UNIVERSITÀ POLITECNICA DELLE MARCHE

PhD course in LIFE AND ENVIRONMENTAL SCIENCES
Curriculum MARINE BIOLOGY AND ECOLOGY

INVESTIGATION OF ACCLIMATION POTENTIAL OF ALGAL CELLS

PhD Candidate
Andrea Pessina

PhD supervisor
Mario Giordano

TABLE OF CONTENT

1. SUMMARY

The project I have conducted intended to investigate the energetic requirements of acclimation and whether the cost of acclimation, understood as energy consumed, when the culture medium contains acetate (as in this case) is impinged mainly on photosynthesis or oxidative metabolism. Cell energy, as ATP and/or reducing power, is transformed in the mitochondria and/or in the chloroplasts. The energy production from chloroplast or mitochondria may depend on environmental conditions. For instance, the production of energy in the chloroplast will be affected by the availability of light (below saturating irradiance) and on the demand for electrons by the various competing sink of energy (e.g. assimilation of C, N, S, responses to stressogenic conditions). The mitochondrial energy depends on the availability of substrate for oxidative metabolism (it should not be forgotten that also chloroplasts are capable of substantial oxidative metabolism) and, in extreme cases, on the availability of O_2. It is unclear to what extent a deficiency in the energetic metabolism in one of the two organelles can be compensated by the energy produced by the other.

In order to address these questions and test the hypothesis that acclimation can only occur when sufficient energy is available, I set up experiments in which algal cells were subject to an environmental perturbation. The acclimation to that perturbation (increased of growth temperature or S-starvation) was then studied in conditions of different energy availability, manipulating the capacity of both photosynthetic and oxidative metabolism.

My results showed that energy availability is a necessary precondition for acclimation and the energy availability determined either the direction of the change, and/or the acclimation timing, and/or the possibility to maintain the modifications at long-term. However, the effects of energy availability on biological response are correlated with the type of perturbation: i) The energy provided by the mitochondria seems essential for the long-term acclimation of *C. reinhardtii* to the S-starvation; ii) The biological response to temperature perturbation seem strictly species-specific. The variation of certain cell components (protein in *C. reinhardtii*; lipid for *D. tertiolecta*) appears crucial for the acclimation of algae since it occurs regardless of the external concentration of O_2 and of the irradiance in the culture regime.

2. INTRODUCTION

2.1 Effects of perturbations on cell composition

Aquatic environments are dynamic and heterogeneous systems, in which abiotic variables such as light, temperature and nutrient availability interact with the biome. Light intensity, surface water temperature and other abiotic variables may have periodic, seasonal or daily (and in some case even shorter) variations, which, as Behrenfeld et al. (2008) reported, may also co-occur. Light, temperature and nutrient availability are certainly among the most important variables regulating productivity and growth of phytoplankton; for this reason, fluctuations of one of these variables can produce large effects in photosynthetic rate, in growth rate and in cell metabolism (Spilling et al. 2015).

Fluctuation of abiotic factors can be short or long - term. The perception of the duration of such environmental perturbations, at least in the range of hours to days, may depend on the growth rate of the organisms that experience them (Giordano 2013). After a perturbation, organisms can choose between two possible modes of response: the maintenance of the *status quo*, i.e. homeostasis (Giordano 2013), or a response enacted through rapid modification of the extant proteome (regulation), the change of the expressed proteome (acclimation) or of the genome (adaptation) (Raven and Geider 2003). Regulation, which does not require the synthesis of new protein, may occur in seconds to minutes (Woods and Wilson 2013). An example of this phenomenon is the enzymatic epoxydation-deepoxydation of xanthophylls in the thylakoidal xanthophyll cycles (Raven 2011). Acclimation, instead, consists of changes of quality and/or quantity of the proteome through the synthesis of new protein (and/or the degradation of existing ones). This change is possibly more demanding in terms of energy and requires more time (hours) to be completed, because the synthesis and accumulation of new protein is needed.
Finally, adaptation occurs when the genome is modified. Gene mutations are essentially instantaneous, but the time needed for the mutation to become a trait of a population can require numerous division cycles, depending on the growth rate and the frequency of the mutation (Raven and Geider 2003).

Literally, the word "homeostasis" means the absolute absence of changes (Giordano 2013), for a cell, the homeostasis can be described as the opposition to intracellular changes despite strong perturbations in external environmental (Montechiaro et al. 2016); it is a rather elusive concept since absolute homeostasis is rarely observed. More typically, homoeostasis is maintained only for certain traits, whereas others undergo modifications (Giordano 2013). If the new condition persists for a time that is appreciably longer than the rate of reproduction, acclimation is almost unavoidable. In terms of interspecific competition, homeostasis may bring a competitive advantage when the duration of the perturbation is shorter than the time required for reproduction: under these circumstances, investing energy and material resources for acclimation would not be justified by the gain of a reproductive advantage (De La Rocha and Passow 2004). These concepts were experimentally addressed by Fanesi et al. (2013) who showed that, for a given perturbation, cells of the same species had a greater tendency to acclimate if their growth rate was faster, whereas slower growing cells were more prone to homeostasis.

If a cell responds to a perturbation by modifying its proteome and metabolome, it needs to have access to both nutrients and energy. Therefore, it may be hypothesized that acclimation is possible only when sufficient resources are available. It is unclear whether acclimation is only initiated when sufficient resources are available or if partial or incomplete acclimation responses are possible when there is a shortage of energy. Depending on the type of changes needed for acclimation, the energy may be supplied as 5'-adenosine triphosphate (ATP), as reducing power, or as both, in different ratios (Raven 1982).

2.2 ATP production

Acclimation usually produces modifications in the organic composition of cells and/or related functions, which require energy to be carried out. Raven (1982), published a list of common cellular functions and of their energy costs (Table 1.1).

Table 2.1: List of common cellular functions and of their energy costs (Raven 1982).

	Cellular functions	Cost
1	ATP generation from ADP and P_i, in *vivo* condition	55 kJ $\cdot mol^{-1}$ (3 ATP + 2 NADPH)
2	NAD(P)+ reduction using equivalents from water	220 kJ$\cdot mol^{-1}$
3	CO_2 fixation by the photosynthetic carbon reduction Cycle; product at redox level of carbohydrate	605 kJ $\cdot mol^{-1}$
4	CO_2 accumulation by unicellular algal cell	55 kJ $\cdot mol^{-1}$
5	The synthesis of 1 mol organic C from CO_2	896 kJ $\cdot mol^{-1}$
6	The synthesis of cell wall polyhexoses from CO_2	669 kJ $\cdot mol$ C in wall polysaccharide
7	The synthesis of cell wall peptidoglycan from CO_2	838 kJ $\cdot mol$ C in peptidoglycan
8	The synthesis of cell wall lipid from CO_2	946 kJ $\cdot mol$ C in tripalmitin (5.84 ATP + 2.84 NADPH)
9	Protein synthesis from CO_2	63 kJ $\cdot mol$ C in protein (4.98 ATP + 2.77 NADPH)

It is possible to observe that the synthesis of new lipid (946 kJ $\cdot mol$ C), protein (883 kJ $\cdot mol$ C) and carbohydrate (605 kJ $\cdot mol$ C) are among the most expensive activities for the cell.

In photosynthetic organisms, the two main processes for the production of energy are photosynthesis, which takes place in the chloroplast and aerobic (respiration) or anaerobic (fermentation) oxidative metabolisms, which take place in mitochondria and in the cytosol.

The interaction between the processes occurring in chloroplast and mitochondria have long been known (Krömer 1995, Hoefnagel et al. 1998) and more recently it has been shown how much these interactions are crucial also for fundamental processes such as photosynthesis: Bailleul et al. 2015 have demonstrated that in diatoms the CO_2 fixation is limited by ATP availability, so that mitochondrial respiration becomes extremely important to adjust the ATP: NADPH ratio which support growth rate and carbon fixation. These considerations are true to diatoms used by Bailleul et al. 2015; other possibilities are discussed in the next paragraph.

During oxygenic photosynthesis, the two photosystems (PSI and PSII) work in series through linear electron flow, which generates the proton gradient that is then utilized by ATP synthase for the production of ATP (Mitchell 1966, Boyer 1975). Moreover, a cyclic electron transport, primarily around PSI, can be used to increase ATP production (Allen 2002, Cardol et al. 2009). The ratio between ATP and reducing power for the biosynthetic needs of the cells is constrained by a number of environmental (e.g. nutrient chemical form and availability) and intrinsic (e.g. reproduction) factors. Thus, the ratio of generation of ATP and reducing power can be modulated depending on the situation (e.g. Noctor and Foyer 1998 and reference therein The water water cycle (WWC), also called the Mehler reaction, can be used as well to regulate the ATP: NADPH ratio. In WWC the electrons from PSI are transferred from Fd to reduce oxygen and a superoxide is formed. The superoxide is catalyzed by superoxide dismutase and ascorbate peroxidase, consuming NADPH. The consumption of NADPH allows linear electron flow to continue, and thus produce new ATP (Asada 1999). WWC contributes also to reduces PSII photoinhibitory stress (Behrenfeld et al. 2008).

The interaction between chloroplast and mitochondrion can be influenced by external conditions. For instance, low irradiance can negatively affect photosynthesis (i.e. carbon fixation) and the production of ATP and reduce power in the chloroplast (Behrenfeld et al. 2008). Under these circumstances, mitochondrial oxidative phosphorylation can supply energy for plastidial processes. Acclimation to low irradiance often requires an increase in cellular pigment content, chloroplast membrane surface and thylakoid stacking (Falkowski et al. 1985). To promote ATP production and a high ATP :NAD(P)H ratio the electron flow between PSII and PSI can be decoupled; the WWC can be used to increase the transmembrane proton gradient necessary for ATP synthesis by water splitting at PSII. In this condition is generated a cyclic electron flow around PSI and so are developed two distinct pathways (i.e. WWC around PSII and cyclic electron flow around PSI) each supporting ATP production (Behrenfeld et al. 2008). Instead, when a light is saturating and the photosynthetic membranes are overstimulated and electron transport is limited downstream of PSII, it may be necessary to dissipate the excess of reducing power to avoid photoinhibition (Ohad et al. 2000, Andersson and Aro 2001). In both of these cases (low light or excess of reducing power) mitochondrial respiration can play important roles: it can elevate the intracellular level of CO_2 (Saradadevi and Raghavendra 1992); it can provide extra energy to facilitate the fast turnover of D1 protein (Saradadevi and Raghavendra 1992, Andersson and Aro 2001); it can regulate the cell redox state and it can prevent the over-reduction of electron transport chain in the chloroplast (Saradadevi and Raghavendra 1992). The latter process is particularly important when photorespiration is restricted because of either metabolic control or mutations (Raghavendra and Padmasree 2003, Scheibe 2004). The chloroplasts can export excess reducing equivalents to be either stored (e.g. as malate) or to be oxidized by respiration (Scheibe, 2004). Various ways exist for the export of $NA(D)PH/NAD(P)^+$ across membranes; they are mostly based on metabolic shuttles that operate through the reversible reduction/oxidation of organic substrates. Four main shuttles are known; the glyoxylate-glycolate shuttle; the malate/oxaloacetate shuttle (Heber 1974), the oxoglutarate/glutamate shuttle (Lea and Miflin 1975) and triose phosphate/sucrose shuttle (Raghavendra and Padmasree 2003). The ''oxaloacetate-malate shuttle'' (OAA-malate) and the ''dihydroxyacetone phosphate-phosphoglyceric acid shuttle''(DHAP-PGA) are the two more important shuttle systems to connect chloroplastic, cytosolic, and mitochondrial reductant pools. In the malate valve (Scheibe 2004) NADPH is consumed in the chloroplast to reduce OAA to malate. The malate is transported across the chloroplast membrane in the cytosol where it is converted in OAA, which is

exchanged with a new malate molecule and then it can return in the chloroplast. During this operation NADH is regenerated (Heber 1974 and references therein). During DHAP-PGA shuttle, PGA is reduced to GAP-DHAP by NADPH through an ATP-dependent intermediate step which involved glycerate-1, 3-bisphosphate. GAP-DHAP go through the chloroplast membrane and NADH, ATP, and PGA are generate in the cytosol from GAP-DHAP by a reverse sequence (Heineke et al. 1991, Raghavendra et al. 1994). Moreover, the mitochondria can use a modified TCA cycle to export isocitrate to the cytosol, where it is converted to oxoglutarate and transferred to chloroplasts (Padmasree et al. 2002), but no more than 50% of reducing power produced from mitochondria is exported to chloroplast (Krömer 1995).
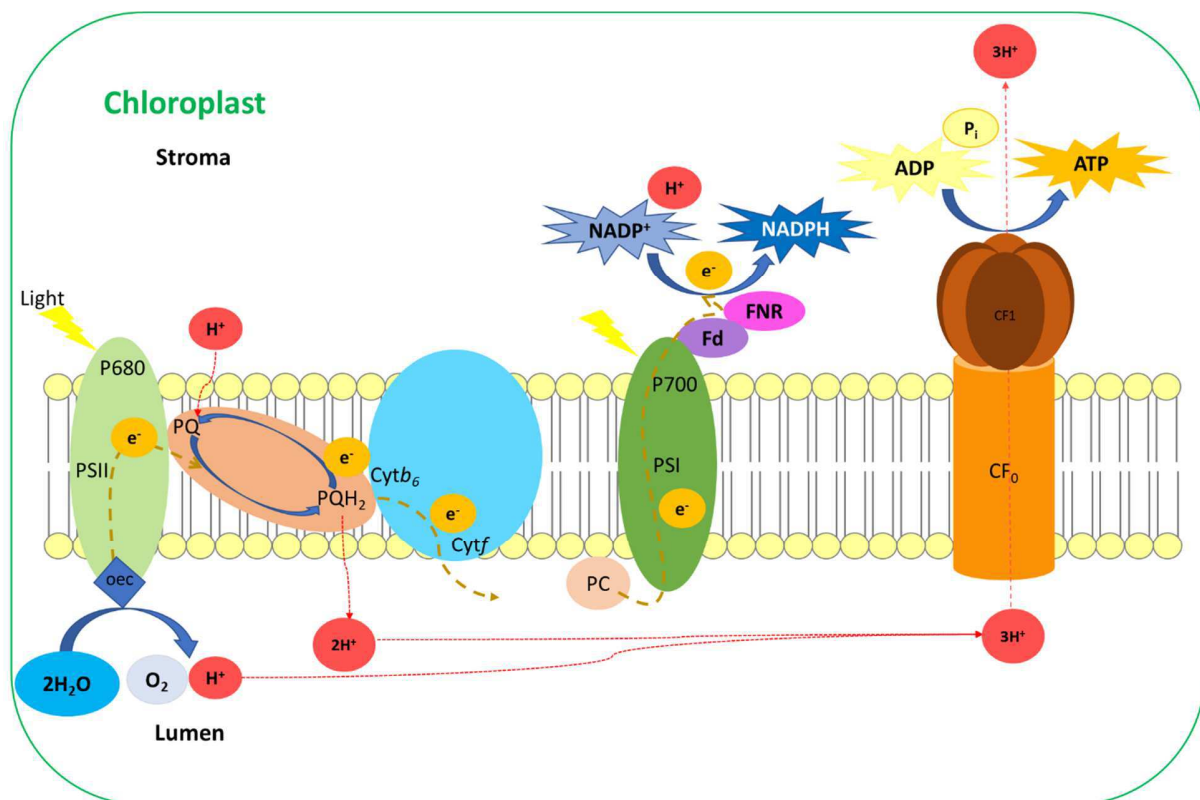

Figure 1.1: Light-dependent reactions, ATP and NADPH productions. Brown arrows stand for electron (e^-) transport along the chloroplast thylakoid membrane (yellow) by molecules of electron transport chain. Red arrows stand for protons (H^+) movements; the H^+ ions translocation from chloroplast stroma into chloroplast lumen produce a proton gradient which is dissipated from ATP synthase during ATP synthesis. The implied $3H^+$:e^- ratio is for non cyclic electron transport. The abbreviations as in thext mean: H2O = water, O_2 = Oxygen, OEC = oxygen evolving complex, PSII = photosystem II, P680 = pigment 680, primary donor of PSII, PQ / PQH2 = " Q cycles", ubiquinone (PQ) /ubiquinol (QH2), Cytb_6 - Cyt$f$ = cytochrome complex b_6-f, Cyt$c6$ = cytochrome c$_6$ can work in substitution of PC (Gupta et al. 2002), PC = plastocyanin, PSI = photosystem I, P700= pigment 700, primary donor of PSI, Fd = ferredoxin, FNR = ferredoxin-NADP$^+$-oxidoreductase, NADP$^+$/H = nicotinamide adenine dinucleotide phosphate, CF$_0$ = "coupling factor 0", membrane-intrinsic domain, CF$_1$ = "coupling factor 1", water-soluble membrane-extrinsic domain, ADP = adenosine diphosphate, P$_i$ = inorganic phophate, ATP = adenosine triphosphate. Redraw from Allen 2002.
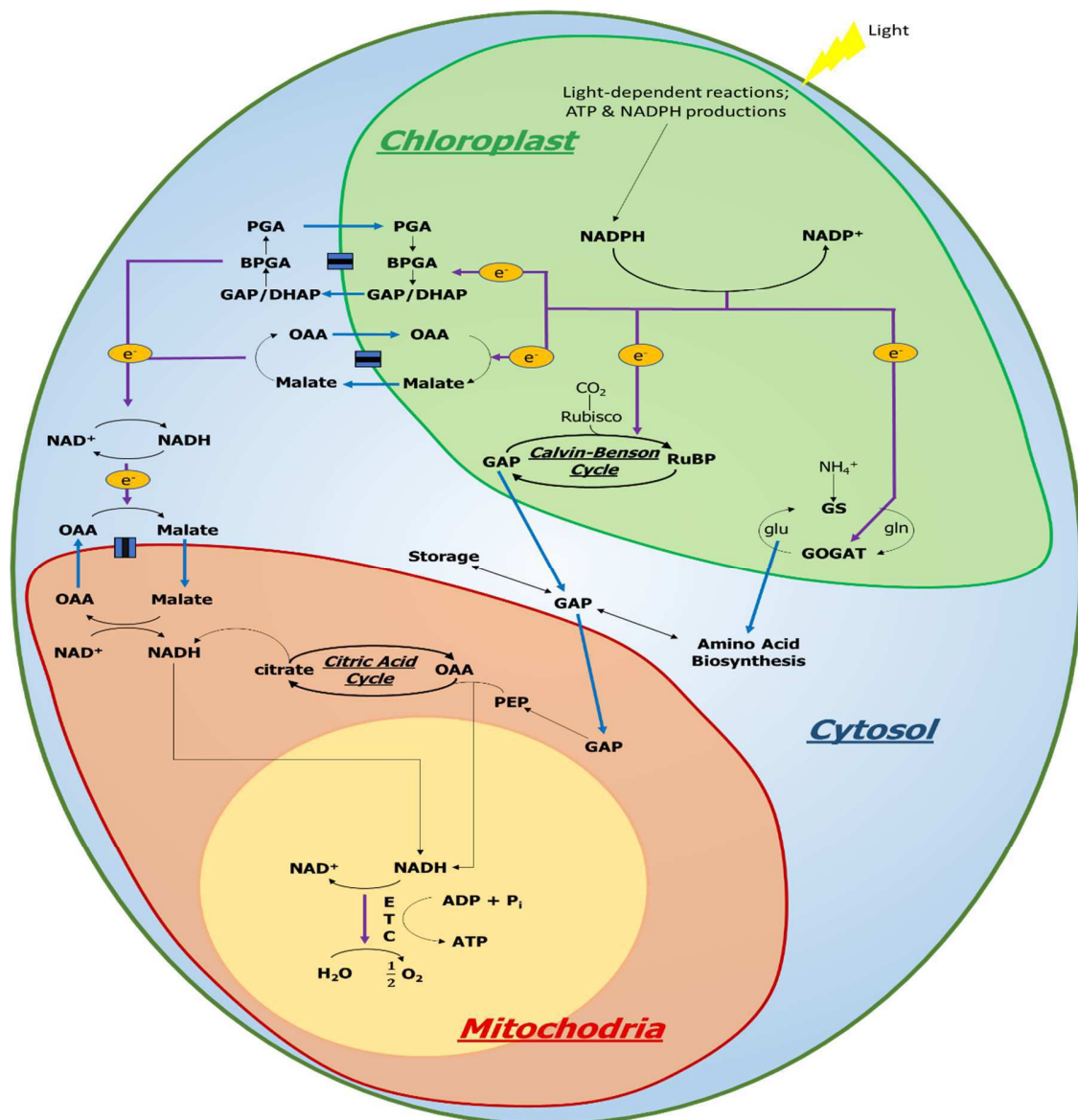
Figure 1.2: Photosynthetic and electron transport pathways. NADPH can be processed in different metabolic pathways: first of all, through nitrogen reduction, glutamate (glu) synthesis (GS) and glutamine:2-oxoglutarate aminotransferase (GOGAT) via the GS-GOGAT cycle in the chloroplast; secondly through glyceraldehyde 3-phosphate (GAP), exported from plastid to cytosol and, finally, into mitochondria, where it can be processed through oxidative phosphorylation, in order to produce ATP, or one other possible way to process NADPH is through substrate shuttles (Membrane-embedded rectangular with black bar) which link the chloroplast, cytosol, and mitochondria. The two shuttles represented in the picture are the oxaloacetate-malate (OAA-Malate) and the dihydroxyacetone phosphate-phosphoglyceric acid (DHAP-PGA) shuttles. GAP produced by the Calvin-Benson cycle can be used for carbon storage, for producing carbon skeletons needed to amino acid biosynthesis, or mitochondrial ATP synthesis by citric acid cycle. Blue arrows stand for transport across membranes; violet arrows stand for electrons (e⁻) transport; ETC = electron transport chain; RuBP = ribulose-1,5-bisphosphate; gln = glutamine; PEP = phosphoenolpyruvate; BPGA = glycerate-1, 3-bisphosphate. Redraw from Behrenfeld et al. 2004.

The enzymes Glyceraldehyde-3-phosphate dehydrogenase (GAPDH) and triosephosphate isomerase (TPI) play a crucial role during the glycolysis. In animals, both enzymes are cytosolic enzymes, however, in photosynthetic eukaryotes exist also isoforms of GAPDH and TPI in the chloroplast, furthermore, Liaud and colleagues (2000) in diatoms' mitochondria discovered a second isoform of GAPDH and TPI. With this enzyme the Glyceraldehyde 3-phosphate (GAP) can be easily processed in diatoms' mitochondria to produce ATP (Kim et al. 2016). The mitochondrial metabolism becomes very important in the darkness when it produces 100% of cell energy from stored substrates (Hoefnagel et al. 1998). However, also in the light, with aerobic metabolism (TCA cycles and oxidative phosphorylation), mitochondria have a greater capacity than chloroplast to synthesize ATP, because the chemical conditions in this organelle generate a greater amount of energy from the oxidation of NAD(P)H than in the chloroplast (2.5 ATP equivalents per NADH, Raven and Beardall 2017, versus 1.28-1.5 ATP per NADH in the chloroplast, Kramer and Evans 2011). Furthermore, the molecular structure of mitochondrial ATPase allows it to produce more ATP for each electron moved to the electron transport chain compared to chloroplast ATPase (Allen 2002) (Table 2.2). However, this ATP production in mitochondria is true only if mitochondrial Complex I is present and functioning. In organisms with mutations in complex I and in dinoflagellates, which are lacking this complex, the production of ATP in the mitochondria is reduced of 30% compared to organisms with a functioning complex I (Raven and Beardall 2017). The mitochondrial ATP/ADP translocator operates at faster rates than its chloroplast counterpart (Hoefnagel et al. 1998, Heldt 1969). This is the reason why the cytosolic ATP pool is mainly maintained by mitochondrial oxidative phosphorylation (Krömer 1995).

Table 2.2: Different in ATP production between chloroplast and mitochondria per NADH

	Chloroplast	Mitochodria
Coupling Factor	CF_0	F_1
Fold rotational (1 fold rotational = 1 H^+ binding sites)	14	12
H^+ / ATP	4.67	4
N° of protons extruded in lumen	6	10
Number of rotation	0.42	0.83
ATP production	1.29	2.5

Several pathways exist for the conversion of pyruvate to acetyl-CoA in algae (Hemschemeier and Happe 2005; Atteia et al. 2006; Grossman et al. 2007): pyruvate formate lyase (PFL1), pyruvate ferredoxin oxidoreductase (PFR, often referred to as PFOR), and the pyruvate dehydrogenase (PDH) complex. In aerobic condition mitochondria, cells use PDH to convert pyruvate in acetyl-CoA which can be oxidated during the TCA cycle in CO_2 (Catalanotti et al. 2013). In hypoxia or anoxia, eukaryotes can continue to produce ATP and consume the NAD(P)H, generated through catabolism, using alternative (to O_2) electron acceptors (e.g. NO_3^-, SO_4^{2-} or fumarate) and fermentation (Atteia et al. 2013). In anaerobic condition, the pyruvate is typically oxidate to acetyl-CoA by PFL1 and PFR. In Chlamydomonas spp, fermentation can produce ethanol, formate, glycerol and lactate (Mus et al. 2007). In hydEF-1 mutant, during fermentation, it is possible to find succinate (Dubini et al. 2008), while in pfl1 mutant, it can be

observed an increase of lactate (Catalanotti et al. 2012). Instead, in both genes PFL1 and ADH1 mutant, it is possible to find glycerol (Catalanotti et al. 2012).

Fermentation requires the synthesis of specific enzymes, whose genes are expressed only in hypoxic or anoxic condition (Catalanotti et al. 2013): PFL1 catalyzes the conversion of pyruvate to acetyl-CoA and formate, while the reaction catalyzed by PFR oxidizes pyruvate to acetyl-CoA and CO2 and reduces ferredoxin (FDX). The reduced FDX can be used as a substrate for nitrite and sulfate/sulfite reductases (Ghirardi et al. 2008). In *Chlamydomonas reinhardtii*, FDX is oxidized by the hydrogenase enzyme (HYDA1 and HYDA2), with the production of H2 as secondary metabolite (Happe and Naber 1993, Timmins et al. 2009) (Figure 1.3 A). The acetyl-CoA produced by PFL1 and PFR can be processed through the reaction catalyzed by Alcohol/aldehyde dehydrogenase1 (ADH1), which reduces acetyl-CoA to ethanol (Hemschemeier and Happe, 2005) (Figure 1.3 B). Alternatively, acetyl-CoA can be converted to acetate by sequential action of phosohotransacetylase, PTA or PAT (Atteia et al. 2006) and acetate kinase (ACK or AK) with the transformation of ATP (Atteia et al. 2006) (Figure 1.3 C).

Pyruvate can also be metabolized to ethanol thanks to the cartalysis of pyruvate decarboxylase (PDC3). PDC3 operates a direct decarboxylation of pyruvate to CO2 and acetaldehyde, which is then reduced to ethanol by an acetaldehyde dehydrogenase (ADH1 or ADH2) (Figure 1.3 D).

The two pathways to convert acetyl-CoA to ethanol produce different amount of NADH: 2 NADH molecules per acetyl-CoA are generated in the reaction catalyzed by ADH and only one in the PDC3 pathway (see figure 1.3).

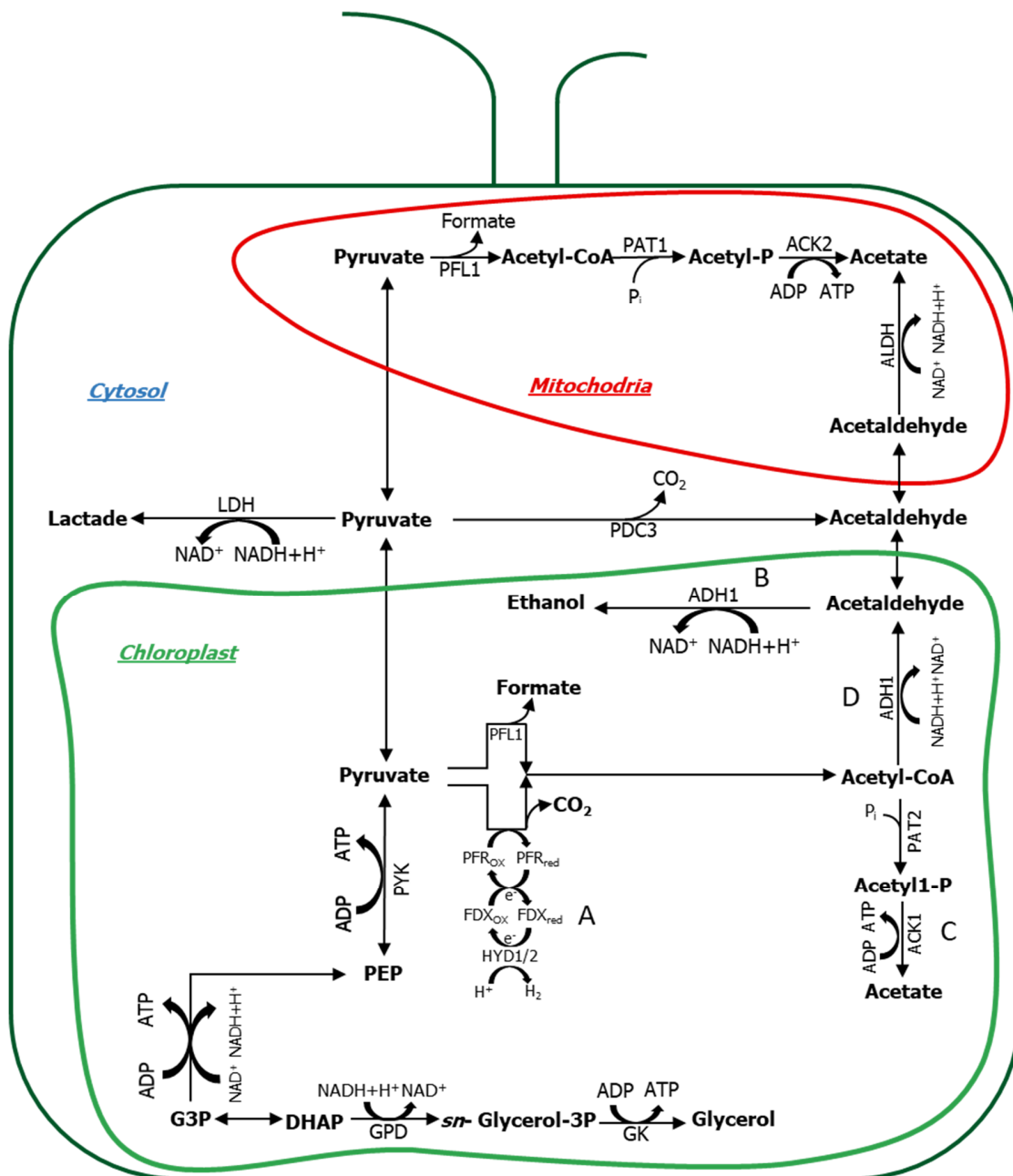The complexity of fermentation pathway is shown in figure 1.3.

Figure 1.3: Fermentation pathways in Chlamydomonas. Formate, acetate and ethanol, CO_2 and H_2 are the main products obtained in wild-type (WT) Chlamydomonas reinhardtii cells during fermentation. Green circle represents the chloroplast, while red circle represents the mitochondria. The single protein represented in figure means: ACK1 and ACK2 = acetate kinase 1 and 2; ADH1 = alcohol dehydrogenase; FDX = ferredoxin; GK = glycerol kinase; GDP = sn-glycerol-3-phosphate dehydrogenase; HYDA1 and HYDA2 = Hydrogenase 1 and 2; LDH = lactate dehydrogenase; PAT1 and PAT2 = phosphotransacetylase 1 and 2; PDC3 = pyruvate decarboxylase 3; PYK = pyruvate kinase. Redraw from Catalanotti et al. 2013.

2.3 Origin of the energy required for acclimation of algal cells to environmental stimuli

The activity of the two main processes for energy production in photosynthetic organisms, i.e photosynthesis and oxidative metabolism, can be modulated respectively by irradiance and oxygen concentration (Lehninger 1962, Allen 2002 and reference therein). A low irradiance can decrease the GAP transformation in the chloroplast and, as a consequence, the substrates for both organic pools biosynthesis and mitochondrial metabolism (Behrenfeld et al. 2008), with a possible reduction of oxidative phosphorylation and production of energy. The total oxidation of glucose to CO_2 and H_2O in the mitochondrion produces about 2870 kJ $\cdot$mol^{-1} (Tran and Unden 1998); 27 mol ATP are produced through the tricarboxylic acid cycle (TCAC) for each mol of glucose oxidized to CO_2 (Raven and Beardall 2017); if we assume that the hydrolysis of a phosphodiester bond in ATP yields 55 kJ $\cdot$mol^{-1} (Raven 1982), we can conclude that about 52% of the energy derived from the oxidation of each mole of glucose is stored in form of ATP during mitochondrial respiration. O_2 is the final electron acceptor of oxidative phosphorylation (Lehninger 1962 and references therein). Therefore, in anaerobic condition, cells use fermentation to produce ATP. The energetic yield of fermentation is such that the oxidation of one glucose molecule produces up to 5 ATP (Atteia et al. 2013). Davies and colleagues (1993) using mung bean root had estimated that the free-energy released by ATP hydrolysis in anaerobic condition at pH 6.8 is 31.4 kJ $\cdot$mol^{-1} and not 55 kJ $\cdot$mol^{-1} as observed in cytosolic condition at pH7.3 (Raven 1982, Davies et al. 1993). pH, as well as ATP availability, has a big effect on free-energy released by ATP (Davies et al. 1993), and it is possible to observe a decrease of pH during anaerobic condition (Kennedy et al. 1992). Considering an average of 43 kJ $\cdot$mol^{-1} for ATP hydrolysis, it can be calculated that, with fermentation, only around 7% of the energy derived from the oxidation of glucose is stored in ATP, a value significantly lower compared to the energy stored in ATP with aerobic metabolism. Processes such as the assimilation of nitrate into glutamate (2255 kJ $\cdot$mol^{-1}), of sulfate into cysteine (1815 kJ $\cdot$mol^{-1}) (Giordano and Raven 2014), the fixation of CO_2 in triose-P (605 kJ $\cdot$mol^{-1}), and the synthesis of lipid from CO_2 (946 kJ $\cdot$mol C in tripalmitin) (Raven 1982) are some of the most costly biological processes, which account for a major part of the cellular energy demand. Algal cells that respond to environmental perturbation by rearranging their cell composition need energy for acclimation. No energy is virtually required by algae that keep their cellular composition stable despite modifications in the external environment (i.e. homeostasis). Whether the energy required for acclimation originates from an equal contribution of chloroplast and mitochondrion is currently unknown.

In this context the project I have conducted intended to test the hypothesis that acclimation can only occur when sufficient energy is available in cells and whether the cost of acclimation impinges mainly on photosynthesis or oxidative metabolism. Considering the great importance of interaction between mitochondria and chloroplast (Bailleul et al. 2015 and Saradadevi and Raghavendra 1992), it is possible to hypothesize that cells living in anaerobic conditions with a low oxidative metabolism are more prone to be homeostatic than cells living under aerobic conditions. In both aerobiosis and anaerobiosis, cells that grow at a high irradiance (HL) should have more energy available to respond to environmental perturbations compared to cells grown at a low irradiance (LL). To verify the hypothesis I set up experiments in which algal cells were subject to an environmental perturbation, change in O2 availability or growth temperature. If the hypothesis true, more compositional changes are expected in cultures at HL in aerobic conditions, and no or little changes at LL in anaerobic conditions.

3. MATERIALS AND METHODS

3.1 Experimental organisms

Chlamydomonas reinhardtii cc-125 and *Dunaliella tertiolecta* ccap 19/24 were chosen as experimental organisms.

Chlamydomonas reinhardtii cc-125 was obtained from the Chlamydomonas Resource Center (University of Minnesota, Minneapolis, USA). *Chlamydomonas reinhardtii* is a unicellular green alga belonging to the phylum Chlorophyta, class Chlorophyceae, order of Chlamydomonadales, family Chlamydomonadaceae (Guiry, M.D. & Guiry, G.M. 2017. *AlgaeBase*). *C. reinhardtii*, are considered as a model organism for the study of photosynthesis and energetic metabolism, for the production of molecular hydrogen (H_2) in anaerobic metabolism (Melis and Happe 2001; Catalanotti et al., 2013) and also for the structure, assembly, and function of flagella (Merchant et al. 2007). *Chlamydomonas reinhardtii* is a green algae that inhabits freshwater and soil algae (Roberts et al. 1972). Its cell is surrounded by a cellulosic cell wall, with two anterior flagella and contains multiple mitochondria and a cup-shaped chloroplast that occupies most of the cell volume (Merchant et al. 2007). The nuclear, plastidial and mitochondrial genomes of C. reinhardtii have been sequenced (Merchant et al. 2007, Gonzalez-Ballester et al. 2010) and this information makes *C. reinhardtii* a robust system for molecular studies (Catalanotti et al2013).

Dunaliella tertiolecta ccap 19/24 was obtained from the Culture Collection of Algae and Protozoa (Scottish Marine Institute, Scotland, United Kingdom).
Dunaliella tertiolecta belongs to the phylum Chlorophyta, order Chlamydomonadales, family Dunaliellaceae (Guiry, M.D. & Guiry, G.M. 2017. *AlgaeBase*). *Dunaliella tertiolecta* cells are a biflagellate green alga (Ben-Amotz et al. 1987), with a single cup-shaped chloroplast and numerous mitochondria (Ben-Amotz and Avron 1980). Besides, chloroplast and mitochondria, also pigments, Golgi apparatus, eyespot of *Dunaliella spp*. are similar to *Chlamydomonas* (Ben-Amotz and Avron 1990). *Dunaliella cells* are enclosed in a mucous coat (Ben-Amotz and Avron 1990) possibly derived from the glycoprotein cell wall of an ancestral chlamydomonadalean (Buccheim et al. 1996) *D. teriolecta*, like all its congeneric species, lacks of a proper cell wall. The genus *Dunaliella* is widely studied and used for biotechnological application mostly, due to its ability to produce a large amount of glycerol and β-carotene (Ben-Amotz and Avron 1990).

Dunaliellaceae are phylogenetically close to Chlamydomonadaceae (Merchant et al. 2007, Leliaert and Lopez-Bautista 2015). For this reason, *Dunaliella* spp. are good seawater equivalents of Chlamydomonas.
Moreover, BLAST similarity searches showed as unique sequences of *D. tertiolecta* produced by next-generation DNA pyrosequencing technology were more similarity at *Chlamydomonas reinhardtii* than at *Dunaliella viridis* or *D. salina* (Rismani- Yazdi et al. 2011). Similar results were obtained with phylogenetic analysis performed by Assunção and colleagues (2012); internal transcribed spacers (ITS1+ITS2) of genus Dunaliella showed that *D. tertiolecta* is closer to *C. reinhardtii* than other Dunaliella species such as *D. salina* or *D. parva*.

3.2 Culture conditions

Experimental 1:

Six cultures of *C. reinhardtii* were grown in Tris-Acetate-Phosphate medium (TAP; Table 3.1) (Harris 1989). On day 0 of the experiment, three cultures were washed and resuspended in fresh TAP medium to free sulfate (-S) (Table 3.1), the other three cultures in TAP medium were used as a control. Cultures grew in batch condition and they were maintained at 100 µmol photons $m^{-2} \cdot s^{-1}$, under continuous light (PAR = λ = 400-700 nm) in 250-ml Erlenmeyer flasks containing 250 ml of algal suspension. Cultures were at constant temperature, 25°C. The experiment was conducted in aerobic and anaerobic conditions. Samples were collected over time to RNA analysis, from immediately after the application of the perturbation (time 0, T0), to six hours after the start of the perturbation (T6h), with intermediate sampling at 4 days after the start of perturbation (T4h). It has been chosen to use a photo-organo-trophic organism because this experiment wanted to study the genes involved in S-uptake in a condition which did not permit photosynthesis (-S and -O_2) and the fermentation was possible only in TAP medium. In an attempt to minimize the variables which could produce biological effects also the control cultures have been grown in TAP medium.

Experimental 2:

In order to investigate the relative contribution of photosynthetic and respiratory energy to acclimation *C. reinhardtii* and *D. tertiolecta* were grown at two different irradiances and in aerobic and anaerobic condition. *C. reinhardtii* grown in Tris-Phosphate minimal medium (TP; Table 3.2); the same medium was used for *D. tertiolecta*, but with the addition of 0.5 M NaCl, since *D. tertiolecta* is a marine species (Table 3.2). The irradiances were such that one would saturate growth (High Light – HL) and the other would limit growth (Low Light – LL). Preliminary tests were conducted to choose the photon flux densities for both species (Figure 3.1): for *C. reinhardtii*, HL was 250 µmol photons$\cdot m^{-2} \cdot s^{-1}$ and LL was 100 µmol photons$\cdot m^{-2} \cdot s^{-1}$; for *D. tertiolecta*, HL was 250 µmol photons$\cdot m^{-2} \cdot s^{-1}$ and LL was 50 µmol photons$\cdot m^{-2} \cdot s^{-1}$. Cultures were allowed to acclimate to each photon flux densities for 4 generations before starting the experiments.

In this case, the perturbation consisted in a change of temperature. The initial condition was 15 ° C; when the experiments started, the flasks were moved to 30 °C (start of perturbation).

In all cases, cell composition and cells physiology were monitored over time, from immediately before the application of the perturbation (time 0, T0), to seven days after the start of the perturbation (T7), with intermediate sampling at day 1 (24 hours after the start of perturbation – T1), and day 4 (96 hours after the start of perturbation – T4). Both species were cultured in 250 ml flasks with 200 ml of algal suspension; during the experiment, for each the sampling days, a volume of 100 ml of algal suspension was collected for analysis. In order to maintain the same ratio between gaseous and liquid phase and therefore to ensure the same anaerobiotic conditions through the experiment, cultures were refilled with 100 ml of the new medium after each sampling. The new medium used to refill cultures was preventively balanced with the same gaseous phase of the cultures by bubbling of N_2

For both experiments, in aerobic condition algae were cultivated in autoclaved flasks provided with cotton plugs while in anaerobic conditions, the flasks were closed with silicone plugs, in which three tubes were inserted to allow gassing and sampling. The tubes were sealed with "water and gas-proof"

silicone (Incofar, Modena, Italy). To induce anaerobic condition, or at least hypoxic conditions hence considered to be anoxic, twenty-four hours prior to experimental manipulation, N_2 gas was insufflated directly into the medium through a 0.2 μm gas filter. Preliminary tests with O_2 electrode system (Chloroview 2, Hansatech, Kings Lynn, Norfolk, UK) based on a Clark-type O_2 electrode, had demonstrated that a flow of 950 ml·min^{-1} for 40 minutes was enough to saturate the cultures with N_2 (2ppm ≤ O_2) and remove O_2 present in the medium and headspace (Figure 4.17). In order to keep the anaerobic condition during the seven days the experiment lasted at HL and LL, N_2 was bubbled each day. For each species/treatment combination, three independent biological replicates were used.

Table 3.1: Recipe for TAP (+S TAP) and free sulphate TAP media (-S TAP). Each stock solution was prepared separately and then mixed in the proportions indicated in the table (A). The salts that contain sulphate during the preparation of -S TAP medium were replaced with salts with Cl and they are listed on the left of /. The salts and the solutions were added in the same order they appear in the table. All media were autoclaved at 120° C for 20 minutes at 2 bars (and then cooled to growth temperature), before being used.

(A) Filner's medium for 1 L of growth medium	+S TAP medium	-S TAP medium
4 X Filner's Beijerinks Solution (mL)	12.5	12.5
Modified Trace Mineral Solution (mL)	5	5
Potassium Phosphate Solution (mL)	1	1
Tris base (g)	2.42	2.42
$C_2H_4O_2$ (mL)5	Adjust pH with HCl to 7,2	Adjust pH with HCl to 7,2
NaCl (g)	0	27.58
4 X Filner's Beijerinks Solution Recipe for 1 L solution (+S / -S)		
NH_4Cl (g)	32	32
$CaCl_2$ (g)	4	4
$MgSO_4 \cdot 7H_2O$ (g) / $MgCl_2$	8	6.6
Modified Trace Mineral Solution Recipe for 500 ml solution (/ -S)		
Na2EDTA (g)	5 g dissolved by heating and stirring	5 g dissolved by heating and stirring
NaOH 5N	Adjust pH with NaOH to 6.5	Adjust pH with NaOH to 6.5
$FeSO_4 \cdot 7H_2O$ (g) / $FeCl_2 \cdot 4H_2O$	0,5	0.357
$ZnSO_4 \cdot 7H_2O$ (g) / $ZnCl_2$	2.2	1.04
H_3BO_3 (g)	1.14	1.14
$MnCl_2 \cdot 4H_2O$ (g)	0.51	0.51
$CuSO_4 \cdot 5H_2O$ (g) / $CuCl_2$	0.16	0.11
$NaMoO_4 \cdot 2H_2O$ (g)	0.073	0.073
$CoCl_2 \cdot 6H_2O$ (g)	0.16	0.16
1M Potassium Phosphate		
1M KH_2PO_4	Mix them together to have a final solution with a 7.2 pH	Mix them together to have a final solution with a 7.2 pH
1M K_2HPO4		

Table 3.2: Recipe for TP and modified TP media. Each stock solution was prepared separately and then mixed in the proportions indicated in the table (A). The salts and the solutions were added in the same order they appear in the table. All media were autoclaved at 120° C for 20 minutes at 2 bars (and then cooled to growth temperature), before being used.

(B) Filner's medium for 1 L of growth medium	TP medium	Modified TP medium
4 X Filner's Beijerinks Solution (mL)	12.5	12.5
Modified Trace Mineral Solution (mL)	5	5
Potassium Phosphate Solution (mL)	1	1
Tris base (g)	2.42	2.42
HCl 12M (mL)	Adjust pH with HCl to 7.2	Adjust pH with HCl to 7.2
NaCl (g)	0	27.58
4 X Filner's Beijerinks Solution Recipe for 1 L solution		
NH_4Cl (g)	32	32
$CaCl_2$ (g)	4	4
$MgSO_4 \cdot 7H_2O$ (g)	8	8
Modified Trace Mineral Solution Recipe for 500 ml solution		
Na2EDTA (g)	5 g dissolved by heating and stirring	5 g dissolved by heating and stirring
NaOH 5N	Adjust pH with NaOH to 6.5	Adjust pH with NaOH to 6.5
$FeSO_4 \cdot 7H_2O$ (g)	0,5	0.5
$ZnSO_4 \cdot 7H_2O$ (g)	2.2	2.2
H_3BO_3 (g)	1.14	1.14
$MnCl_2 \cdot 4H_2O$ (g)	0.51	0.51
$CuSO_4 \cdot 5H_2O$ (g)	0.16	0.16
$NaMoO_4 \cdot 2H_2O$ (g)	0.098	0.098
$CoCl_2 \cdot 6H_2O$ (g)	0.16	0.16
1M Potassium Phosphate		
1M KH_2PO4	Mix them together to have a final solution with a 7.2 pH	Mix them together to have a final solution with a 7.2 pH
1M K_2HPO4		

Figure. 3.1: Identification of the photon flux densities that saturates (250) or limits (100 or 50) the growth rate of *C. reinhardtii* (left) and *D. tertiolecta* (Right). Different letters indicate statistically different mean values ($p < 0.05$; 2-ways ANOVA and Fisher's LSD test).

3.3 Determination of cell number, growth rate, and cell size

Cell number, cell volume and cell size were determined with an automatic cell counter (CASY® TT, Innovatis AG, Reutlingen, Germany). Aliquots of 100 µl of algal cultures were mixed with 10 ml of an electrolyte solution (CASYton, Innovatis AG, Reutlingen, Germany). A small volume of this mix was pumped into a capillary with a 60 µm pore size, at a constant flow. The capillary separates two electrodes, the inner electrode in silver and outer electrode in platinum. The silver electrode is closed in the capillary, while the platinum one is immersed in the electrolyte solution. The two electrodes produce a cyclic low voltage field of 1 MHz; when a cell enters in the measuring pore, it interfere with the electric field and produces a signal. This signal is measured as a cell count. The flow of cell displaces an amount of water equal to the volume of moving cell; thus the duration of the event of increased resistance is used to estimate the cell volume.

For both species, the growth in batch cultures was measured with daily cell counts.
- Ln cells number (N) counted in exponential phase was plotted vs time;
- The slope of the line obtained was the specific growth rate (μ).

$$\Delta N = N_0 \cdot e^{\mu t}$$

From which μ is derived:

$$\mu = \ln (N_t / N_0) \cdot 1/t$$

3.4 Cell dry weight and ash weight

The cell dry weight was determined according to Ratti et al. (2011). Fifteen ml of culture were centrifuged (3500 g, 5 min) with a centrifuge (MPW 551e centrifuge, MPW MED INSTRUMENT, Warzlawa, Poland). The pellet was washed once in an 0.5 M ammonium formate solution isosmotic to the culture media for *D. tertiolecta* and in deionized water for *C. reinhardtii*, and resuspended in the

same media used for washing. The cell suspension was then filtered on pre-combusted glass fibers filter (GF/C, Whatman, Kent, England) under mild vacuum. The filters were pre-combusted in a muffle furnace at 450°C, for 4 hours or until their dry weight was stable and then brought back to room temperature. The filtered samples were left in an oven (T6 Heraeus, ThermoFisher scientific, Waltham, MA, USA), at 80 °C, for 24 hours or until their weight was constant and were then allowed to equilibrate at room temperature. The dry weight was calculated from the difference between the dry weight of the filter with the sample and the weight of the pre-combusted filter. The dry weight of cells was estimated by dividing this number by the number of cells deposited on the filter. The dry cells were then incinerated in a muffle furnace, at 450 °C, for 4 hours (or until their weight was stable) and weighed again to obtain the weight of the ashes, i.e. the weight of what remains after all organic compounds have been fully combusted.

3.5   Ananlysis of organic composition by Fourier-transformed infrared (FTIR)

The organic composition of algae subject to different growth condition was analyzed over time by means of Fourier Transform Infrared (FTIR) spectroscopy, as described by Domenighini and Giordano (2009). For both species, the sample size that gave the highest signal to noise ratio was $4 \cdot 10^8$ cells. Cells ($1.6 \cdot 10^9$) were harvested by centrifugation (3500 g, 5 minutes; MPW 551e centrifuge, MPW MED INSTRUMENT, Warzlawa, Poland), washed three times with either a 0.5 M ammonium formate solution (for *D. tertiolecta*) or deionized water (for *C. reinhardtii*). Finally, the cells were resuspended in 0.2 ml of the same solution used for the washes, with a final cell concentration of $8 \cdot 10^6$ cells$\cdot \mu l^{-1}$. Fifty μl of this cell suspension were deposited in the center of a silicon window (Crystran, Ltd, Poole, UK) and heated for 24 hours at 80 °C in an oven (T6 Heraeus , ThermoFisher scientific, Waltham, MA, USA). As a blank, 50 μl of 0.5 M ammonium formate solution were deposited on a silicon window and treated as the samples. The reading from this blank measurement was subtracted from the sample measurements (although the heating of the ammonium formate usually left no residue that could be detected by the spectrometer).
For each of the three biological replicates, three instrumental replicates were done.

FTIR spectroscopy is based on the principle that each molecule that has a dipole moment can absorb IR radiations. The wavelengths that are absorbed depend on the normal (vibrational) modes of the molecule, which are influenced by the strength of the dipoles, by the number of atoms in the functional group and by their geometry (Smith 1998) (Figure 3.2).
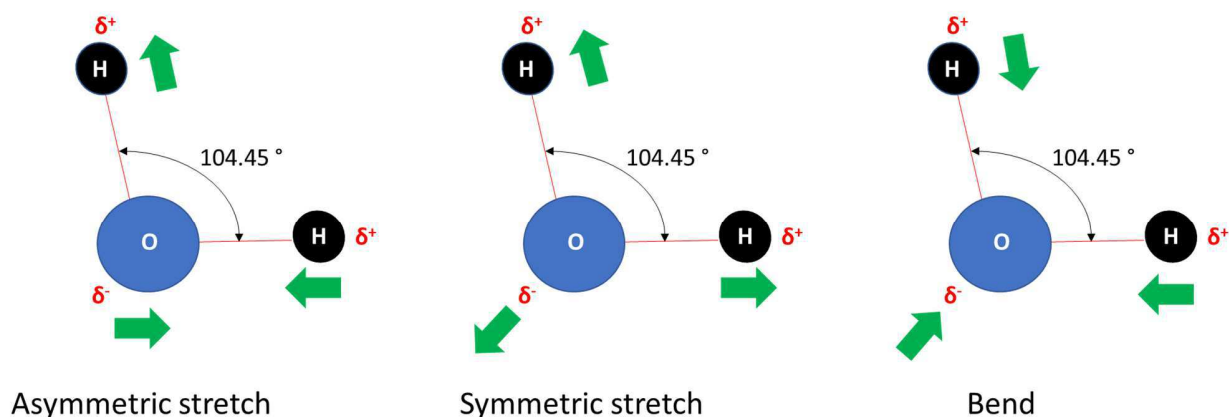
Figure 3.2: Normal (vibrational) modes of a water molecule. δ+ and δ- are the partial positive or negative charge of element, it is the dipole moment of water. The green arrows are the only possible movements of atoms.

A FTIR spectrometer (Fig. 3.3) is equipped with an infrared source, which emits a broad range IR radiation towards a beam splitter. Fifty percent of the IR radiation is deviated by the beam splitter towards a fixed mirror; the other 50% is directed towards a mobile mirror. The ensemble of the two mirrors and the beam splitter is the "Michelson interferometer". The two mirrors reflect the IR beams towards the beam splitter, where the reflected beam interact; such interaction can be constructive (the two beams are in phase) or destructive (the beams are in counter-phase). The recombined beam, after crossing the sample, reaches the detector and generates an interferogram (Figure 3.3). The interferogram represents the intensity of the radiation as a function of the displacement of the mobile mirror. Such function is of difficult chemical and biological interpretation because it does not explicitly provide information on the IR frequency absorbed by the sample (frequency is usually expressed as its spatial analogue, the wavenumber, with units of cm^{-1}). This function of the position of the mirror is converted to a function of the wavenumber through a mathematical operation, the Fourier Transform.

1a = Split Beam, 1b = Delayed Split Beam, 2 = Recombined Beam
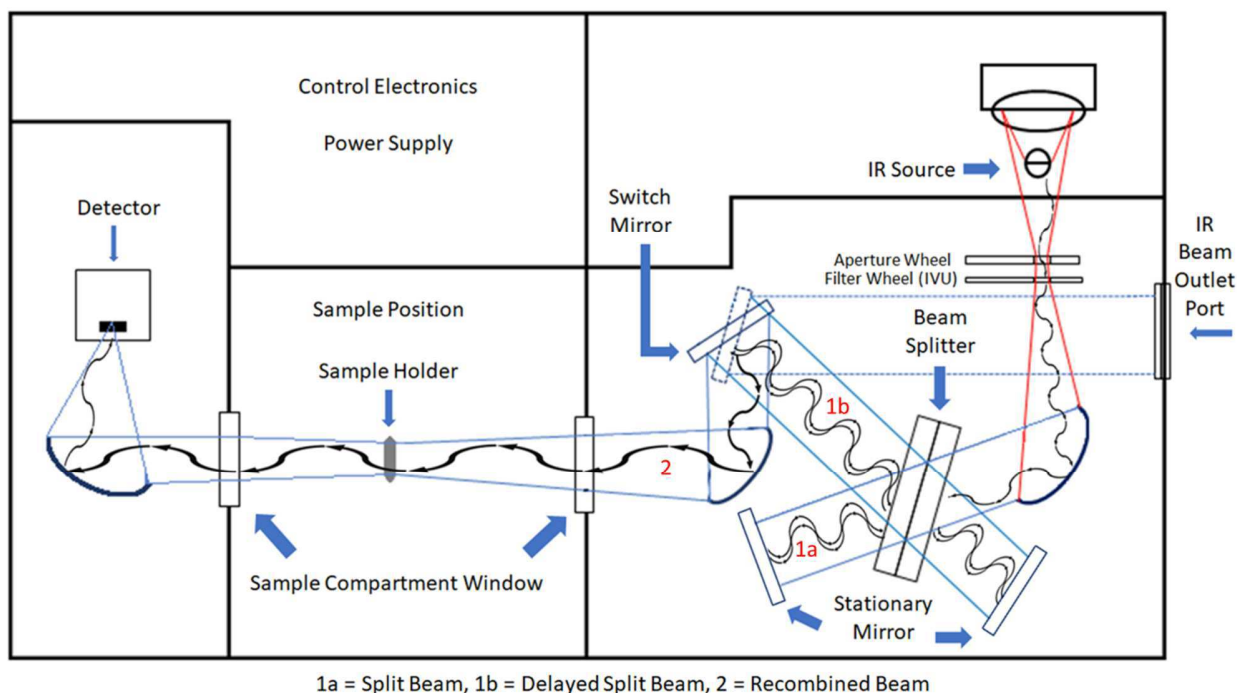
Figure 3.3: Schematic representation of a FTIR spectrometer and of the path of the IR beam. The fixed mirror, the mobile mirror and the beam splitter constitute the "Michelson interferometer"

The main organic pools (protein, carbohydrate and lipid) have characteristic functional groups that absorb at different wavelengths. The intensity of the absorbance of these functional groups can be used to identify them in whole cells (Domenighini and Giordano, 2009).

In this thesis, FTIR spectra were acquired with a Tensor 27 spectrometer (Bruker Optics GmbH, Ettlingen, Germany) and they were obtained through the software OPUS 6.5 (Bruker Optics GmbH, Ettlingen, Germany). The acquisition parameters are listed in Table 3.2.

Table 3.3: Parameters used for the acquisition of FTIR spectra.

Parameters	Value
Spectral resolution	4 cm^{-1}
Number of scans	32
Range of acquisition	4000-400
Apodization function	3-terms Blackman-Harris
Zero-filling factor	2
Pinhole aperture	3 mm

A baseline correction was applied with the "Rubber band" algorithm (64 baseline points): the CO_2 and H_2O bands were excluded. Regarding the peaks attribution was done according Giordano et al. (2001). The position of the peaks in the absorbance spectrum was identified by application of a second derivative with 9 smoothing points to the spectrum. The peaks with negative value in the second derivative indicate the position of peaks. The peak identified with this procedure was used to constrain

spectra deconvolution. The "Curve fit" function of the software OPUS 6.5 (Bruker Optics GmbH, Ettlingen, Germany) was used for peak deconvolution. The area of the relevant peaks was calculated using the integration routine of OPUS 6.5 (Figure 3.4).
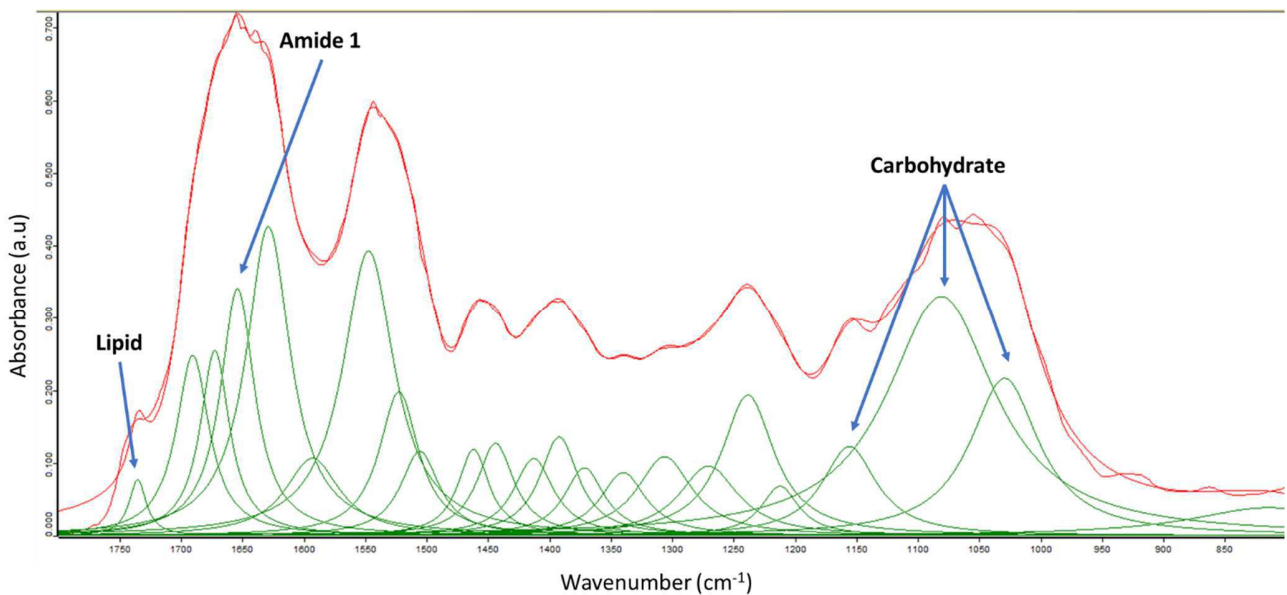
Figure 3.4: An FTIR spectrum (1800–800 cm^{-1}) with peak deconvolution representative of *Chlamydomonas reinhardtii* cells grown in aerobic condition at 15 °C.

The peaks that were used for this work were those at: 1650 cm^{-1} ("amide I", C=O of amides associated with protein), as proxy for protein; 1740 cm^{-1} (C=O of ester functional groups of triglycerides and phospholipids), used as proxy for lipid; as proxy for carbohydrate the sum of the integrals of the peaks at 1024 cm^{-1}, 1050 cm^{-1} and 1150 cm^{-1} (C-O-C of polysaccharides) was used (Giordano et al. 2001). The absorbance of the cell population deposited on a silicon window is influenced by thickness and unevenness of samples. For this reason, absolute quantification is not possible. In this thesis, relative quantification was used. Furthermore, based on the procedure described in Palmucci et al. (2011), semi-quantification of cell pools was conducted using protein as reference. It is worthwhile to stress the fact that this semi-quantification allows for the comparison of the same peak in different conditions, but does not allow to compare peaks at different wavenumbers.

3.6 Chlorophyll *a/b*

Chlorophyll amount was determined on samples containing from 5x10^5 to 7x10^6 cells. Cells were harvested by centrifugation at 3,000 g for either 5 minutes (for *C. reinhardtii*) or 3 minutes (for *D. tertiolecta*) (MPW 551e centrifuge, MPW MED INSTRUMENT, Warzlawa, Poland). The pellet was resuspended in 1 mL of 90 % (v /v) acetone and remained in 90 % acetone, in the dark and at 4 °C, for 1 hour or until no green pigment was visible. The samples were then centrifuged (3000 g for 5 or 3 minutes) to separate the water soluble phase and the cell fragments (pellet) from the acetone extract (supernatant).

Chlorophyll quantification was conducted with a spectrophotometer (Beckman Coulter, Bea, California, USA). Jeffrey and Humphrey (1975) equations were used:

$$\text{Chl } a \text{ (µg/ml)} = (11.93 \cdot A664) - (1.93 \cdot A647)$$
$$\text{Chl } b \text{ (µg/ml)} = (20.36 \cdot A647) - (5.5 \cdot A664)$$
$$\text{Chl TOT (µg/ml)} = \text{Chl } a + \text{Chl } b$$

Where Chl is Chlorophyll *a* or *b* and A is the absorbance at different wavelengths (nm).

3.7 Protein determination

The pellets remaining after chlorophyll extraction were used for protein quantification.
The protein content was determined according to Peterson (1977): the pellet was resuspended in 500 µl of a solution containing 1% SDS and 0.1 M NaOH. The samples were then whirl-mixed for at least 1 minute. Five hundred µl of freshly made "reagent A" were subsequently added. Reagent A contained equal volumes of Milli-Q water, 10% SDS, 0.8 M NaOH and CTC (CTC contained 0.1% $CuSO_4 \cdot 5H_2O$; 0.2% Na-K Tartrate; 10% Na_2CO_3; w/v). The samples were immediately vortexed and then incubated for 10 minutes at room temperature. Subsequently, 250 µl of freshly made "reagent B", containing 5 parts of Milli-Q water and 1 part of Folin-Ciocalteu (v/v), were added. After whirly-mixing, the samples were left for 30 minutes at room temperature and their absorbance was then measured spectrophotometrically at 750 nm by a Beckman DU 640 spectrophotometer (Beckman Coulter, Bea, California, USA). Milli-Q water was used as a blank. To calculate protein concentration, the absorbance of the samples was interpolated within a standard curve prepared with increasing amounts from 0 to 100 µg of Bovine Serum Albumin (BSA A-8022, SIGMA, St. Louis, MO, USA). The final volume of BSA samples was brought to a volume of 500 µl with a solution of 0.1 M NaOH. Reagent A and B were subsequently added in the BSA standards, as for the samples.

3.8 Elemental composition

The elemental composition of algal cells in different growth conditions were determined with an elemental analyzer ECS 4010 (Costech International S.p.A., Pioltello, Mi, Italy) for C and N, and with a Total Reflection X-ray Fluorescence (TXRF) spectrometer (Picofox S2, Bruker Nano GmbH, Berlin, Germany) for P, S, Cl, K, Ca, Mn, Fe and Zn.

Cells for the determination of C and N contents were collected by centrifugation at 1,000 g for 10 minutes, with a Biofuge fresco Heraeus (Kendro Laboratory Products, Osterode am Harz, Germany). After centrifugation, the pellets were washed twice with either 0.5 ammonium formate (*D. tertiolecta*) or deionized water (*C. reinhardtii*); this was necessary to get rid of the salts in the medium, which would otherwise have introduced an artifact in the weight of the samples (cells). The pellets were then dried in an oven at 80°C for 24 hours, or until the weight was stable. For each sample, 0.07-2.0 mg of dry weight were transferred into tin capsules. The capsules were then carefully closed. The capsules were weighed before and after their closure, in order to make sure that no sample had escaped from the capsules in the closing process. For analysis, empty tin capsules were used as blanks, while sulphanilamide (41,84% C; 16,27% N; 18,62% S; w/w) was used as a standard for the preparation of a

calibration curve. Standards were used every time a measurement was conducted to check for the retention time of the different elements; the calibration curve type was set as linear for N and quadratic for C. To facilitate the complete oxidation of samples and standards, a small amount of V_2O_5 was added. Before each working session, a "leak check" was performed to ensure that no gas leak occurred in the system.

During C and N determination, a carrier gas (He) circulates through an analytic circuit made of a combustion reactor, a gas chromatographic (GS) separation column (Poropak Q/S 0/80 mesh) and a Thermal Conductivity Detector (TDC). With a presetting time, samples, blanks and standards, were one by one dropped into the combustion reactor, contained WO_3 as an oxidation catalyst and copper wires as reduction catalyst, where they were combusted at 980 °C in the presence of saturating O_2. Samples reacted with O_2 and all C is converted to CO_2, all N to NOx; the copper wires converted NOx into N_2. The gases containing the elements were transported by the carrier gas into a water trap column filled with magnesium perchlorate, where the water generated in the combustion was trapped. Finally the gases entered the GC separation column and determined by the TCD. The EAS 4010 clarity (DataApex Ltd., Prague, Czech Republic) compares the elemental peak to sulphanilamide and generates a report for each element; the abundance of C and N were normalized over the mg of dry matter used for the analysis.

In order to have the best possible signal to noise ratio, for the samples with a weight lower than 1 mg the TCD control panel was set as follows;
<div align="center">
Range switch = High (x10)

Gain control = 1
</div>

Instead, when the sample weight was more than 1 mg the TCD control panel was set as follows:
<div align="center">
Range switch = Low (x1)

Gain control = 3
</div>

The smallest possible amount of oxygen was used during the combustion of the sample. The amount of O_2 injected in the combustion reactor was set on "μ = 5 ml of O_2 for sample" for samples with a weight lower than 1 mg, while for the analysis of samples with weight higher than 1 mg the amount of O_2 injected was increased and set to "Semi-μ = 10 ml of O_2 for sample".

The flow of He in the system was 100 ml·min^{-1}; the O_2 flow into the combustion reactor was 30 ml·min^{-1}.

The following time cycle parameters were adopted:
- Autosampler is activated and the sample dropped into the combustion reactor;
- 12 of sample delay = It is the time for the samples to arrive in the combustion reactor. The samples should arrive almost 2 seconds before O_2 flow;
- 20 s of sample stop = it determines the time of sample combustions;
- 40 s of Oxy stop = time waiting for electrovalves from activating of autosampler before starting to refill the instrument of oxygen volume needed for the next samples;
- 70 s of run time = it is the time from the beginning of a cycle to the end of it.

For the analysis with TXRF, were prepared as for the C: N analyses. In the end, however, the samples of both species were resuspended, at a concentration of $8 \cdot 10^6$ cells·ml^{-1}, in 1 mL of Milli-Q water. The analysis was done following the protocol of Fanesi et al. (2013).

To allow an absolute quantification, 5 µl (5 mg·ml^{-1}) of a gallium standard solution (Sigma-Aldrich Co. LLC, Saint Louis, United States) were added to each sample as an internal standard. An aliquot of 10 µL of sample was deposited on a quartz sample carrier (Bruker AXS Microanalysis GmbH, Berlin, Germany) and dehydrated on a hot plate prior to measurement. A Picofox S2 spectrometer (Bruker AXS Microanalysis GmbH) was used to measure the X-ray fluorescence of the various elements. The elements determination was performed with a measurement time of 1000 s. The software SPECTRA5.3 (Bruker AXS Microanalysis GmbH, Berlin, Germany) was used to acquire and analyze the spectra. In order to correct for the natural drift of the detector, which may cause a change in the energy to channel ratio, a recalibration of the energy to channel ratio by gain correction was performed prior to each analysis. One µg of arsenic was positioned on quartz sample carriers used for this purpose. Only the quartz sample carriers that had been previously checked and considered clean were used for the analyses.

The quartz sample carriers were cleaned by washing them with Milli-Q water; then, they were left to sit in water for 5 minutes at 70 °C and then treated for 10 minutes at 70 °C in a solution with the detergent RBS 50X (5% v/v - Sigma-Aldrich Co. LLC, Saint Louis, United States). After this, the sample carriers were washed with Milli-Q water and let sit for 2 hours in a 20% (v/v) solution of nitric acid, at room temperature. Finally, the sample holders were put in an M 1000-VF oven (Instrument Bernareggio, Bernareggio, Mi, Italy) at 60 °C to dry. Before the measurement, each disc was checked with the TXRF spectrometer for 60 seconds, in order to ensure that they were not contaminated; if no element had an abundance higher than the background noise, the quartz sample carriers were used.

3.9 Chlorophyll fluorescence: maximum PSII quantum yield (Fv/Fm)

Photosynthetic efficiency was measured with an AquaPen-C AP-C 100 (Photon Systems Instruments, Brno, Czech Republic). Cells ($1 \cdot 10^6$ cells) for photosynthetic efficiency analysis were collected in a 1.5 ml tube and were kept in the dark for 20 minutes before being analysed. The maximum quantum yield at PSII was measured in dark-adapted cells by providing a blue light (455 nm) to excite chlorophyll.

F_v / F_m was calculated according to the following equation:

$$F_v / F_m = (F_m - F_0) / F_m$$

Where Fm is the maximal fluorescence yield observed in dark-adapted cells after stimulation with a saturating light pulse (3000 µmol photons·m^{-2}·s^{-1}); Measuring Light – a weak measuring light (0.15 mmol photons m^{-2} s^{-1}) that induces fluorescence but not photosynthesis. F0 is the fluorescence yield measured in dark-adapted sample when all PSII reaction centers are open and it was measured with a measuring light (0.045 µmol photons·m^{-2}·s^{-1}).
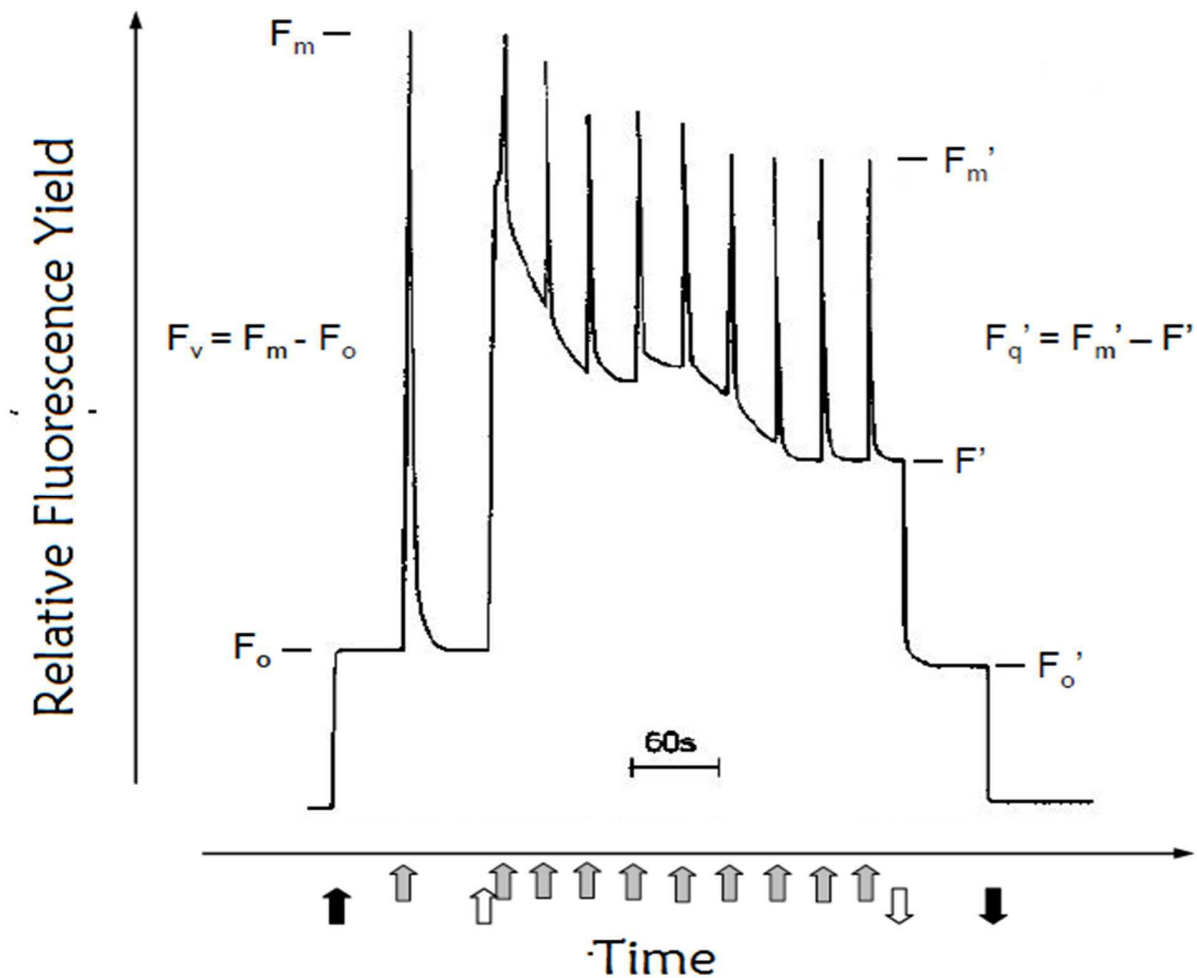
Figure 3.5: Analysis of variable fluorescence y saturation pulse method. Upward arrow = light on; downward arrow = light off. White arrows: actinic light; grey arrows: application of a short pulse of saturating light; black arrow: activation of non-actinic measuring light (Schreiber et al. 1986 modified from Büchel and Wilhelm 1993). F_o = fluorescence dark-adapted sample; F_m = maximal fluorescence in dark-adapted sample after application of saturating light pulse; F_v = variable fluorescence; F_m' = maximum fluorescence yield in illuminated sample; F' = fluorescence in illuminated sample; F_0' = minimal fluorescence yield in non dark-adapted sample.

3.10 RNA extraction, cDNA synthesis and real-time PCR

Total RNA was extracted from a cells suspension of *C. reinhardtii* containing approximately $4 \cdot 10^7$ cells, using th e Eurogold TriFast kit (Euroclone SPA, Pero, Italy). The cells pellet was harvested in a 15 ml tube by centrifugation (3500 g, 5 minutes) with a MPW 551e centrifuge (MPW MED INSTRUMENT, Warsaw, Poland). The supernatant was discarded and 1 ml of TriFast lysis solution was added, in order to facilitate the cells lysis; ten mg of 425-600 µm glass beads were also added (Sigma-Aldrich Co. LLC, Saint Louis, USA). The sample was then transferred to a 2 ml tube and it was whirly mixed for 30 seconds; subsequently, the sample was incubated for 5 minutes at room temperature. At the end of the 5 minutes, 0.2 ml of chloroform were added and the solution was energetically mixed by hand for 20 seconds and then incubated at room temperature for 10 minutes. The Eurogold TriFast / chloroform

solution was centrifuged at 12000 x g for 20 minutes at 4 °C with a Biofuge fresco Heraeus (Kendro Laboratory Products, Osterode am Harz, Germany). The resulting aqueous phase was transferred to a new 2 ml tube, and 0.5 ml of Isopropanol were added. The aqueous phase/ Isopropanol mix was kept at 4°C for 15 minutes and then centrifuged at 12.000 x g for 10 minutes at 4°C. The supernatant was carefully removed and 1 ml of 75% ethanol was added to the pellet.

The samples was centrifuged again at 7500 g for 8 minutes at 4°. The ethanol was removed with a pipette and the RNA pellet was air-dried, for about 5 minutes. The dry RNA pellet was resuspended in 20-40 µl of RNase-free water and whirly-mixed for 2 seconds. The RNA resuspended in water was immediately put on ice or stored at -80°C for further analyses.

To remove genomic DNA, the extract was treated with RNase-free DNase I (Euroclone SPA, Pero, Italy), as described by the manufacturer. The concentration of RNA extracted was assessed using a nanophotometer (P330 Implen GmbH, Munich, Germany) at a wavelength of 260 nm. RNA integrity was checked by horizontal electrophoresis in a minisub cell GT box (Bio-Rad, Hercules, California, USA). The electrophoretic migration was carried out at 100 volts for 30 minutes in 1 % agarose (Sigma-Aldrich Co. LLC, Saint-Louis, USA) gels (1 g of molecular biology grade agarose in 100 ml of Tris-Acetate-EDTA buffer, TAE). Five µl of EuroSafe (Euroclone SPA, Pero, Italy) in 100 ml of 1% TAE (4.84 g/l TRIS + 0.02% 0,5 M EDTA at 8 pH + 0.1142% of glacial acetic acid in RNA-free Milli-Q water) were used as fluorescent RNA intercalant; a TFX-20 M UV transilluminator (Vilber Lourmat, Marne-la-vallée, France) was used to detect the fluorescence. The samples for the electrophoresis were prepared according to RNA concentration in the samples, one volume with 0.4 ng of total RNA mixed with 0.5 volume of gel loading Solution (Sigma-Aldrich Co. LLC, Saint Louis, Unite State) and RNase-free Milli-Q water was added to make a final volume of 20 µl.

The complementary DNA (cDNA) was synthesized by retrotranscriptase (RT) reaction carried out in a thermocycler. RT was performed by 500 ng of total RNA, 4 µl of 5X PrimerScript Buffer, 1 µl of PrimerScript RT Enzyme Mix I, 1 µl of Oligo dT Primer, 1 µl of Random 6 mers; the final volume was brought to 20 µL with RNase-free Milli-Q water. The PrimeScript kit was manufactured by Takara Holdings Inc. Kyoto, Japan. The PCR conditions were: 37 °C for 15 min, 85 °C for 5 sec. Before running the real-time PCRs, for each gene studied, a PCR was performed with both forward and reverse primers, in order to check the presence of genomic DNA in the cDNA solution. The final amplification was loaded on a 2% agarose gel (2% gel allow having a good separating resolution even for small fragments of DNA) with EuroSafe, and run together with the samples, and a molecular weight ladder (Sigma-Aldrich Co. LLC, Saint Louis, USA). For each gene, two primers were designed to be in two distinct exons adjacent to an intron; they allowed to amplify segments of known length; in addition, through the molecular weight ladder, it was possible to determine the length (molecular weight) of the amplified segments. If the amplification mix contained cDNA and DNA, two bands would appear on the gel after the electrophoretic run: a longer band for the genomic DNA containing both intron and exons in the amplified fragment, one band of lower molecular weight corresponding to the cDNA, which did not contain the intron. If only cDNA was present, only one band would appear. In all runs, no genomic DNA band was observed. Both reverse transcription and PCR were performed with a Biometra T3 Thermocycler (Biometra GmBH, Göttingen, Germany). The primers for gene analysis were specific for *C. reinhardtii*; according to Aksoy et al. 2013, *CBLP* gene (G-protein β-subunit-like protein) was used as housekeeping gene (Table 3.4).

Table 3.4: List of primers used in this work. The primers for the PCR are shown in the 5'- 3' orientation.

Gene	Primer sequnce	Reference
ACK 1	CAACTGCGTGTTGAAGGCTA	Catalanotti et al. 2012
	AAGGTGCTCGACACGTTCTC	Catalanotti et al. 2012
ARS 1	GTACTGCCGCGTGCGTGATTCC	
	CCTAAACATTTGGCTCCGCAGTCC	
CBLP	CTTCTCGCCCATGACCAC	Aksoy et al. 2013
	CCCACCAGGTTGTTCTTCAG	Aksoy et al. 2013
ECP76	CCTCGCTCTCCTCGCTGCTG	Aksoy et al. 2013
	CGGCCGCCTTGGGTAATTGC	Aksoy et al. 2013
HYDA 1	CGGGAACGTGGGTAGCATTTAGG	Catalanotti et al. 2012
	CGCCAAGGGTCCACATCAGAGT	Catalanotti et al. 2012
PFR 1	CGCGCAGGGCACAATCACAC	Catalanotti et al. 2012
	ATCAGACGGCGCCACAAACACA	Catalanotti et al. 2012
SLT 1	ACGGGTTCTTCGAGCGAATTGC	Aksoy et al. 2013
	CGACTGCTTACGCAACAATCTTGG	Aksoy et al. 2013
SLT 2	TTCTTCGCCACCGATGAGC	Aksoy et al. 2013
	GTACGGAGTTCCTTACGCGC	Aksoy et al. 2013
SULTR 2	ACGTGGCATGCAGCTCAT	Aksoy et al. 2013
	CTTGCCACTTTGCCAGGT	Aksoy et al. 2013

The genes analyzed involved in S metabolism (*ARS 1*, *ECP 76*, *SLT1*, *SLT 2* and *SULTR 2*) or in anaerobic metabolism (ACK, *HYDA 1* and *PFR 1*). Arylsulfatase (*ARS1*) is a periplasmic protein released in growth medium during S-deprivation condition (de Hostos 1988 and references therein); *SLT1*, *SLT2* and *SULTR2* are high-affinity transporters for sulfate (Yildiz et al. 1994, Pootakham el al. 2010); ECP76 is a polypeptide that contains almost no S-containing amino acids, *ECP76* is used to replace S-rich amino acids of cell wall protein during S-starvation and thus the S of amino acids can be recycled (Takahashi et al. 2001). Regarding the genes involved in anaerobic metabolism refer to the chapter 2.2.

A preliminary real-time PCR was performed for each pair of primers to check annealing temperature and enzymatic efficiency (Ef) in working condition. For all couple of primes, the best annealing temperature turned out to be 60 °C. To test the real-time PCR efficiency, serial dilutions of cDNA, each in duplicate, were amplified using the specific primers for the target genes, only a Efs of 100% ± 10% were accepted. A specific temperature protocol was used for real-time PCR: the preincubation was conducted at 95 °C for 5 min; it was followed by 50 cycles of denaturation at 95° C for 10 s; annealing was allowed to take place at 60 °C for 20 s; elongation occurred at 72 °C for 30 s; one final extension was added at 72 °C for 5 min.

The RT-PCRs were performed with IQ5 real-time PCR (Bio-Rad, Hercules, California, USA). Each sample was prepared in a final volume of 10 μl and was mixed with 5 μl of ITAQ UniverSyber Green master mix

(Bio-Rad, Hercules, California, USA), 0.2 µl of 10 µM forward primer, 0.2 µl of 10 µM reverse primer, 1 µl of cDNA (25 ng/µl), and 3.6 µl of RNase-free water.

Housekeeping gene expression was used to standardize the results by eliminating variations in mRNA and cDNA quantity and quality, due to a different amount of impurities (e.g. DNA, phenols, protein) that may have remained in the sample cDNA. The data was analyzed by IQ5 optical system software version 2.0 (Bio-Rad, Hercules, California, USA). The analyses of the denaturation curves for the reactions showed a single peak in all cases and no amplification product and primer-dimer formation were observed in the controls. To calculate the relative amount of gene expression, the $\Delta\Delta Ct$ method was used (Pfaffl 2001):

$$\Delta Ct_1 = Ct \ (Target \ A \ \text{-treated}) - Ct \ (Ref \ B \ \text{- treated})$$
$$\Delta Ct_2 = Ct \ (Target \ A \ \text{- control}) - Ct \ (Ref \ B \ \text{- control})$$
$$\Delta\Delta Ct = \Delta Ct_1 \ (treated) - \Delta Ct_2 \ (control)$$
$$Normalized \ target \ gene \ expression \ level = 2\Delta\Delta Ct$$

Where Ct is the first cycle in which it was possible to detect a significant increase of PCR reaction products. Ct was calculated by the IQ5 software.

3.11 ATP measurement

ENLITEN ATP Assay System (Promega Corporation, Madison Wisconsin, USA) was used for the quantitative detection of adenosine 5'-triphosphate (ATP). An amount from 10^{-10} to 10^{-16} moles of ATP could be detected through the following process:

$$ATP + D\text{-Luciferin} + O_2 \rightarrow Oxyluciferin + ADP + PPi + CO_2 + Light \ (560nm)$$

The reaction is catalyzed by a recombinant. When ATP is the limiting component in the luciferase reaction, the intensity of emitted light is proportional to ATP concentration. The fluorescence intensity was measured with the Infinite F200PRO luminometer (Tecan Trading AG, Männedorf, Switzerland). The luciferine (substrate) is provided in dehydrated form and was therefore rehydrated in the "reconstitution buffer", the mix produced was rL/L reagent; the resulting solution was gently swirled and then left at room temperature for 1 hour. About $2\cdot10^7$ cells were collected by centrifugation (15.000 x g, 10 minutes); the pellet was washed once with Milli-Q water and then centrifuged at a higher speed for a shorter time (35,000 x g, 2 minutes), in order to reduce contaminations by salts. In order to reduce the degradation of ATP and the change in the concentration of the metabolite, the dry pellet was immediately frozen at -20 ° C and stored at -80 ° C until the day of the analysis, which was performed no more than a week after pellet preparation (Fernie et al. 2011). As suggested by Lapaille et al. (2010), the defrost pellet was resuspended in 300 µl of Milli-Q water and 15 µl of 1 M $HClO_4$, with 5 mg of 425-600 µm glass beads (Sigma-Aldrich Co. LLC, Saint Louis, USA); this mix was vortexed for 20', in order to break the cell wall and extract the ATP; 485 µl of 1M $NaHCO_3$ were added to the solution to neutralize $HClO_4$. The samples were then subjected to a fast centrifugation (35000 g, 2 minutes at 4°C); the supernatant was collected and, if needed, its pH was adjusted to 7.75 (pH optimum for the luciferase activity) with 1M HCl. All steps were performed on ice. A 96-wells plate was used to perform the analysis; in each well, 100 µl of rL/L reagent and 10 µl of supernatant were added. Each plate contained

an ATP standard curve. The ATP standard (10^{-7} M) was diluted with ATP-free water (both provided in the ENLITEN ATP Kit), to obtain serial dilution from 10^{-7} M to 10^{-13} M. The fluorescence was immediately detected.

3.12 Statistics

All experiments were conducted on three distinct algal cultures (biological replicates). The statistical significance of mean differences was determined by Two-way ANOVA followed by Fisher's LSD test, using GraphPad Prism 5 (San Diego, California, USA); the significance level was set at $p < 0.05$. The term 'post hoc' means that the groups to be compared are selected after the experiment; for this reason, the Fisher's LSD test does not qualify as a "post hoc". Fisher's LSD test is a set of individual t-test between all experimental data groups performed by multiple comparison tests. Multiple comparison tests consist in several comparisons conducted at the same time; in this case, the comparisons are called "non-orthogonal" because at least one sample value is used for at least two comparisons test. Normally, with the post hoc tests, the significance level is applied to the whole set of comparisons (familywise error rate), but with Fisher's LSD test, the significance level applies only to one comparison at a time (no correction for multiple comparisons); we refer to this process as a "per-comparison error rate".

4. RESULTS

4.1 Impact of O$_2$ concentration on the acclimation potential of *C. reinhardtii* to S starvation

C. reinhardtii gene expression was evaluated by real-time PCR 0, 4 and 6 hours (h) after the cells were transferred to S-free medium. Gene expression changed in response to S-starvation in both aerobic and anaerobic conditions (Figure. 4.1 and Figure 4.2). At both oxygen concentrations, S-starvation induced gene expression of all genes involved in S-uptake, which instead were not appreciably expressed in S-replete conditions (Figure 4.1). In aerobic conditions, each gene had a specific trend: *ARS1* increased in 4 hours and then it decreased; *ECP76* expression increased until 6 hours; the expression of *SLT1* and *SL2* increased until hour 4 and then remained stable while *SULTR2* increased only after 6 hours. In anaerobic condition, the expression of *ARS1, ECP76* and *SLT2* increased over the whole experimental time; expression of *SLT1* after 4 h was similar that at 6 h. *SULTR2 expression decreased after 4 h.* The expression of the anaerobic markers *ACK1*, *HYDA1*, *PFR1* was modulated by the presence or absence of both O$_2$ and S (Figure 4.2). Only *HYDA1* expression did not increase in aerobic condition. In both S conditions, *ACK1* and *PFR1* increased their expression in aerobic condition already at 4 hours, but only in S-starvation. In anaerobic condition, S-starvation was necessary to induce *ACK1* and *PFR1 expression*; S was instead needed for the expresison of *HYDA1* (6 h).
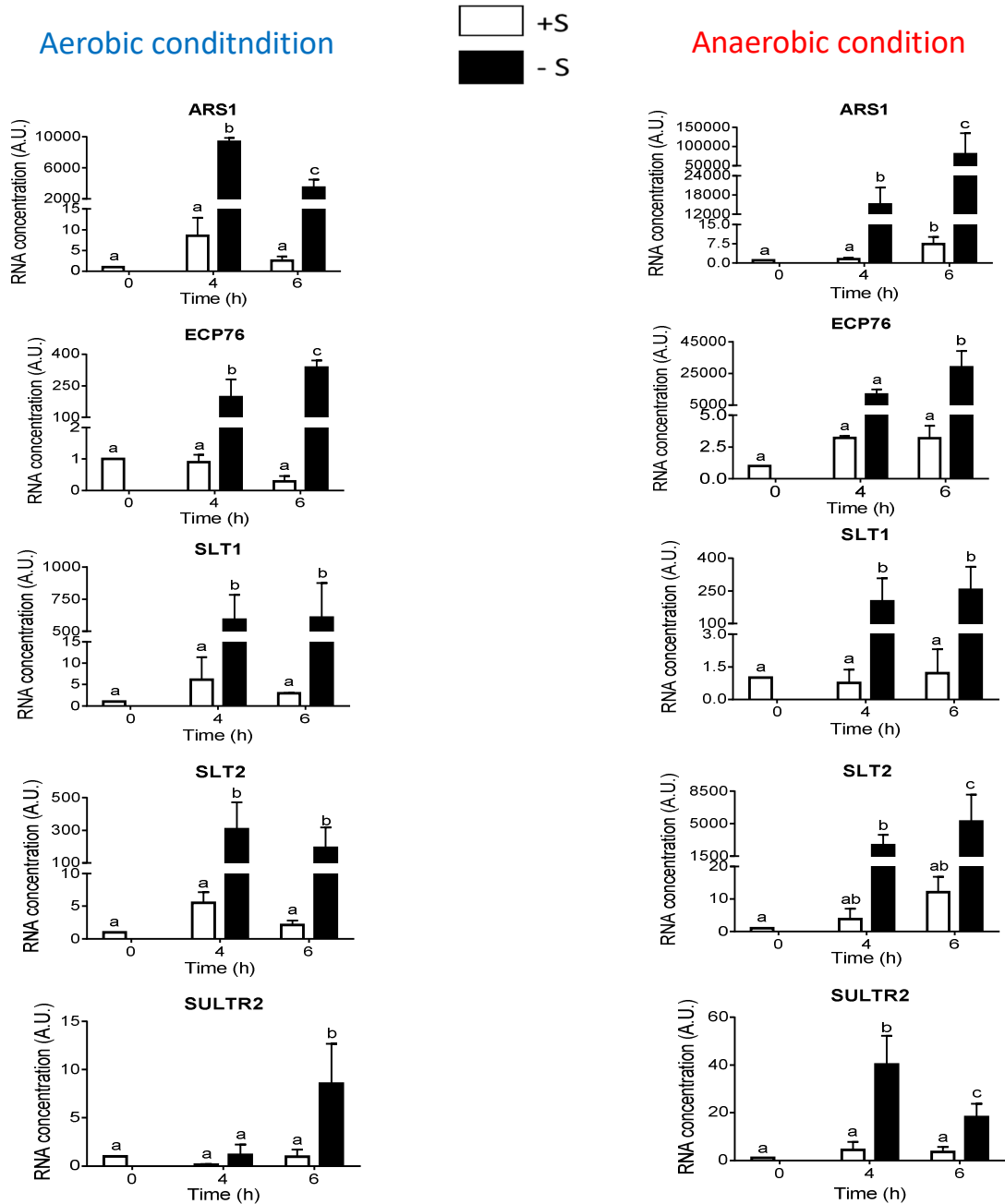
Figure 4.1: Relative changes in mRNA transcript level of genes involved in S-uptake. *ARS1* = extracellular arylsulfatase 1; *ECP76* = extracellular polypeptides 76; *SLT1* = SAC1-like transporter 1; *SLT2* = SAC1-like transporter 2; *SULTR2* = Sulfate transporter 2*; CBLP* = G-protein β-subunit-like protein. *ARS1, ECP76, SLT1, SLT2, SULTR2* expressions were normalized against *CBLP* expression measured in respective oxygen condition. For this reason, the gene expressions measured in an oxygen condition cannot be compared with the other one. RNA samples were collected 0, 4 and 6 hours (h) after the start of perturbation (S-derivation). Right column is for samples analyzed in aerobic condition, left column is for samples analyzed in anaerobic condition. White and black bars represent the gene expression in, respectively, cells grown with S and cells grown in S-starvation. Error bars indicate mean ± SD; different letters on bars indicate significant differences (p < 0.05) among sampling mean values (two-way ANOVA and Fisher's LSD test, N=3).
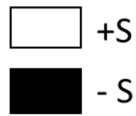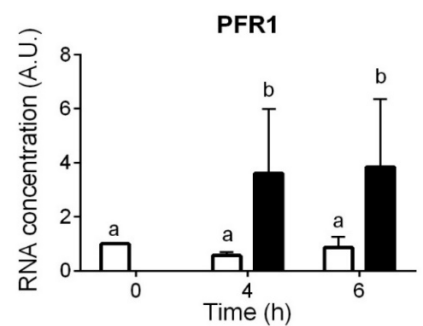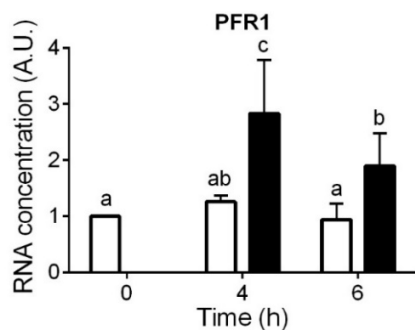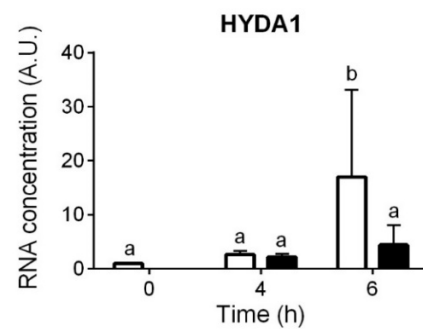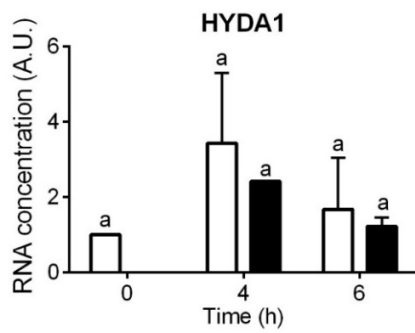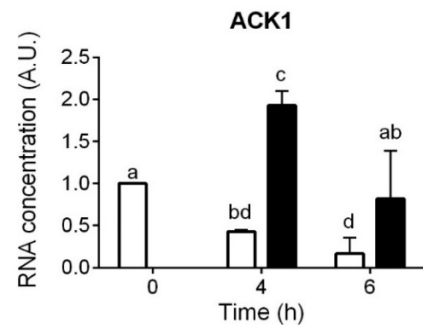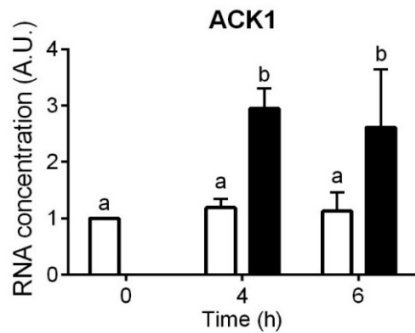
Figure 4.2: Relative changes in the mRNA transcript level of genes involved in anaerobic metabolism. *ACK1* = Acetate kinase 1; *HYDA1* = [Fe-Fe]-hydrogenase isoform 1; *PFR1* = pyruvate-ferredoxin-oxidoreductase 1. *ACK1, HYDA1, PFR1* expressions were normalized against *CBLP* expression measured in respective oxygen condition. For this reason, the gene expressions measured in an oxygen condition cannot be compared with the other one. mRNA samples were collected at 0, 4 and 6 hours (h) after the start of S-starvation. THE results for aerobic conditions are shown in the left columns; those for the cells cultured in anaerobiosis are shown on the right. White and black bars represent the gene expression in, respectively, cells grown with S and cells grown in S-starvation. The error bars indicate the standard deviations. Different letters on the bars indicate significant differences (p < 0.05) among mean values (two-way ANOVA and Fisher's LSD test, N=3).

4.2 Impact of temperature variation on *C. reinhardtii* and *D. tertiolecta* cell composition in aerobic condition

4.2.1 ATP measurement

For both examined species, free ATP cell content was more affected by the duration of perturbation than by the difference in irradiance. Only after 7 days and only in *D. tertiolecta* the two irradiances had an effect on ATP content, with the ATP cell content being higher in LL cells than in HL cells (Figure 4.3 b). For both species, free ATP content increased over time in response to the change in growth temperature, but with different trends. For both species, free ATP content were not correlated with cell number (Figure 4.4 a and c).

In *C. reinhardtii*, after 4 days, ATP content was two orders of magnitude higher than on day 0, but after 7 days its value decreased drastically. These trends were irrespective of the irradiance used for growth (Figure 4.3 a).

In *D. tertiolecta*, regardless of irradiance, ATP content continued to increase until the seventh day, when its value was two orders of magnitude higher than on day 0 (Figure 4.3 b).
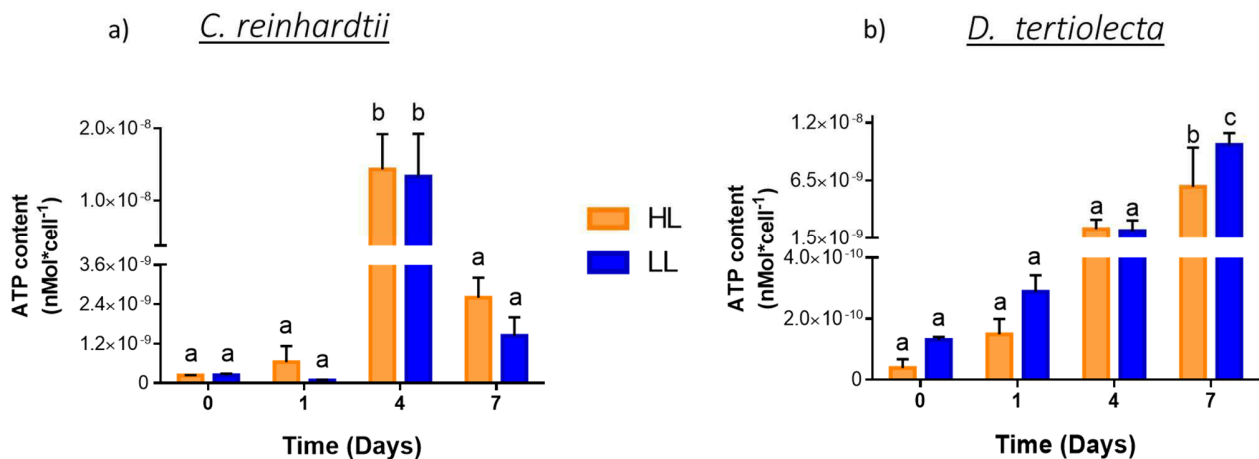
Figure 4.3: ATP content in *C. reinhardtii* (a) and *D. tertiolecta* (b) in aerobic condition, at two different irradiances; High light (HL – orange bars) and Low light (LL – blue bars). On day 0 the growth temperature was changed from 15 °C to 30 °C. Different letters indicate statistically different mean values ($p < 0.05$; 2-ways ANOVA and Fisher's LSD test). The error bars show the standard deviations.

4.2.2 Cell number, cell volume

Cells number and volume were measured with an automatic cells counter before and 1, 4 and 7 days after the application of the perturbation, i.e. the change of growth temperature from 15 °C to 30 °C. Cell number values were normalized taking into account the dilution rate.

In *C. reinhardtii*, the change of growth temperature, especially at HL, induced a strong increase of cells number after 24 hours (T1); this increase was not maintained over time: after 7 days, in fact, the cells number was similar to that on day 0. At LL, 24 hours of perturbation induced a significant increase of cell number compared to day 0 but it was lower than the value at HL. Subsequently, the cell number

decreased until reaching, after 4 days, values similar to those on day 0 (Figure 4.4 a). At HL the temperature had no effect on cell volume, while with LL we can observe a decrease of cell volume only in the central samplings, T1 and T4 (Figure 4.4 b).

In *D. tertiolecta* different irradiances produced a significant effect on the cell number only on day 7, with cell number at LL higher than at HL; growth temperature was the main player in modulating the cell number, which increased oneday one and then decreased 4 days after the onset of the perturbation (Figure 4.4 c). Cell volume was not affected by irradiance and showed a slight decline (around 20%) over time (Figure 4.4 d).
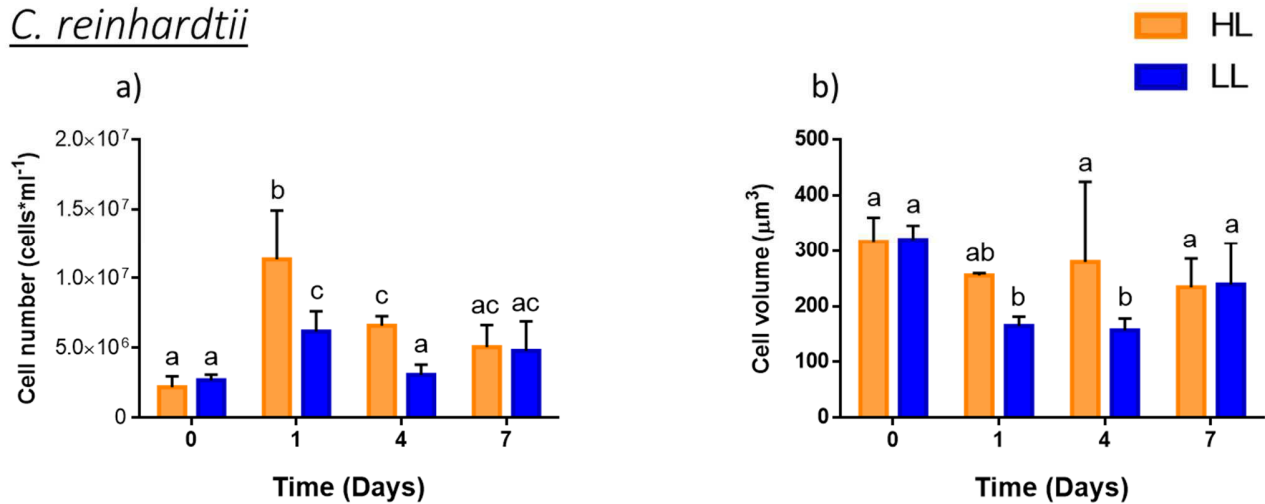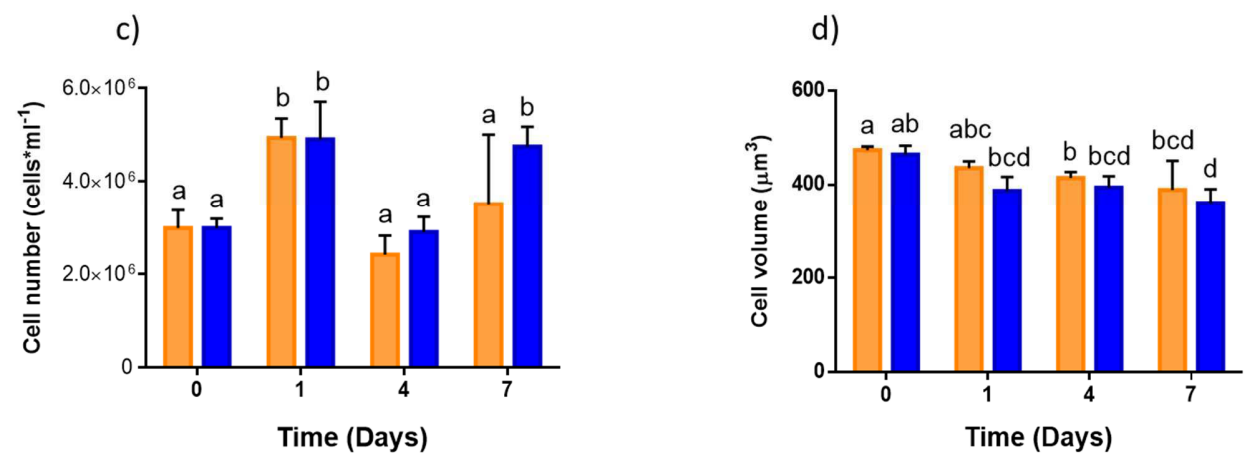
Figure 4.4: Cell number, and cell volume of *C. reinhardtii* (a and b) and *D. tertiolecta* (c and d). For both species, the results are related to aerobic condition at two different irradiances; High light (HL – orange bars) and Low light (LL – blue bars). On day 0 the cells were grown at 15 °C while on days 1, 4 and 7 cells were grown at 30 °C. Different letters indicate statistically different mean values ($p < 0.05$; 2-ways ANOVA and Fisher's LSD test). The error bars show the standard deviations (N=3).

4.2.3 Cell dry weight and ash weight

The dry weight of *C. reinhardtii* cells did not change significantly as a function of time and irradiance, with the only exception of day 4, when the dry weight was higher at LL than at HL (Figure 4.5 a). The amount of *C. reinhardtii* culture that was collected for the analysis was not enough to calculate the ash weight. In *D. tertiolecta* dry weight and ash weight followed the same trends, with an increase up to day 4 followed by a decline on day 7 (Figure 4.5 b, c). Different irradiances did not have any significant effect on both dry weight and ash weight. Consequently, the ratio between dry weight and ash weight did not show any change (Figure 4.5 d).
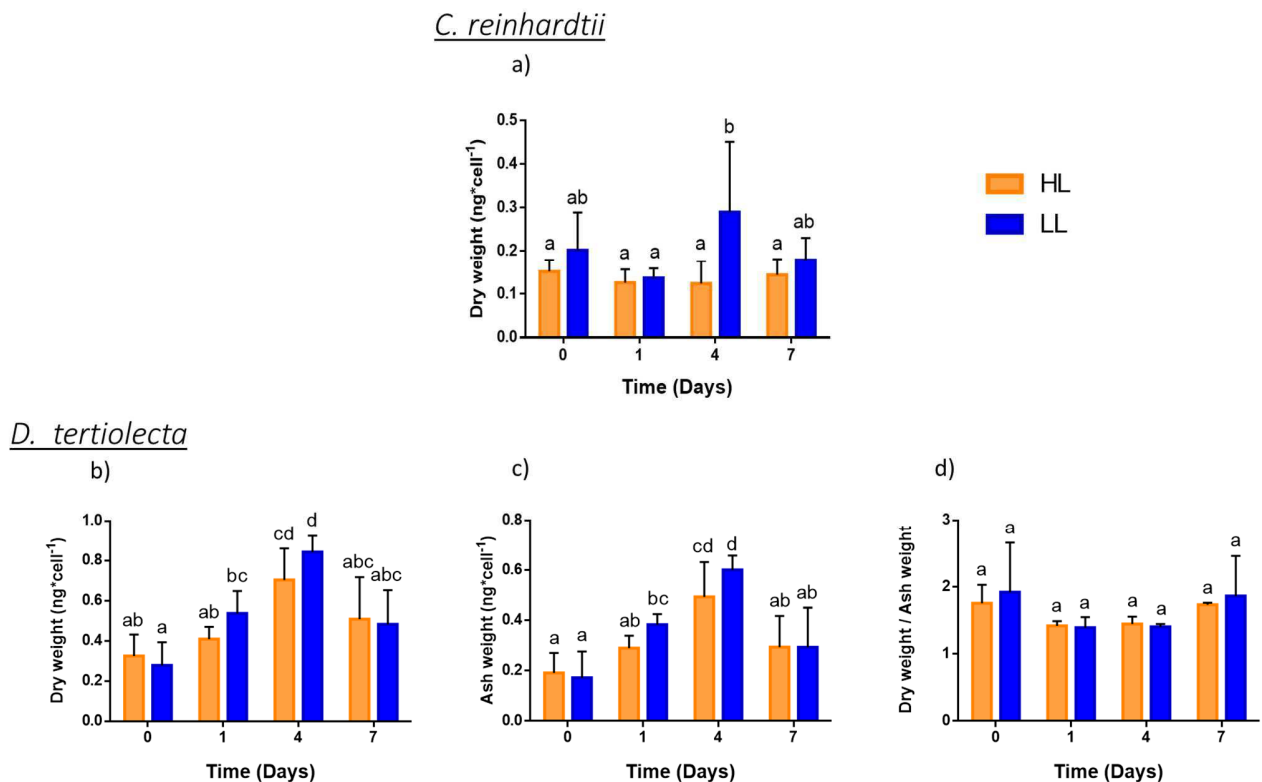
Figure 4.5: Dry weight, ash weight and dry weight/ash weight ratio of *C. reinhardtii* (a) and *D. tertiolecta* (b, c and d) grown at High light (HL – orange bars) and Low light (LL – blue bars) and subjected to a change of growth temperature from 15 °C to 30 °C. Different letters indicate statistically different mean values (p < 0.05; 2-ways ANOVA and Fisher's LSD test). The error bars show the standard deviations (N=3).

4.2.4 Chlorophyll fluorescence: maximum quantum yield (Fv/Fm)

In both *C. reinhardtii* and *D. tertiolecta*, irradiances and perturbation of temperature influenced the photosynthetic maximum quantum yield. The quantum yield of the two species was similar at HL, but at LL the Fv/Fm of *C. reinhardtii* was higher than that of *D. tertiolecta*. In both species, 4 days after the onset of the perturbation, the photosynthetic efficiency was higher at LL than at HL. In *C. reinhardtii* at

HL, the photosynthetic efficiency on day 1 was not significantly different from that at day 0, while it was higher than on day 4 and day 7 (Figure 4.6 a). In *D. tertiolecta* cultured at HL the maximum quantum yield was higher at T1 than at the other sampling times. At LL, instead, the Fv/Fm remained constant over time (Figure 4.6 b).
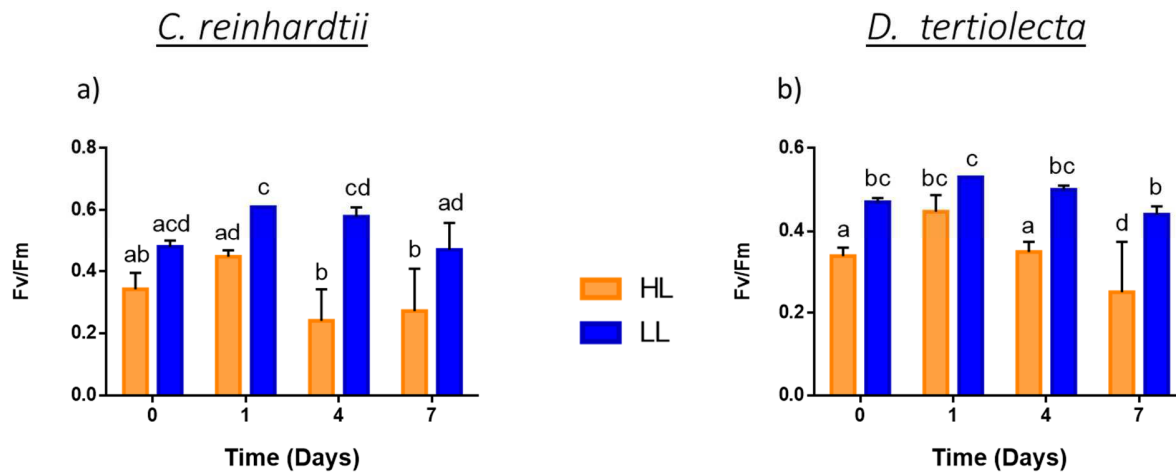
Figure 4.6: Photosynthetic efficiency in *C. reinhardtii* (a) and *D. tertiolecta* (b). For both species, the results are related to aerobic condition at two different irradiances; High light (HL – orange bars) and Low light (LL – blue bars). On day 0 the cells were grown at 15 °C while on days 1, 4 and 7 days cells were grown at 30 °C. Different letters indicate statistically different mean values ($p < 0.05$; 2-ways ANOVA and Fisher's LSD test). The error bars show the standard deviations (N=3).

4.2.5 Chlorophyll *a/b*

In both *C. reinhardtii* and *D. tertiolecta*, chlorophyll *a* was more abundant than chlorophyll *b*; *D. tertiolecta* had about 3 times more chlorophyll per cell than *C. reinhardtii*.
 In *C. reinhardtii*, the chlorophyll *a* concentration at HL increased significantly on day 7; at LL, chl a decreased after 1 day at high temperature, and the decrease continued over the experimental period. On day 0, chlorophyll *a* was two times higher at LL than at HL: at LL, at the end of the experiment, it was about 3 times lower than at HL (Figure 4.7 a). Chlorophyll *b* abundance had different fluctuations but these were not generally significant, with two exceptions: in *C. reinhardtii* cells cultured at LL, the chlorophyll *b* was higher at T4 than at T7 –(Figure 4.7 b). Total chlorophylls in *C. reinhardtii* followed the same trend as chlorophyll *a*, and at HL its value was constant until the fourth day after perturbation and then it increased significantly; at LL, instead, the total chlorophyll cell content was three times lower on day 7, compared to day 0. (Figure 4.7 c).
In *D. tertiolecta* the change of chlorophyll *a*, chlorophyll *b* and total chlorophylls values followed the same trends; the chlorophylls abundance increased after one day of perturbation and then it went back to the initial value (Figure 4.7 d, e, f). With both irradiances, the increase of chlorophylls on day 1 was three times higher compared to the other days (Figure 4.7 f). Only on day 1, the two irradiances produced different effects on chlorophylls, with chlorophyll *a*, chlorophyll *b* and so, the total chlorophylls higher at LL rather than HL (Figure 4.7 d, e, f). In *D. tertiolecta* after 4 days of perturbation, it was possible to observe the bleaching of cultures that grew at HL; this did not happen in cultures grown at LL. The bleaching continued until the end of the experiments (Figure 4.8).
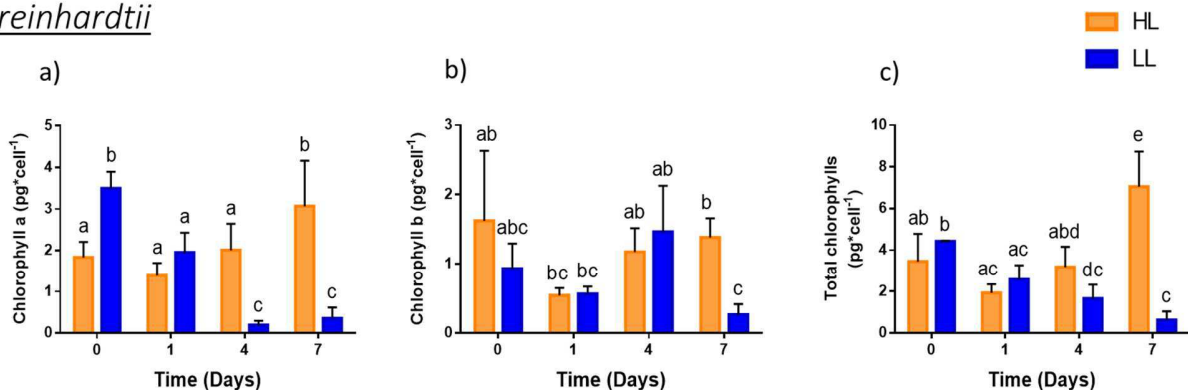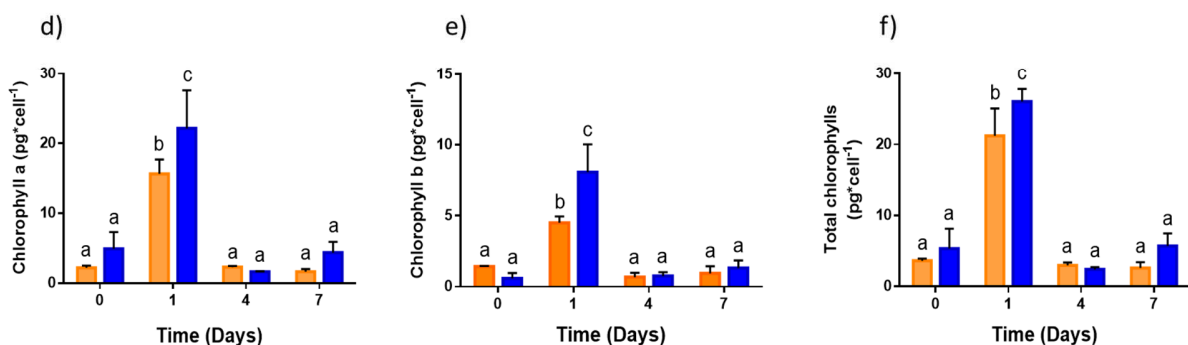
Figure 4.7: Chlorophyll *a/b* and total chlorophylls in *C. reinhardtii* (a, b and c) and *D. tertiolecta* (d, e and f). For both species, the results are related to aerobic condition at two different irradiances; High light (HL – orange bars) and Low light (LL – blue bars). On day 0 the cells were grown at 15 °C while on days 1, 4 and 7 days cells were grown at 30 °C. Different letters indicate statistically different mean values ($p < 0.05$; 2-ways ANOVA and Fisher's LSD test). The error bars show the standard deviations (N=3).
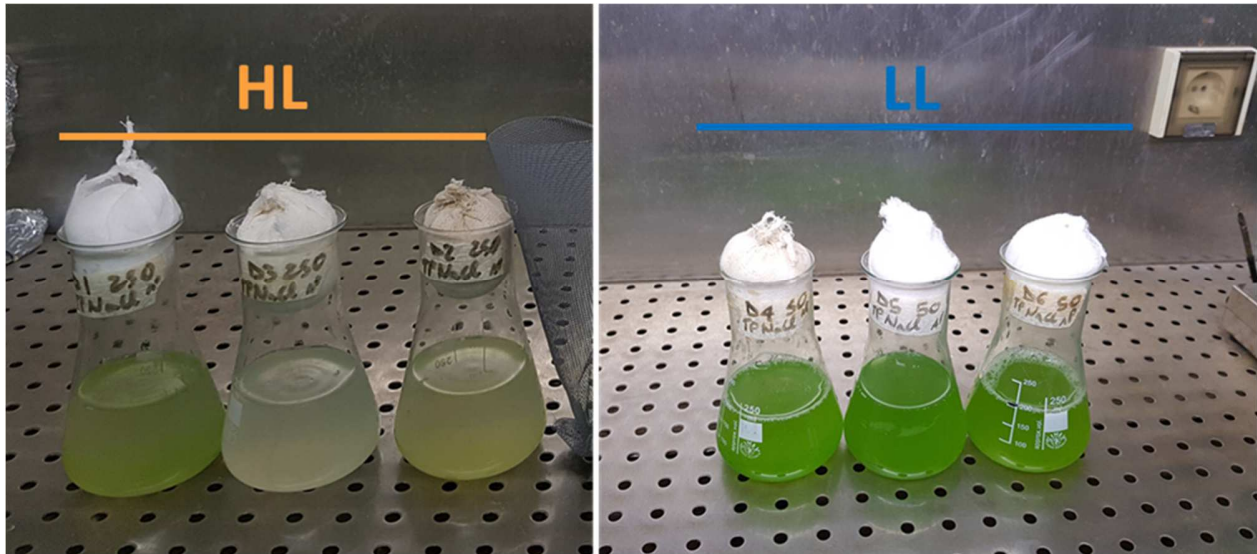
Figure 4.8: Cultures of *D. tertiolecta* in aerobic condition. Left - HL: Cultures of *D. tertiolecta* grown at HL, 7 days after the onset of the perturbation (30 °C). The cultures were much paler than the cultures grown at LL. Right – LL: Cultures of *D. tertiolecta* grown at LL after 7 days of perturbation (30 °C).

4.2.6 Protein content

The protein abundance changed, after the T change, in opposite ways in the two species under examination; in *C. reinhardtii*, the protein abundance increased over time; in *D. tertiolecta*, instead, the protein abundance decreased over time. There were clear and significant differences also between the two irradiances. *C. reinhardtii* had more protein than *D. tertiolecta*, the protein content on day 7 of *C. reinhardtii* was almost 3 times higher than that of *D. tertiolecta*. In *C. reinhardtii* on day 0, the cells grown at LL had almost double protein content than cells grown at HL; after 4 days of perturbation, growth irradiance made no difference for the protein content, while the protein content in HL increased; in LL, the protein content did not change. On day 7, with both irradiances, there was an increase of protein content, but it was higher at LL than at HL (Figure 4.9 a). In *D. tertiolecta*, cells grown at HL had higher protein content than cells grown at LL, but after 7 days the protein content in cultures grown at different irradiances were equal. In *D. tertiolecta*, at LL, the protein content decreased immediately after perturbation until the end of experiment; on day 7, instead, at HL there is a general trend of decrease (Figure 4.9 b).

C. reinhardtii   D. tertiolecta
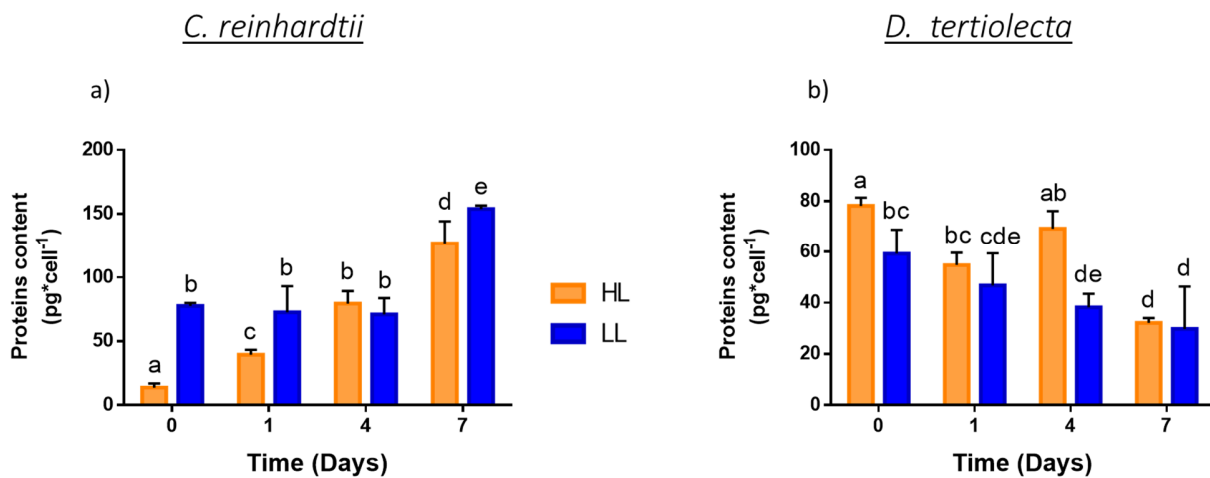
Figure 4.9: Protein content in *C. reinhardtii* (a) and *D. tertiolecta* (b). For both species, the results are related to aerobic condition at two different irradiances; High light (HL – orange bars) and Low light (LL – blue bars). On day 0 the cells were grown at 15 °C while on days 1, 4 and 7 days cells were grown at 30 °C. on day 0. Different letters indicate statistically different mean values ($p < 0.05$; 2-ways ANOVA and Fisher's LSD test). The error bars show the standard deviations (N=3).

4.2.7 Organic composition determined by Fourier-transform infrared (FTIR) spectroscopy

In *C. reinhardtii*, the carbohydrate/protein ratio of HL and LL cells changed over the experimental time at both irradiances. The carbohydrate/lipid ratio showed similar trends in both LL and HL cells, with an overall increasing trend over time (Figure 4.10 a). Also the carbohydrate/lipid ratio showed a similar pattern at LL and HL, with an increase till day 4 and a somewhat downward trend in the last section of the curve (Figure 4.10 b). The Protein/lipid ratios were not affected by light and remained approximately constant throughout the experiment (Figure 4.10 c).

In *D. tertiolecta*, the carbohydrate/protein ratio at LL increased after the perturbation but, after day one, it decreased until reaching a value similar to that on day 0. At HL, on day 1 the carbohydrate/protein ratio had an opposite trend compared to LL, but from the 4th day, the ratio increased (Figure 4.10 d). The carbohydrate/lipid ratio at LL increased after the day one, whereas at HL it showed an increasing tren only after the fourth day. (Figure 4.11 e). The protein/lipid ratios increased after perturbation at LL while at HL it was generally constant (Figure 4. 10 f).
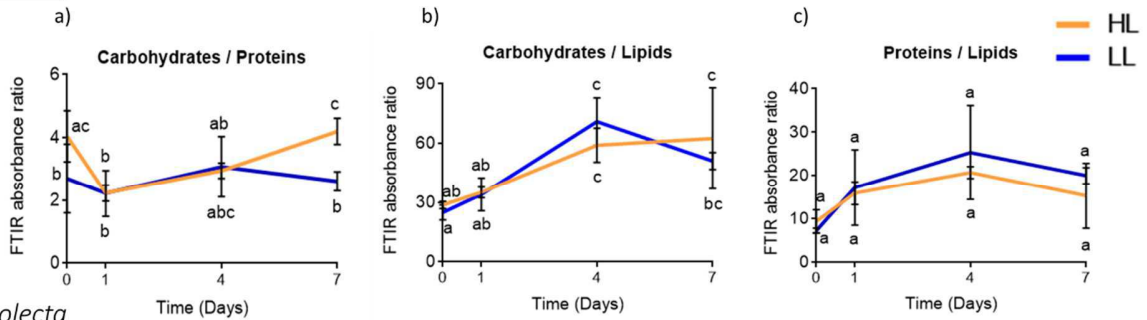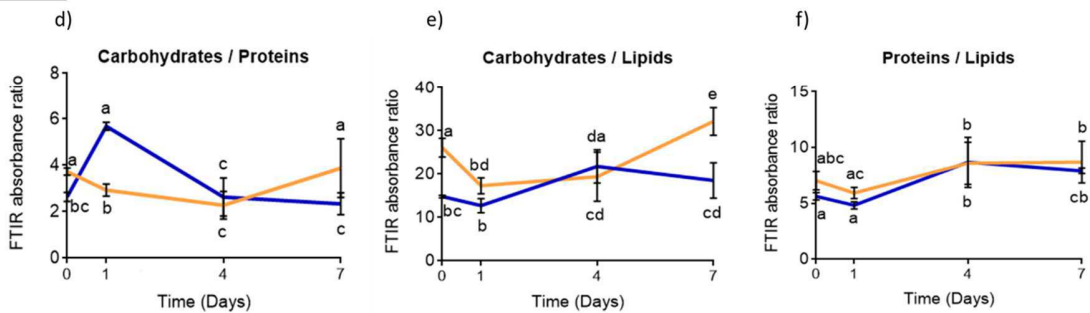
Figure 4.10: FTIR absorbance ratio between the main organic pools (carbohydrate, protein and lipid) in *C. reinhardtii* (a, b and c) and *D. tertiolecta* (d, e and f), in aerobic condition at high (HL – orange bars) and Low light (LL – blue bars). On day 0 the cells were transferred from 15 °C to 30 °C. Different letters indicate statistically different mean values ($p < 0.05$; 2-ways ANOVA and Fisher's LSD test). The error bars show the standard deviations (N=3).

In *C. reinhardtii* at HL, the content of lipid and carbohydrate increased over time (respectively more than 8 times and more than 10 times compared to day 0), while at LL the concentration of lipid and carbohydrate was homeostatic (Figure 4.11 and b). In *D. tertiolecta*, lipid contents at the two irradiances were not significantly different. The carbohydrate content at LL was not affected by the temperature change until day 7, when the carbohydrate content was half compared to T0 (Figure 4.11 c). At HL the carbohydrate decreased after the temperature change but then remained stable until the last experimental time (Figure 4.11 d).
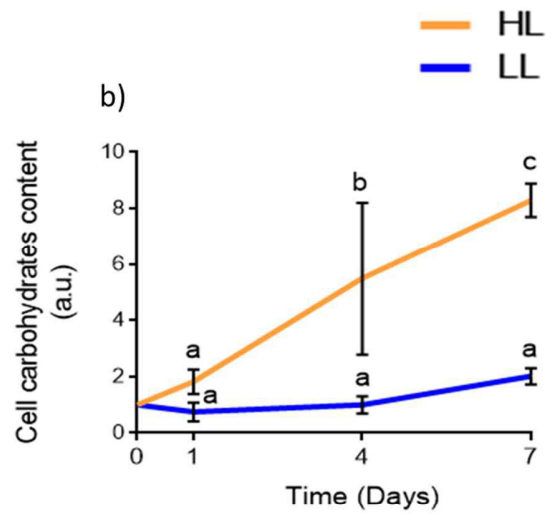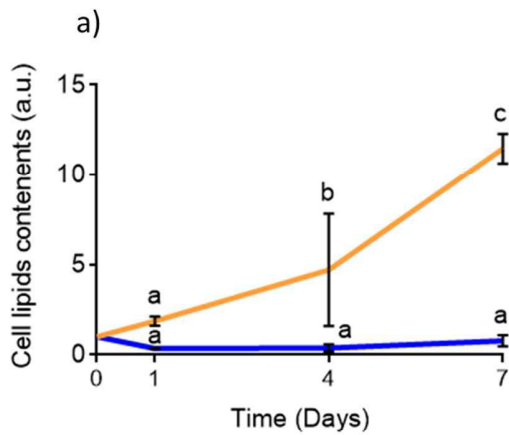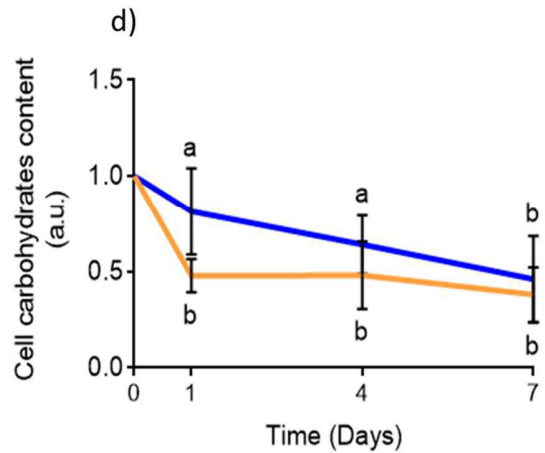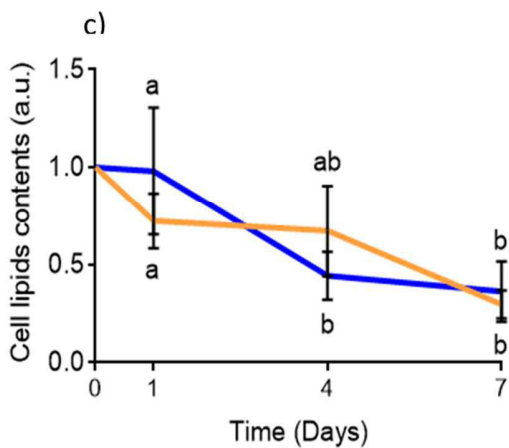
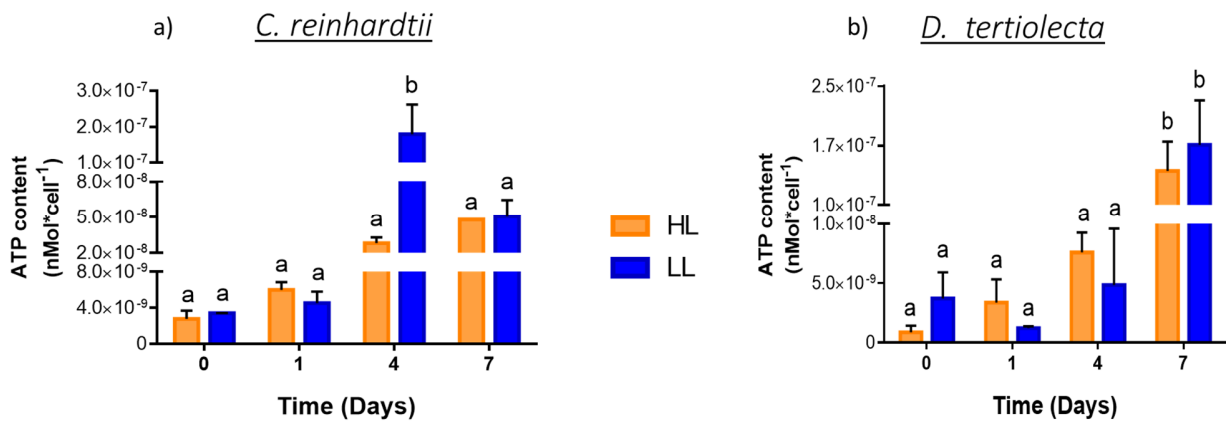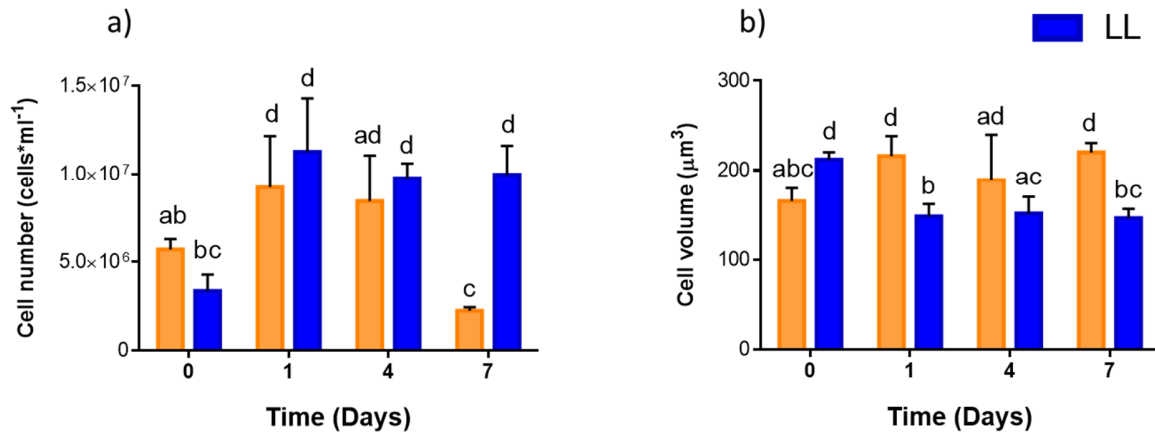**Figure 4.11:** Relative amount of lipid and carbohydrate in *C. reinhardtii* (a and b) and *D. tertiolecta* (c and d). For both species, the results are related to aerobic condition at two different irradiances; High light (HL – orange bars) and Low light (LL – blue bars). On day 0 the cells were transferred from 15 °C to 30 °C. Different letters indicate statistically different mean values ($p < 0.05$; 2-ways ANOVA and Fisher's LSD test) within the same light condition. The error bars show the standard deviations (N=3).

4.2.8 Elemental cell quotas

The C content of *C. reinhardtii* changed only on day 4 and at LL, at HL the C content was homeostatic (Table 4.1). The N content had the same trend of C content (Table 4.1), while P content did not change overall. Regarding HL, on day 0, the P content in HL was significantly lower than in LL; on day 7, however, the two values were similar (Table 4.1). The S content remained constant in LL, whereas in HL it decreased after one day at 30°C, but then it increased to values similar to those of day 0 and in LL (Table 4.1).

Also in *D. tertiolecta* the C and N contents changed following the same trend, with the highest value on day 4. Irradiances had no effect on C and N cell quotas (Table 4.2). At LL, after a small but significant decrease on day 1, the P concentration remained constant; at HL, on day 1 and on day 7 the P content

was lower compared to day 0 and 4. (Table 4.2). The S cell quota increased after four days at 30°C at HL, while it increased after seven days at LL (Table 4.2).

Figures 4.12 and 4.14 depict the C/N, C/P, C/S and N/S and N/P atomic ratios. The ratios among elements followed very different trends in the two species. In addition, irradiances strongly influenced the stoichiometry, even if no clear trend could be identified. Table 4.1 and 4.2 show the cell quotas of K, Ca, Fe, Cu and Zn. In both species, the main changes happened after 4 days from the onset of the perturbation. While in *C. reinhardtii* the highest values were determined in LL cells, in *D. tertiolecta* irradiance had no or little effect on micronutrients cell contents.

Table 4.1: Cell quotas of C, N, P, S, K, Ca, Fe, Cu and Zn in *C. reinhardtii cells cultured at* either high (HL) or low light (LL) in an aerobic condition. On day 0, the cells were transferred from 15 °C to 30 °C. Different letters indicate statistically different mean values ($p < 0.05$; 2-ways ANOVA and Fisher's LSD test). The error bars represent the standard deviations (N=3).

Elements	Cell quota pg·cell^{-1}															
	T0				T1				T4				T7			
	HL		LL		HL		LL		HL		LL		HL		LL	
C	65.92^a	(0.59)	68.09^a	(9.63)	52.13^a	(12.15)	63.28^a	(4.77)	60.31^a	(10.52)	127.09^b	(84.42)	61.96^a	(16.87)	64.65^a	(9.16)
N	16.24^a	(1.05)	16.98^a	(2.57)	13.94^a	(1.82)	16.57^a	(1.18)	14.18^a	(2.9)	29.3^b	(19.05)	13.54^a	(3.16)	15.85^a	(1.75)
P	7.09^{ab}	(1.07)	4.66^c	(1.51)	1.58^d	(0.82)	5.63^{bc}	(0.5)	3.41^b	(0.53)	5.9^c	(0.5)	7.79^c	(4.65)	6.79^c	(0.39)
S	1.72^{abcd}	(0.88)	1.18^{acd}	(0.32)	0.49^b	(0.25)	1.77^c	(0.71)	0.74^{ab}	(0.07)	1.51^{cd}	(0.34)	1.75^{abc}	(1.12)	1.74^{ac}	(0.13)
K	1.52^{ab}	(0.09)	2.66^{bc}	(0.65)	1.49^{ab}	(0.89)	2.54^{cd}	(0.36)	1.3^{ab}	(0.08)	2.08^{abd}	(0.23)	1.83^a	(0.65)	2.84^c	(0.95)
Ca	1.02^a	(0.47)	1.07^a	(0.21)	0.81^a	(0.31)	0.96^a	(0.28)	0.76^a	(0.07)	0.91^a	(0.279)	1.19^a	(0.36)	1.03^a	(0.53)
Fe	0.16^a	(0.07)	0.102^{ab}	(0.03)	0.05^b	(0.02)	0.11^{ab}	(0.01)	0.16^a	(0.1)	0.16^a	(0.06)	0.18^a	(0.06)	0.12^{ab}	(0.04)
Cu	0.03^{ab}	(0.02)	0.07^{acd}	(003)	0.02^b	(0.01)	0.11^c	(0.02)	0.05^{ab}	(0.01)	0.12^{ce}	(0.06)	0.13^{ce}	(0.02)	0.1^{cd}	(0.01)
Zn	0.15^{ab}	(0.04)	0.15^{ab}	(0.03)	0.09^a	(0.06)	0.15^{ab}	(0.07)	0.08^a	(0.02)	0.06^a	(0.01)	0.15^{ab}	(0.06)	0.25^b	(0.13)

Table 4.2: Cell quotas of C, N, P, S, K, Ca, Fe, Cu and Zn in *D. tertiolecta* at two different irradiances; High light (HL) and Low light (LL) in an aerobic condition. On day 0 the cells were grown at 15 °C while on days 1, 4 and 7 the cells were grown at 30 °C. Different letters indicate statistically different mean values (p < 0.05; 2-ways ANOVA and Fisher's LSD test). The error bars represent the standard deviations (N=3).

Elements	Cell quota pg·cell^{-1}															
	T0				T1				T4				T7			
	HL		LL		HL		LL		HL		LL		HL		LL	
C	222.48^{ab}	(9.40)	160.3^{b}	(71.1)	213.8^{ab}	(32.2)	239.45^{ab}	(39.7)	412.4^{c}	(70.2)	389.96^{c}	(8.26)	290.24^{a}	(56.2)	228.8^{ab}	(77.6)
N	45.3^{ab}	(3.39)	24.9^{b}	(8.76)	42.8^{ab}	(6.56)	40.8^{ab}	(7.23)	84.6^{c}	(20.2)	73.4^{cd}	(1.72)	54.8^{ad}	(14.5)	43.0^{b}	(16.4)
P	8.24^{ab}	(0.50)	8.92^{b}	(1.55)	4.96^{cd}	(0.66)	6.37^{ac}	(1.82)	6.38^{dc}	(0.06)	6.94^{abc}	(0.12)	3.55^{d}	(1.51)	7.43^{ab}	(1.02)
S	0.97^{a}	(0.48)	0.59^{a}	(0.32)	0.75^{ab}	(0.08)	0.65^{ab}	(0.27)	1.81^{c}	(0.48)	0.56^{a}	(0.01)	0.98^{a}	(0.31)	1.09^{b}	(0.08)
K	3.74^{a}	(1.18)	3.30^{ab}	(0.26)	1.81^{cd}	(0.23)	2.48^{bcd}	(0.55)	2.71^{bcd}	(0.36)	2.49^{bcd}	(0.32)	2.03^{d}	(0.40)	2.75^{bd}	(0.28)
Ca	0.96^{ab}	(0.36)	0.87^{ac}	(0.20)	0.43^{d}	(0.05)	0.58^{cd}	(0.11)	1.28^{be}	(0.32)	1.42^{e}	(0.22)	0.55^{cd}	(0.18)	0.48^{d}	(0.03)
Fe	0.10^{ab}	(0.05)	0.07^{a}	(0.01)	0.05^{a}	(0.00)	0.05^{a}	(0.01)	0.14^{b}	(0.07)	0.06^{a}	(0.01)	0.08^{ab}	(0.04)	0.07^{b}	(0.01)
Cu	0.02^{ab}	(0.01)	0.02^{ac}	(0.00)	0.01^{d}	(0.00)	0.01^{ad}	(0.00)	0.04^{b}	(0.00)	0.02^{ac}	(0.00)	0.02^{ac}	(0.01)	0.01^{cd}	(0.00)
Zn	0.37^{a}	(0.13)	0.30^{ad}	(0.04)	0.10^{b}	(0.01)	0.17^{ab}	(0.04)	0.26^{c}	(0.07)	0.30^{ab}	(0.04)	0.14^{ad}	(0.05)	0.25^{bd}	(0.02)
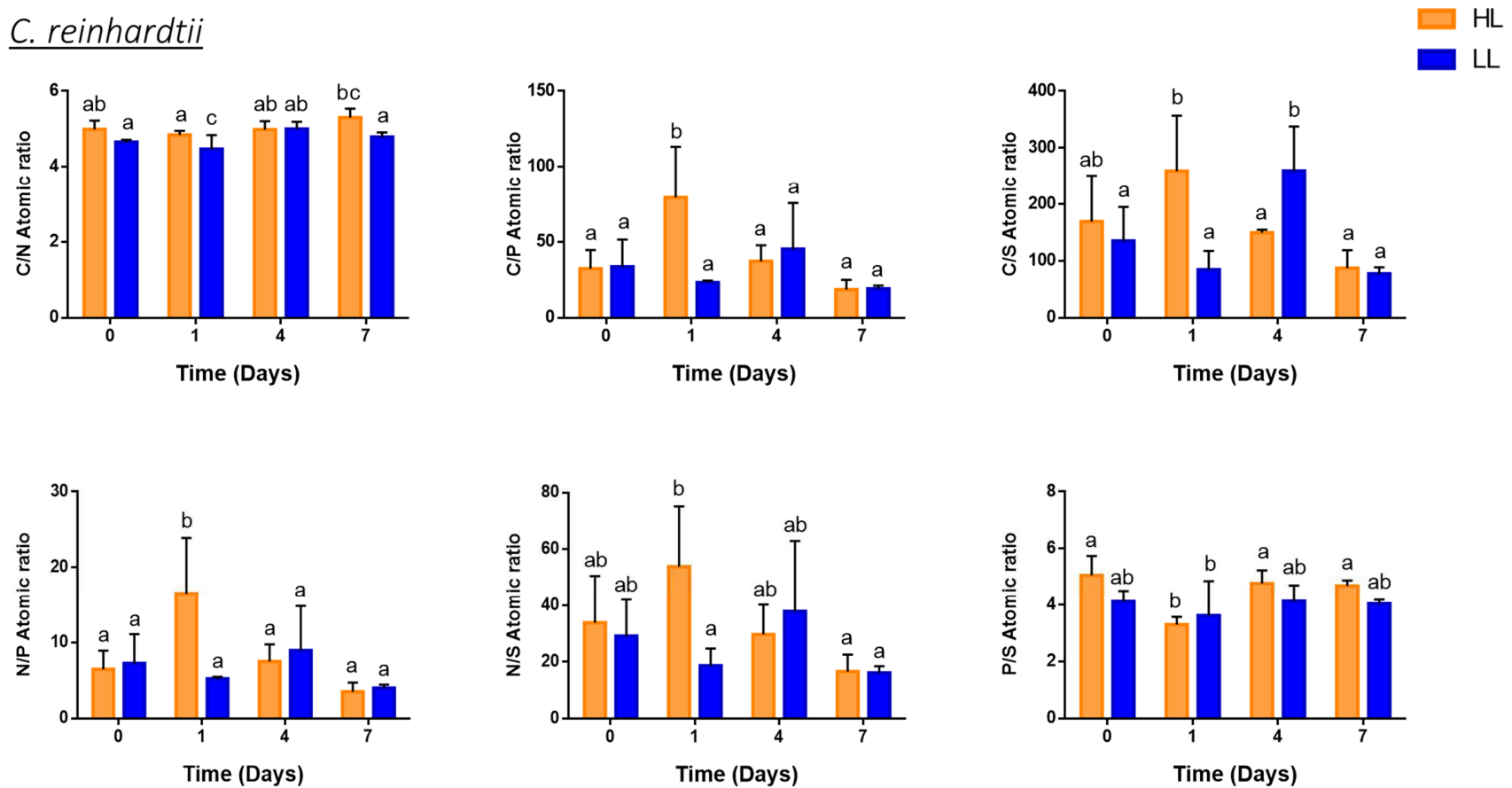
Figure. 4.12: Elemental stoichiometries (atomic ratios) in *C. reiharditii*, in aerobic condition, High light (HL - orange bars) e and Low light (LL – blue bars). On day 0, the cells were transferred from 15 °C to 30 °C. Different letters indicate statistically different mean values ($p < 0.05$; 2-ways ANOVA and Fisher's LSD test). The error bars represent the standard deviations (N=3).
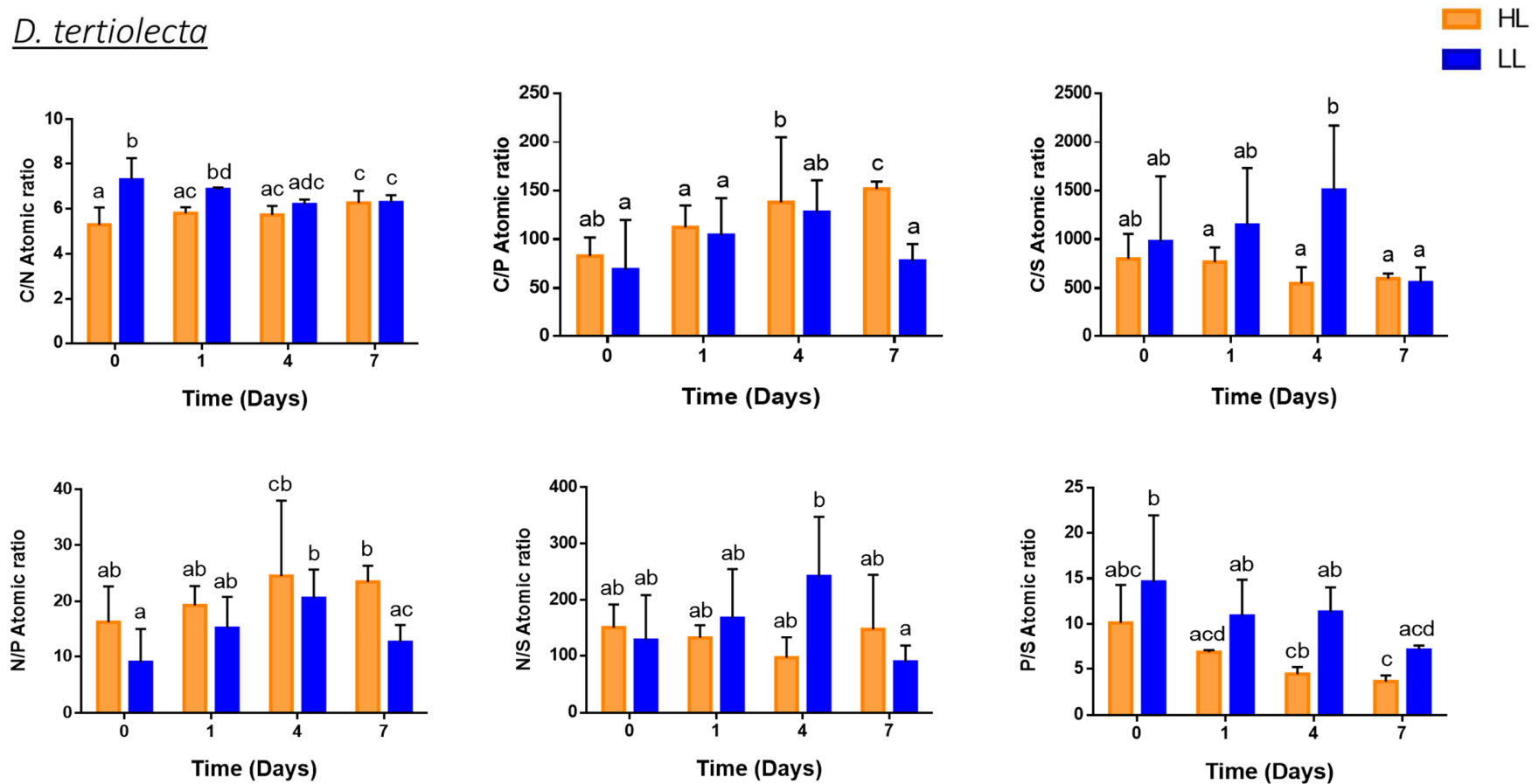
Figure. 4.13: Elemental stoichiometries (atomic ratios) in *D. tertiolecta,* at two different irradiances; High light (HL - orange bars) e and Low light (LL – blue bars) in aerobic condition. On day 0 the cells were grown at 15 °C while on days 1, 4 and 7 the cells were grown at 30 °C. Different letters indicate statistically different mean values (p < 0.05; 2-ways ANOVA and Fisher's LSD test). The error bars represent the standard deviations (N=3).

4.3 Impact of temperature variation on cell composition of *C. reinhardtii* and *D. tertiolecta* in anaerobic condition

4.3.1 Acclimation to Anaerobic condition

To induce anaerobic condition, 950 ml·min^{-1} of N_2 were bubbled for 40 minutes into the growth medium. Preliminary tests were performed to select the adequate N_2 flow (950 ml·min^{-1} of N_2 were for 40 minutes, Figure 4.14). The O_2 concentration was measured with a Clark type O_2 electrode system. In previous experiments (Fanesi and Giordano, unpublished) gas analysis performed by GC-TDC detected 2.98·10^{-3} (3.07·10^{-5}) ppm O_2 in the air space above the medium, after sparging the medium with a N_2 flow of 589 ml·min^{-1} for 7 minutes. As mentioned in paragraph 3.2, the anaerobic condition was induced one day before day 0; this time was deemed sufficient because, as shown in paragraph 4.1 and figure 4.2, the necessary genes for anaerobic metabolism, among which PFR1 and ACK1, are already fully expressed four hours after the start of the anaerobic condition. Data from Fanesi and Giordano (unpublished) proved that lipid and carbohydrate contents in *C. reinhardtii,* after the temperature increase*,* were stable only in anaerobic conditions (Figure 4.15).
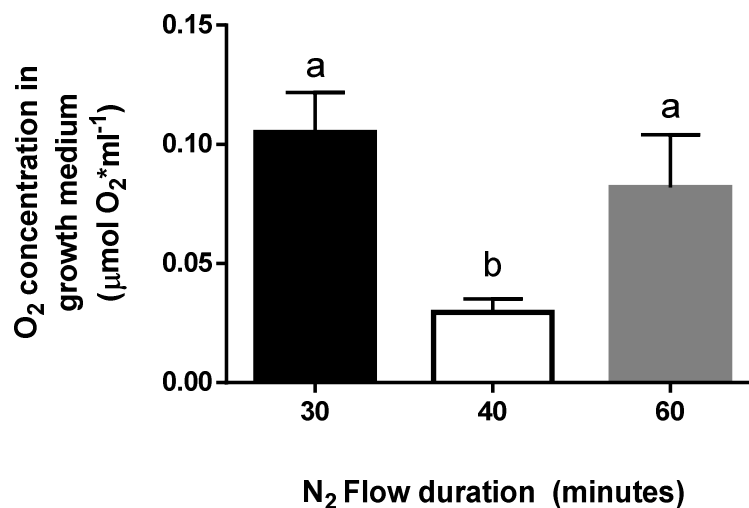
Figure 4.14: Preliminary determination of the duration of the N_2 flus (950 mL·min^{-1}) necessary to induce anaerobiosis in *C. reinhardtii.* Different letters indicate statistically different mean values ($p < 0.05$; 2-ways ANOVA and Fisher's LSD test). The error bars represent the standard deviations (N=3).
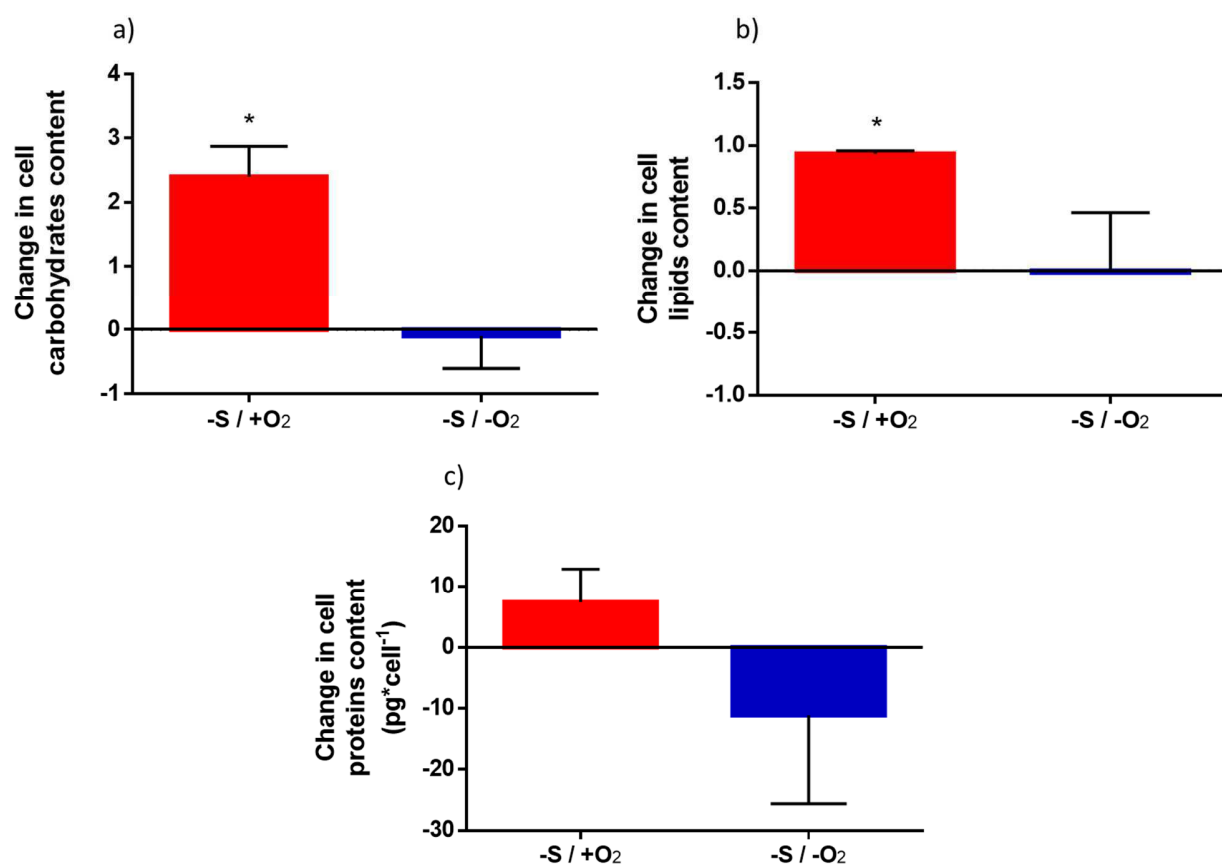
Figure 4.15: Carbohydrate and lipid amounts in *C. reinhardtii*, in anaerobic conditions, in S-starved (black bars) or S replete(white bars) cells. Asterisk indicate statistically different mean values ($p < 0.05$; Student t-test). Each value was compared to value 0. Zero was used as control in an ideal homeostasis condition. The error bars represent the standard deviations (N=3).

4.3.2 ATP measurement

In both aerobic condition and anaerobic conditions, in both species, the free ATP content in the cells was more affected by the temperature change than by the irradiance. Only after 4 days and only in *C. reinhardtii* the irradiances had an effect on ATP content: in LL, free ATP was higher than in HL (Figure 4.16 a). ATP concentration in the two species was similar. In *D. tertiolecta*, the free ATP content increased only on day 7, with similar trends between HL and LL. (Figure 4.16 b). In *C. reinhardtii*, ATP content in HL did not increase significantly over time, while in LL, the ATP content had its highest value on day 4, but then decreased again (Figure 4.16 a). For both species, free ATP content were not correlated with cell number (Figure 4.17 a and c).

Figure 4.16: ATP content in *C. reinhardtii* (a) and *D. tertiolecta* (b). For both species, the results are related to anaerobic condition at two different irradiances; High light (HL, orange bars) and Low light (LL, blue bars). On day 0 the cells were grown at 15 °C while on day 1, 4 and 7 days cells were grown at 30 °C. Different letters indicate statistically different mean values ($p < 0.05$; 2-ways ANOVA and Fisher's LSD test). The error bars show the standard deviations (N=3).

4.3.3 Cell number, cell volume

In *C. reinhardtii*, perturbation determined a significant cell number reduction on day 7 at HL, while at LL it produced an increase of cell number from day 0 to day 1 and the new growth rate is maintained until day 7 (Figure 4.17 a). Both irradiances and temperature had an effect on volume; with a HL, the cell volume increased after perturbation (temperature change) and then stabilized. The cell volume was larger in LL than in HL, but after perturbation, its value decreased in LL and increased in HL (Figure 4.17 b). In *D. tertiolecta*, the perturbation at LL stimulated the cells growth, but after day 1, the cell concentration decreased over time. At HL the cell growth was not affected from by perturbation until day 7; at this time the cells concentration decreased (Figure 4.17 c). At HL, the cell volume decreased with time, while at HL the cell volume showed a tendency to homeostasis (Figure 4.17 d).
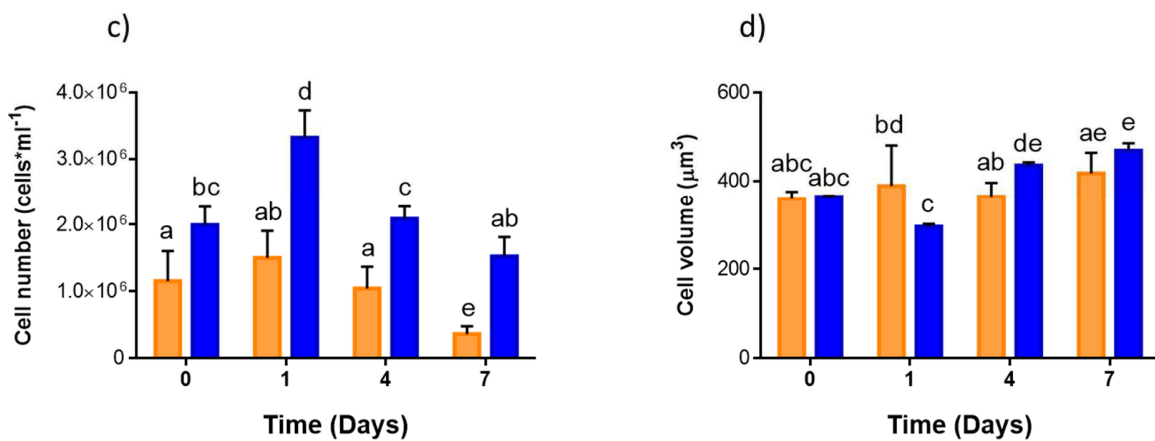
Figure 4.17: Cell number and cell volume of *C. reinhardtii* (a and b) and *D. tertiolecta* (c and d)*. For both species, the results are related to anaerobic condition at two different irradiances; High light (HL - orang bars) e and Low light (LL – blue bars). On day 0 the cells were grown at 15 °C while on days 1, 4 and 7 days cells were grown at 30 °C. Different letters indicate statistically different mean values (p < 0.05; 2-ways ANOVA and Fisher's LSD test). The error bars show the standard deviations (N=3).

4.3.4 Cell dry weight

The dry weight of *C. reinhardtii* cells was about the same in both irradiances conditions; after one day of perturbation, dry weight increased significantly with both irradiances but only at HL on day 7 was observed a new increase of cells weight of 3 magnitude orders (Figure 4.18 a). In *D. tertiolecta* dry weight was not affected by irradiances and perturbations, apart from the case of HL on day 7, where dry weight was almost 5 times higher than in all other sampling days (Figure 4.18 b).
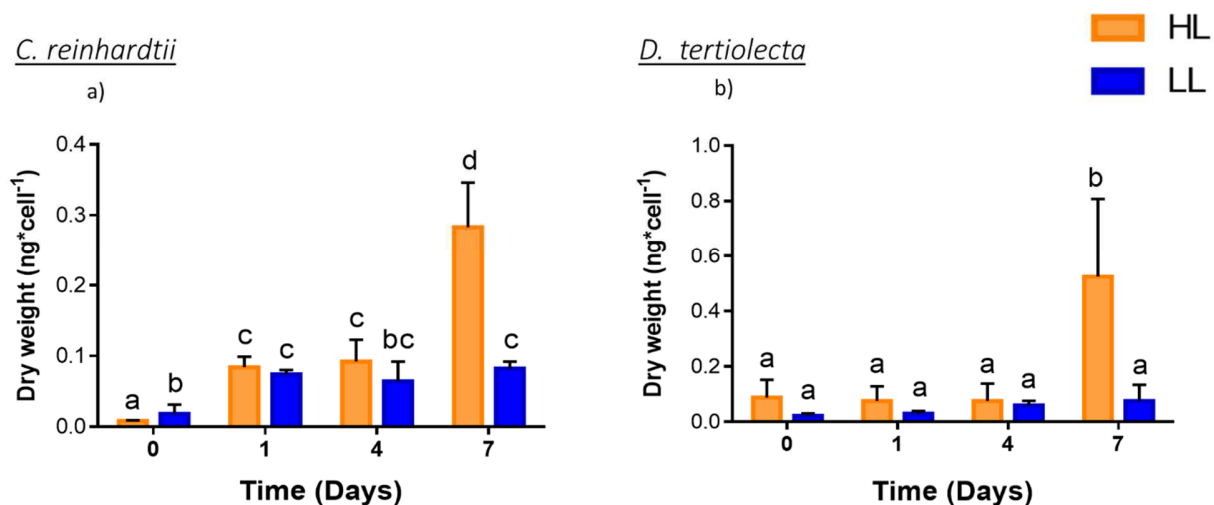
Figure 4.18: Dry weight of *C. reinhardtii* (a) and of *D. tertiolecta* (b). For both species, the results are related to anaerobic condition at two different irradiances; High light (HL - orange bars) e and Low light (LL – blue bars). At day 0 the cells were grown at 15 °C while on days 1, 4 and 7 days cells were grown at 30 °C. Different letters indicate statistically different mean values (p < 0.05; 2-ways ANOVA and Fisher's LSD test). The error bars show the standard deviations (N=3).

4.3.5 Maximum PSII quantum yield (Fv/Fm)

In *C. reinhardtii*, the photosynthetic efficiency in anaerobic condition was not affected by the change of growth temperature, at both irradiances. Photosynthetic efficiency was always above 0.6 (Figure 4.19 a). In *D. tertiolecta,* the photosynthetic efficiency on day 0 was higher at LL than at HL. After the shift of higher temperature, the photosynthetic efficiency decreased significantly at both irradiances, but at HL the photosynthetic efficiency decreased faster than LL exposure. For both irradiances, the decrease of photosynthetic efficiencies between day 0 and day 7 was by about 50% (Figure 4.19 b).

C. reinhardtii
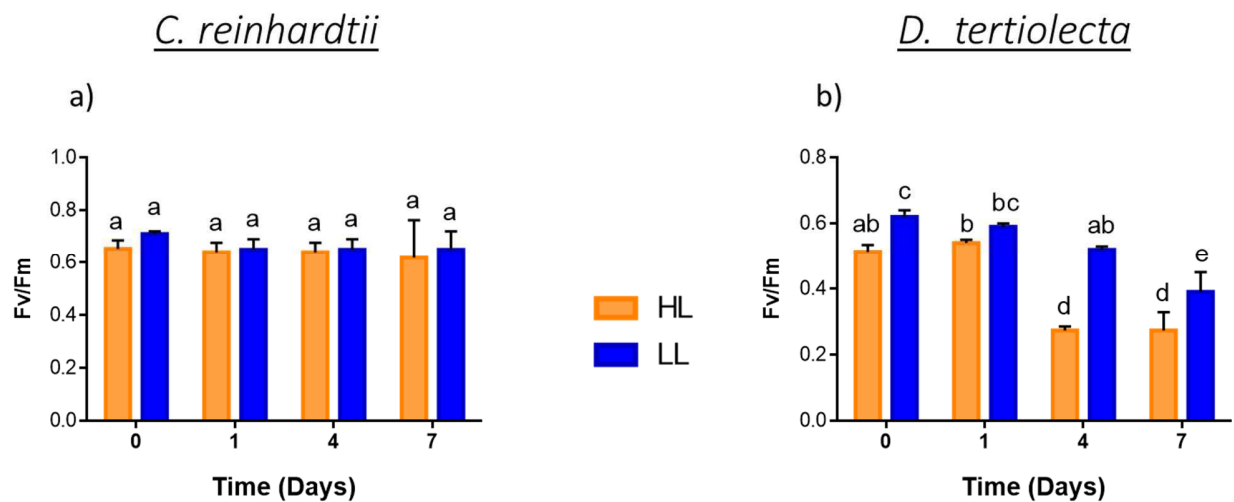
D. tertiolecta

Figure 4.19: Photosynthetic efficiency in *C. reinhardtii* (a) and *D. tertiolecta* (b). For both species, the results are related to anaerobic condition at two different irradiances; High light (HL - orange bars) e and Low light (LL – blue bars). On day 0 the cells were grown at 15 °C while on days 1, 4 and 7 cells were grown at 30 °C. Different letters indicate statistically different mean values (p < 0.05; 2-ways ANOVA and Fisher's LSD test). The error bars show the standard deviations (N=3).

4.3.6 Chlorophyll *a/b*

In *C. reinhardtii*, on day 0, chlorophyll *a* cell content at HL was lower than at LL, but after the change of growth temperature, chlorophyll *a* at HL became higher than at LL. The content of chlorophyll *a* at HL increased significantly over time; on day 7, it was almost twice that on day 0. In contrast, chlorophyll *a* at LL decreased over time after the temperature change, and it was 3 times lower on day 4 than on day 0; on day 7, however, it again reached similar value to those measured on day 1 (Figure 4.20 a). Chlorophyll *b* cell content did not change over time, at HL, while it increased significantly at LL, on day 1 and decreased significantly on day 7 (Figure 4.20 b). Total chlorophyll decreased over time at LL, whereas at HL it was constant until day 4 and then increased significantly (Figure 4.20 c).

In *D. tertiolecta*, chlorophyll *a* was higher at HL than at LL, for the whole duration of the experiment, especially on day 0 and day 4. At HL, chlorophyll *a* was not affected by the changes of growth conditions, while at LL it slightly decreased from day 4 to day 7 (Figure 4.20 d). Irradiance had no effect on chlorophyll *b* content, which had its highest value on day 4 (Figure 4.20 e). Only on day 4 total chlorophyll showed higher value at LL than at HL (Figure 4.20 f).
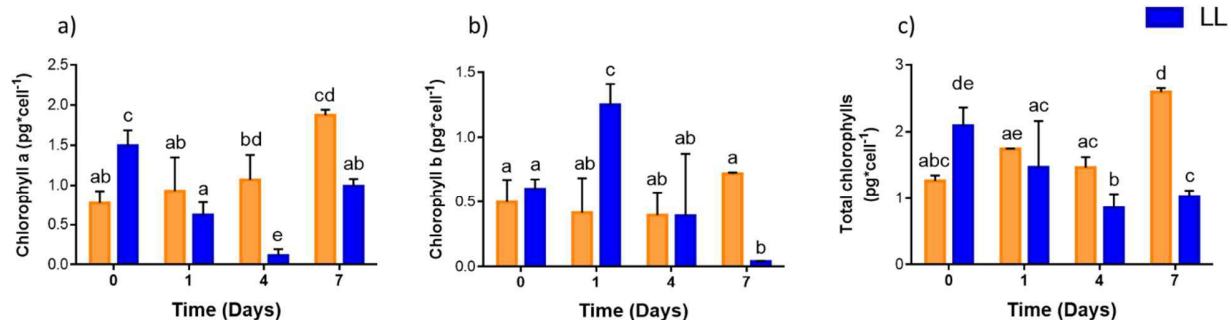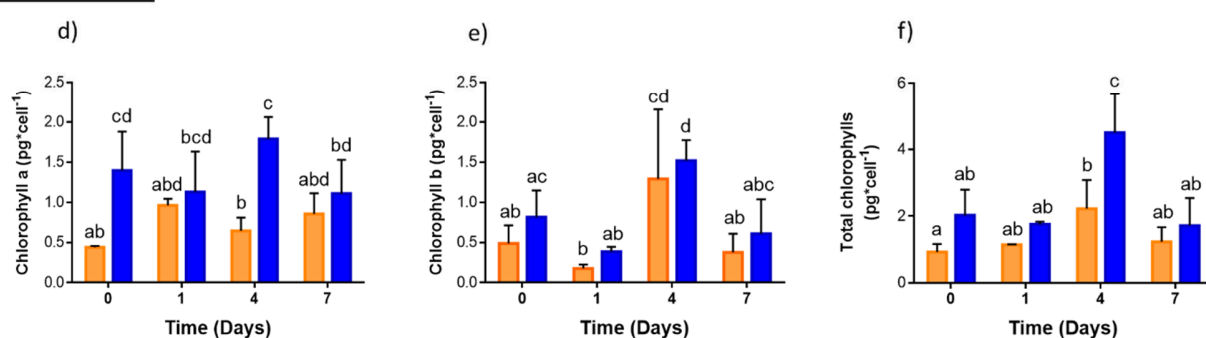
Figure 4.20: Chlorophyll *a/b* and total chlorophylls in *C. reinhardtii,* (a, b and c) and *D. tertiolecta* (d, e and f). For both species, the results are related to anaerobic condition at two different irradiances; High light (HL - orange bars) e and Low light (LL – blue bars). On day 0 the cells were grown at 15 °C while on days 1, 4 and 7 cells were grown at 30 °C. Different letters indicate statistically different mean values ($p < 0.05$; 2-ways ANOVA and Fisher's LSD test). The error bars show the standard deviations (N=3).

4.3.7 Protein content

The change of growth temperature affected protein cell content in both *C. reinhardtii* and *D. tertiolecta*. In *C. reinhardtii*, the protein cell content on day 0 was lower compared to that on all other days and it was similar at the two irradiances. After the temperature change, the protein cell content increased significantly at both irradiances, even though the increase was higher at LL than at HL. After day 1, protein remained constant at HL, that was not true for LL (Figure 4.21 a).

In *D. tertiolecta*, the protein cell content was similar at both irradiances. After the change of temperature, protein remained constant at HL, while, at LL, protein increased significantly from day 0 to day 4, but protein cell content decreased in the last part of treatment (Figure 4.21 b).
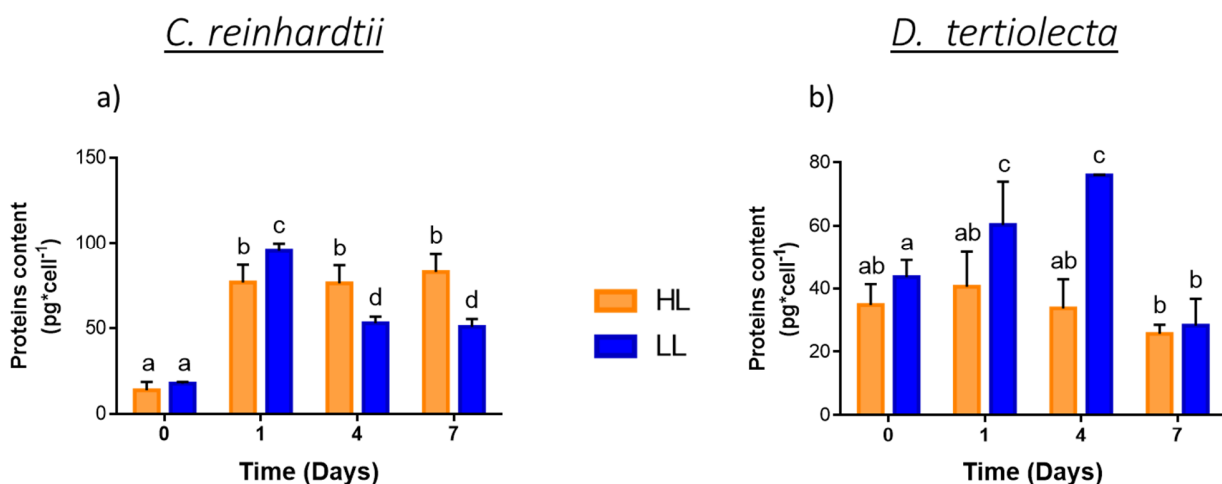
Figure 4.21: Protein content in *C. reinhardtii* (a) and *D. tertiolecta* (b). For both species, the results are related to anaerobic condition at two different irradiances; High light (HL - orange bars) e and Low light (LL – blue bars). On day 0 the cells were grown at 15 °C while on days 1, 4 and 7 cells were grown at 30 °C. Different letters indicate statistically different mean values ($p < 0.05$; 2-ways ANOVA and Fisher's LSD test). The error bars show the standard deviations (N=3).

4.2.8   Organic composition determined by Fourier-transform infrared (FTIR) spectroscopy

In *C. reinhardtii*, on day 0, the carbohydrate/protein ratio at HL was significantly higher than at LL; it was affected by the temperature change. However, carbohydrate/protein ratio had not a clear trend and on day 7 it was similar to day 0 at both irradiances. (Figure 4.22 a). The carbohydrate/lipid ratio was not affected by irradiance; it increased from day 0 to day 4 and then remained unchanged till day 7 (Figure 4.22 b). The protein/lipid ratio was not affected by light or temperature change, throughout the duration of the experiment (Figure 4.22 c).

In *D. tertiolecta, at LL the* carbohydrate/protein ratio increased on day 7 while at HL it was homeostatic (Figure 4.22 d). The carbohydrate/lipid ratio significantly increased at both irradiances HL (Figure 4.22 e). Relative to protein/lipid ratio, at LL it was homeostatic while increased on day 7 at HL (Figure 4.22 c).
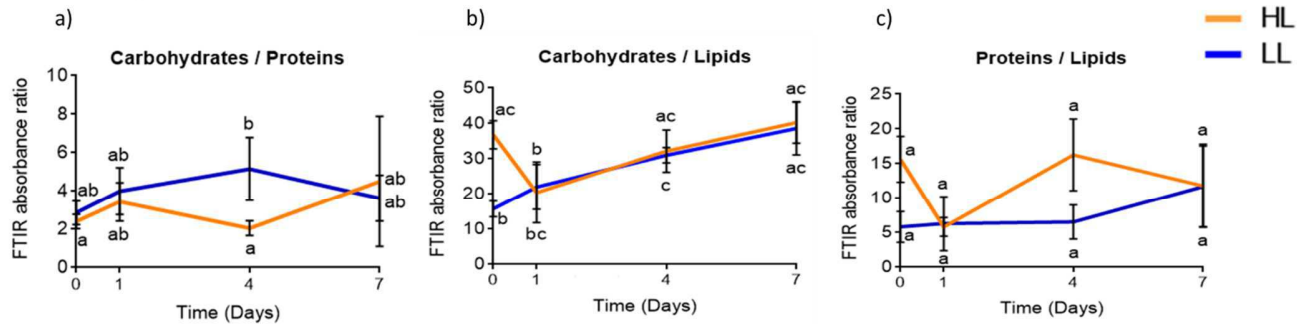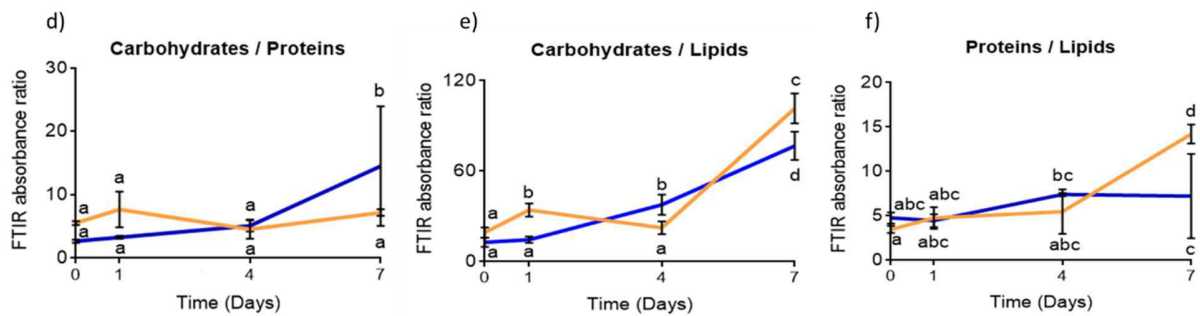
Figure 4.22: FTIR absorbance ratio between main organic pool (carbohydrate, protein and lipid) in *C. reinhardtii* (a, b and c) and *D. tertiolecta* (d, e and f). For both species, the results are related to anaerobic condition at two different irradiances; High light (HL - orange bars) e and Low light (LL – blue bars). On day 0 the cells were grown at 15 °C while on days 1, 4 and 7 cells were grown at 30 °C. Different letters indicate statistically different mean values (p < 0.05; 2-ways ANOVA and Fisher's LSD test). The error bars show the standard deviations (N=3).

In *C. reinhardtii*, the semi-quantification of lipid showed an increase in cell lipid content at HL, while at LL the lipid content was almost constant over time (Figure 4.23 a). The relative carbohydrate content after perturbation increased in both irradiances but on day 7 the decreases were more accentuate in LL than HL (Figure 4.23 b). In *D. tertiolecta*, lipid contents after perturbation decreased at both irradiances (Figure 4.23 c). The carbohydrate content at HL was not affected by perturbation, whereas at LL the relative amount of carbohydrate increased (Figure 4.23 d).
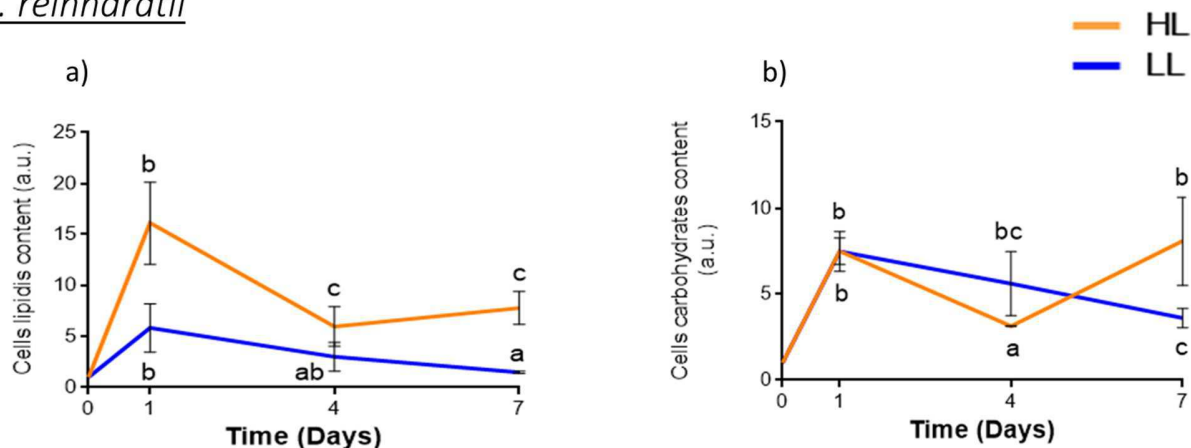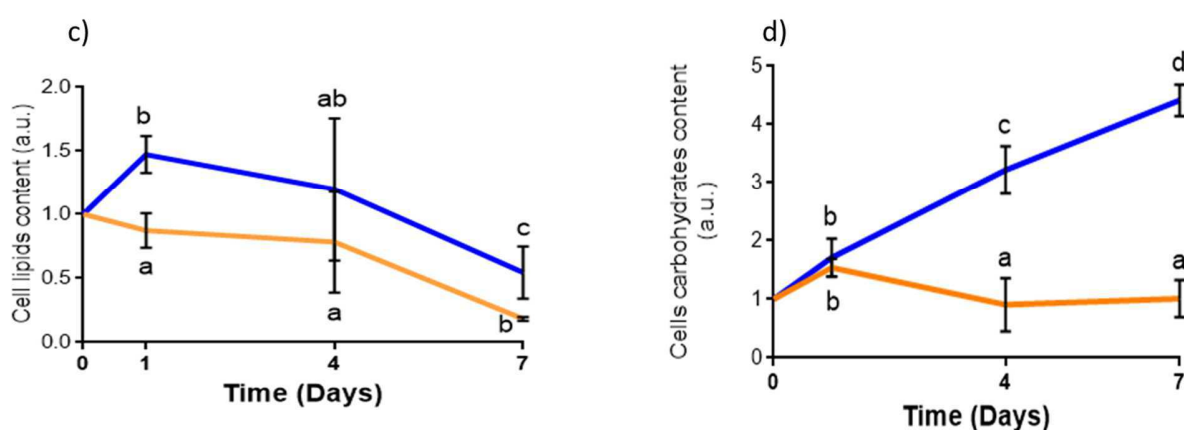
Figure 4.23: The relative amount of lipid and carbohydrate in *C. reinhardtii* (a and b) and *D. tertiolecta* (c and d). For both species, the results are related to anaerobic condition at two different irradiances; High light (HL - orange bars) e and Low light (LL – blue bars). On day 0 the cells were grown at 15 °C while on days 1, 4 and 7 cells were grown at 30 °C. Different letters indicate statistically different mean values ($p < 0.05$; 2-ways ANOVA and Fisher's LSD test). The error bars show the standard deviations (N=3).

4.3.8 Elemental composition

At LL, the C content increased by one order of magnitude after 1 day at higher temperature and then remained unchanged for the rest of the experimental period (Table 4.3). The N content changed with the same trend as Carbon, (Table 4.3). The cell content of P, at LL was constant for 1 day after the change of temperature; it then decreased and remained stable until day 7 (Table 4.3), while at HL its content increased over time (Table 4.3). S abundance on day 0 was similar between the two irradiances, after perturbation, it increased with both irradiances but with HL continued to increase while with LL after day 1 S abundance decreased and stayed constant (Table 4.3).

In *D. tertiolecta* the C and N contents changed by following the same trend, with the highest value on day 7 at HL, while at LL they were homeostatic (Table 4.4). P content at HL was homeostatic, while at

LL it increased only on day 4 but on day 7 it drastically decreased at a value similar to HL (Table 4.4). S abundance was almost constant at LL though on day 7 it decreased compared to day 4. At HL, S abundance significantly decreased after perturbation (Table 4.4).

Figures 4.24 and 4.25 show the atomic ratio between C, N, P and S. The pattern of changes of the atomic ratios were very different between the two species: the ratios between macronutrients increased before at HL in *C. reinhardtii* on day 1, at LL the macronutrient ratios changed on day 4, except P/S which changed on day 1 too (Figure 4.24). Even in *D. tertiolecta*, the macronutrient ratios changed before at HL than at LL (Figure 4.25). Table 4.3 and 4.4 show the cell quotas of K, Ca, Mn, Fe, Cu and Zn; no significant trend was observed.

Table 4.3: Cell quotas of C, N, P, S, K, Ca, Fe, Cu and Zn in *C. reinhardtii* cells exposed to anaerobiosis, at either high light (HL) or low light (LL). On day 0 the growth temperature was changed from 15 °C to 30 °C. Different letters indicate statistically different mean values ($p < 0.05$; 2-ways ANOVA and Fisher's LSD test). The error bars show the standard deviations (N=3).

	Cell quota pg·cell^{-1}															
	T0				T1				T4				T7			
Elements	HL		LL		HL		LL		HL		LL		HL		LL	
C	3.72^a	(0.50)	8.39^{ab}	(6.16)	102.71^{bc}	(30.9)	17.4^c	(4.82)	98.6^c	(18.82)	111.25^{abc}	(22.9)	118.55^d	(17.8)	38.52^{bc}	(1.67)
N	1.01^a	(0.12)	1.76^a	(1.21)	22.0^{ab}	(8.85)	3.70^b	(1.20)	22.0^b	(6.91)	23.1^{ab}	(5.70)	35.4^c	(7.93)	12.7^b	(4.09)
P	4.70^{ab}	(0.29)	5.32^a	(0.72)	7.58^c	(0.26)	5.56^a	(1.55)	3.45^d	(0.14)	3.97^{bd}	(0.53)	12.3^e	(0.46)	4.03^{bd}	(0.45)
S	0.87^a	(0.06)	1.10^a	(0.13)	1.74^b	(0.14)	2.13^c	(0.41)	0.83^a	(0.23)	0.99^a	(0.17)	2.45^c	(0.29)	1.11^a	(0.09)
K	1.73^{ab}	(0.17)	1.85^a	(0.32)	1.64^{ab}	(0.33)	2.03^a	(0.12)	0.98^c	(0.28)	1.61^{ab}	(0.31)	1.82^{ab}	(0.28)	1.38^{bc}	(0.20)
Ca	1.45^{ab}	(0.25)	1.93^a	(0.18)	3.51^c	(0.47)	4.54^d	(1.06)	0.64^e	(0.12)	0.83^{be}	(0.17)	2.28^a	(0.36)	1.70^a	(0.37)
Mn	0.15^a	(0.03)	0.21^b	(0.02)	0.10^{ac}	(0.04)	0.10^{ac}	(0.00)	0.06^c	(0.02)	0.05^c	(0.01)	0.25^b	(0.08)	0.07^{cb}	(0.02)
Fe	0.33^a	(0.07)	0.64^b	(0.09)	0.24^{acd}	(0.06)	0.28^{ad}	(0.11)	0.22^{acd}	(0.06)	0.12^c	(0.05)	1.09^e	(0.13)	0.15^{cd}	(0.04)
Cu	0.04^a	(0.00)	0.06^{ab}	(0.01)	0.14^{bc}	(0.03)	0.12^c	(0.04)	0.08^{abc}	(0.02)	0.08^{abd}	(0.02)	0.33^d	(0.11)	0.09^{abd}	(0.02)
Zn	0.38^{ab}	(0.07)	0.51^c	(0.05)	0.31^b	(0.10)	0.30^b	(0.07)	0.06^e	(0.01)	0.16^{de}	(0.06)	0.48^{ab}	(0.11)	0.26^{be}	(0.05)

Table 4.4: Cell quotas of C, N, P, S, K, Ca, Fe, Cu and Z in *D. tertiolecta* cells exposed to anaerobiosis. at either high light (HL) or low light (LL). On day 0 the growth temperature was changed from 15 °C to 30 °C. Different letters indicate statistically different mean values (p < 0.05; 2-ways ANOVA and Fisher's LSD test). The error bars show the standard deviations (N=3).

Elements	Cell quota pg·cell^{-1}															
	T0				T1				T4				T7			
	HL		LL		HL		LL		HL		LL		HL		LL	
C	30.61^a	(22.1)	10.24^b	(1.80)	28.34^{ab}	(15.5)	13.38^{ab}	(4.65)	103.72^{ab}	(22.7)	46.7^{ab}	(16.2)	87.73^c	(48.4)	19.0^{ab}	(12.2)
N	13.2^{ab}	(10.7)	2.14^b	(0.77)	5.49^{ab}	(3.20)	2.41^{ab}	(0.85)	19.6^{ab}	(3.90)	12.3^{ab}	(3.33)	36.2^c	(12.8)	2.47^{ab}	(1.53)
P	4.05^{ab}	(1.56)	5.79^{ab}	(0.61)	6.34^{ab}	(0.90)	7.94^a	(3.12)	2.92^{ab}	(0.95)	17.0^c	(9.71)	1.44^b	(0.08)	1.29^b	(0.32)
S	0.96^a	(0.47)	0.76^{abd}	(0.15)	0.35^{bcd}	(0.03)	0.70^{abd}	(0.12)	0.83^a	(0.12)	0.92^{ab}	(0.49)	0.23^{cd}	(0.03)	0.36^d	(0.07)
K	2.73^{ab}	(0.74)	2.79^{ab}	(0.55)	2.49^b	(0.55)	3.72^a	(0.59)	3.42^{ab}	(0.17)	3.46^{ab}	(1.44)	0.57^c	(0.03)	0.44^c	(0.01)
Ca	1.03^{ab}	(0.34)	0.87^{abc}	(0.22)	0.72^{abc}	(0.12)	1.25^a	(0.70)	4.92^b	(0.26)	0.69^{bc}	(0.20)	0.58^{bc}	(0.07)	0.44^c	(0.05)
Mn	0.12^{ab}	(0.04)	0.05^{cd}	(0.02)	0.11^{ab}	(0.01)	0.10^{abd}	(0.03)	0.14^b	(0.04)	0.09^{ad}	(0.04)	0.06^{cd}	(0.02)	0.01^c	(0.00)
Fe	0.35^{abc}	(0.09)	0.12^c	(0.01)	0.51^{abd}	(0.12)	0.21^{ac}	(0.10)	0.41^{abcd}	(0.23)	0.61^b	(0.44)	0.75^{bd}	(0.34)	0.29^{abc}	(0.00)
Cu	0.04^a	(0.02)	0.10^b	(0.01)	0.02^a	(0.00)	0.02^a	(0.01)	0.04^a	(0.01)	0.15^c	(0.04)	0.03^a	(0.01)	0.17^c	(0.04)
Zn	0.55^a	(0.22)	0.21^{bc}	(0.06)	0.32^{bc}	(0.05)	0.22^{bc}	(0.08)	0.63^a	(0.02)	0.33^b	(0.14)	0.32^{bc}	(0.09)	0.14^c	(0.01)
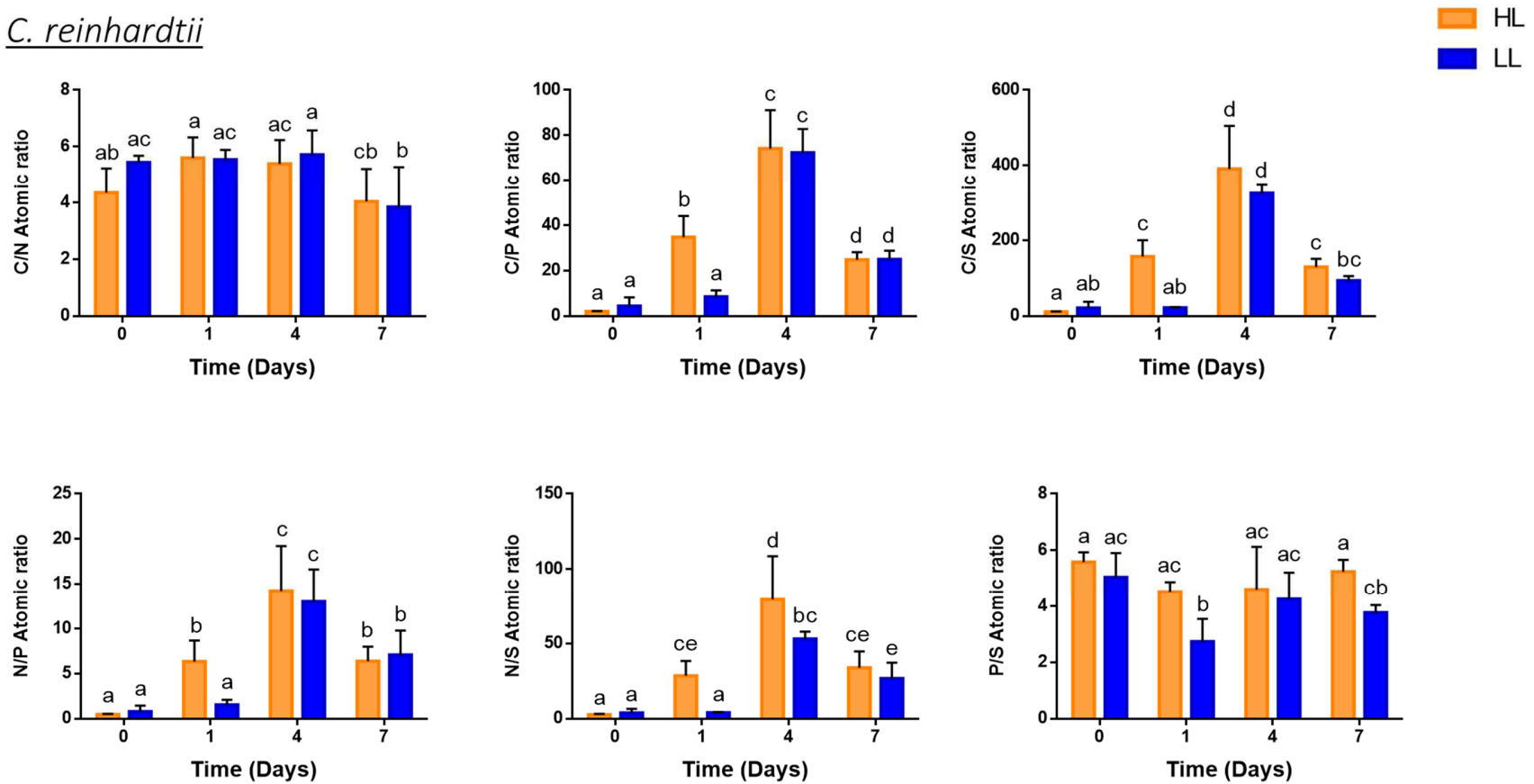
Figure. 4.24: Elemental stoichiometries (atomic ratios) in *C. reihardtii*. in anaerobic condition. High light (HL - orange bars) e and Low light (LL – blue bars). On day 0. the cells were transferred from 15 °C to 30 °C. Different letters indicate statistically different mean values ($p < 0.05$; 2-ways ANOVA and Fisher's LSD test). The error bars represent the standard deviations (N=3).
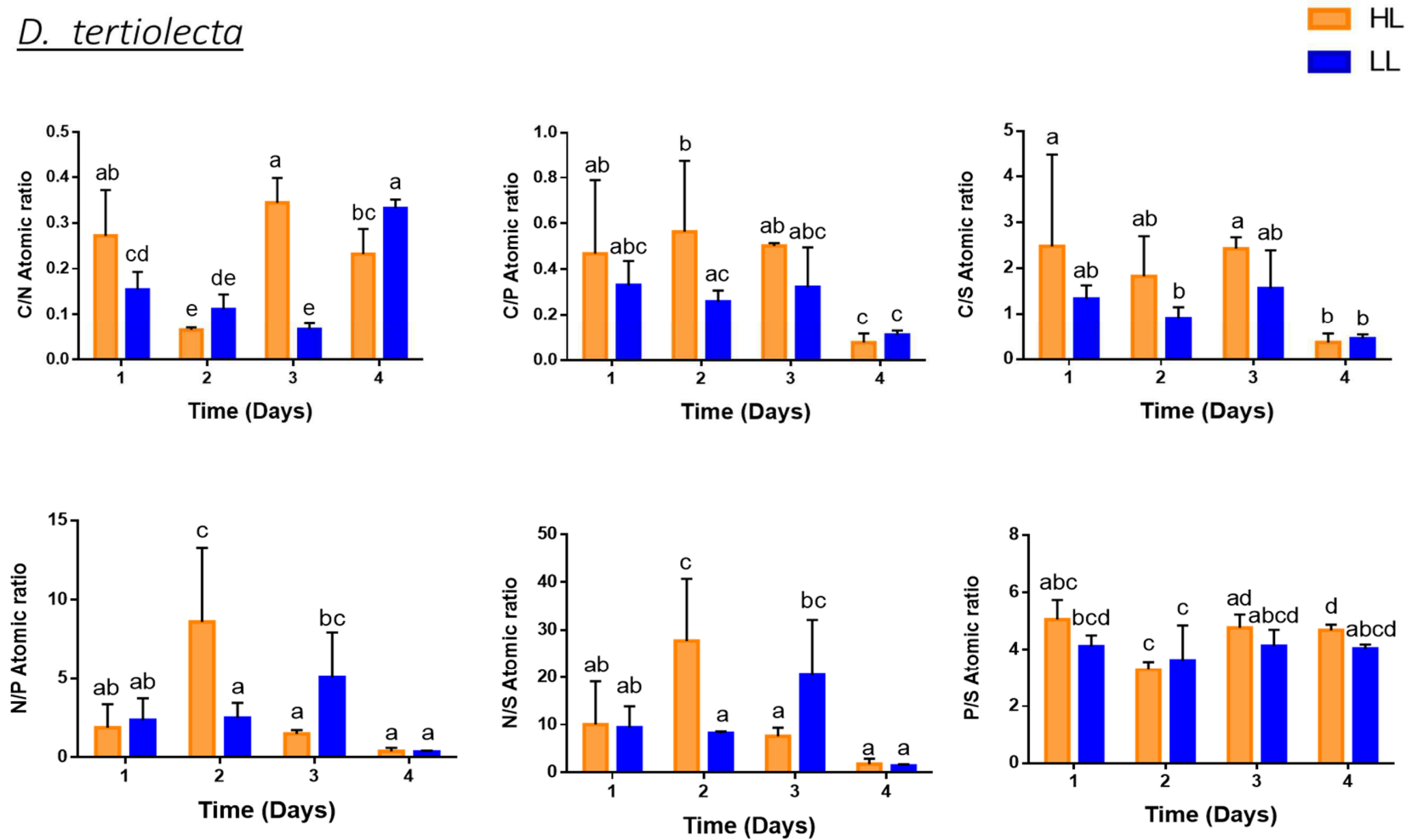
Figure. 4.25: Elemental stoichiometries (atomic ratios) in *D. tertiolecta* in anaerobic condition. High light (HL - orange bars) e and Low light (LL – blue bars). On day 0. the cells were transferred from 15 °C to 30 °C. Different letters indicate statistically different mean values (p < 0.05; 2-ways ANOVA and Fisher's LSD test). The error bars represent the standard deviations (N=3).

5. DISCUSSION

According to my experimental hypothesis (see paragraph 2.3), the energy availability was expected to be a major determinant of the acclimation potential of algal cells.

In the first section of this chapter, I will discuss the results of the first experiment, which was designed to understand whether the higher energetic yield of aerobic metabolism compared to that of anaerobic metabolism could affect the ability of *C. reinhardtii* to respond to an environmental perturbation (i.e. S-starvation).

In the second section of this chapter, I will discuss the results of the second experiment, which was aimed at investigating whether the acclimation potential of *C. reinhardtii* and *D. tertiolecta* is affected by energy availability, the latter determined by either irradiance and/or O_2 availability.

5.1 Impact of extracellular O_2 concentration on acclimation potential after S-starvation in *C. reinhardtii*

The analysis of the responses of *C. reinhardtii* to S-starvation was conducted at two levels (gene expression and C allocation), which correspond to different phases of the algal responses; this allowed me to observe a two-steps response.

The short-term response consists in an increase of the transcription of the genes associated with S uptake. In fact, as expected according to previous experiments (e.g. Aksoy et al. 2013), the expression of the genes encoding for sulfate transporters, arylsulfatases and *ECP76*, was up-regulated in 1 to 6 hours after the start of S starvation, in both aerobic and anaerobic condition. This suggests that *C. reinhardtii* cells subjected to S-starvation, regardless of the presence of O_2 in the external environment, and thus, independently on the energy availability provided by the mitochondria, begin to acclimate to the new environmental conditions.

The fact that the different cell metabolisms (cell respiration or cell fermentation) have no significant effect on cell capacity to transcribe mRNA for the genes associated with S uptake does not mean, however, that algae grown in aerobic and anaerobic conditions have, overall, a similar acclimation potential to S-starvation. In fact, we should consider a second step in the acclimation process, which requires more time to occur than gene expression, and consists in the modification of cell composition, aimed at reaching a new favorable equilibrium in the new environmental conditions (Giordano 2013). In the case examined here, only *C. reinhardtii* cells grown in aerobic conditions show a reorganization of the cell organic pools, while cells grown in anaerobic conditions remain homeostatic in terms of cell composition, probably due to the lower energetic availability.

It seems thus that cells grown in both aerobic and anaerobic conditions respond very rapidly to S-starvation, activating an acclimation process. The higher energetic requirement for compositional changes (compared to that for mRNA synthesis), however, prevents the long-term acclimation to S-starvation of cells growing in anaerobiosis, the latter being associated with anaerobic metabolism and therefore with fermentation, which leads to a lower energy production compared to the cellular respiration (Krebs and Jonson 1937, Atteia et al. 2013). Cellular energetics emerges as an important constraint in the strategy of response to environmental perturbations, confirming my first experimental hypothesis (see paragraph 2.3).

When I studied the expression of the genes *PFR1*, *ACK1* and *HYDA1*, which were previously used as indicators of anoxia (Pape et al. 2012; Catalanotti et al. 2012), I found that the transcription of *PFR1* and *ACK1* is stimulated by S-starvation in both aerobic and anaerobic condition. For what concerns the expression of *HYDA1*, it was previously reported as induced by O_2-deprivation (Hemschemeier et al. 2008b; Catalanotti et al. 2012) and S-deprivation (Hemschemeier et al. 2008a). However, I did not observe any effect of S-starvation on the expression of *HYDA1* in both aerobic and anaerobic conditions. I also observed an increase of *HYDA1* expression at T6 in control cells grown in anaerobic conditions. The gene expression in control cells, which were acclimated, prior to the experiment, to S-replete conditions and to either aerobic or anaerobic conditions, was expected to be stable. It is possible that absence of light during culture manipulation (i.e. centrifugation) of control cells was been involuntary longer than for other samples, and the darkness was responsible for the odd effect observed at T6. In fact, the growth in the dark seems to induce high levels of expression of *HYDA1* in *C. reinhardtii* (Gfeller and Gibbs 1984, Philipps et al. 2011).

5.2   Impact of energy availability on acclimation potential after a temperature shift in the green algae *C. reinhardtii* and *D. tertiolecta*

According to Renaud (2002), algal response to temperature changes varies in species-specific manner. I found that the temperature shift from 15°C to 30°C induces changes in the organic composition of both *D. tertiolecta* and *C. reinhardtii* cells in all examined conditions. However, it is possible to identify differences in the timing and in the extent at which these changes occur, which depend on the examined species and/or on the culture regime.

In *C. reinhardtii*, the temperature shift affects all the main organic pools: protein, lipid and carbohydrate. **Protein** increase after the perturbation regardless of irradiance and external [O_2], suggesting that a higher amount of protein is essential for coping with the given temperature increase. However, in anaerobiosis, and thus in absence of the energy produced by the mitochondrion, only a high irradiance allows the maintenance of the elevated cell protein content observed 1 day after the onset of the environmental perturbation.

The light regime seems critical for the **lipid** modifications in *C. reinhardtii*: only high irradiances allow the cells to obtain a significant increase in the lipid content. The concentration of external [O_2], furthermore, has an influence on the long-term acclimation potential of *C. reinhardtii*: only the most energetically-favorable culture regime (aerobiosis, high light) allows the cells to maintain high levels of lipid (about 10 times higher than before the onset of the temperature shift) after a long-term exposure to the perturbation. This is probably due to the fact that lipid require a higher energy expenditure per unit of mass and volume than carbohydrate and protein (Raven 2005; Gushina and Harwood 2006).

For what concerns the **carbohydrate** cell content, it is hard to understand, with the available information, why *C. reinhardtii* cells growing in aerobiosis at low irradiance did not follow the general tendency, evident in all the other culture regimes, toward an increase of the carbohydrate content after the temperature shift. I also observed that, in anaerobic conditions, the light regime determines the ability of cells to maintain high levels of carbohydrate throughout the end of the experiment.

In *D. tertiolecta* the **lipid** content, which has an overall decreasing trend over time, is influenced by neither the irradiance nor the external [O_2]. This suggested that a reduction in the amount of cell lipid is a key response to the temperature changes in this alga.

The exposure of *D. tertiolecta* to a temperature shift induces cells growing in aerobiosis to decrease their **carbohydrate** content. Similarly to what occurs for the protein content in *C. reinhardtii* growing in anaerobiosis, the light regime is crucial for the acclimation timing: the high irradiance permits cells to reduce the amount of carbohydrate more rapidly than low irradiance.

In contrast to what happens in *C. reinhardtii* cells exposed to the temperature change, in *D. tertiolecta* the external concentration of O_2 and the light regime both seem to be major determinants of the observed **protein** changes. This suggests that species-specific biases regulate and define the environmental conditions at which each cell organic pool can vary in response to an external perturbation.

The **ATP** content in *C. reinhardtii* and *D. tertiolecta* appears substantially uncoupled from the production of organic pools; this, however, does not contradict our speculation, which states that energy had a crucial role in determining the observed strategy of response of these algae to the temperature shift. In fact, we should consider that both ATP and reducing power are required for the production of the main organic pools (Table 2.1) and that the exactly ATP/NAD(P)H ratio depends on the physiological requirement of cells at each given condition (Baker et al. 2007). In the case examined here, the metabolic demands associated to the response to the temperature shift may have produces temporary unbalances in ATP/NAD(P)H ratio. The observed accumulation of ATP, rather than as a proxy for a high energy availability, may thus be considered as the result of a temporary inability of cells to exploit all the chemical energy stored in form of ATP because of a limitation induced by NAD(P)H. In *D. tertiolecta*, the ATP content seems to be inversely correlated to the photosynthetic efficiency, the latter being lower after 7 days from the onset of the perturbation than before the temperature change. I cannot exclude that this may have driven metabolic changes that would justify an alteration of the ATP/NAD(P)H ratio. Many processes are known to increase the ATP/NAD(P)H ratio, such as the increase of cyclic electron flow, the Mehler reaction and the malate shuttle (Baker et al. 2007).

The photosynthetic efficiency (**Fv/Fm**) of *C. reinhardtii* is not affected by the temperature change in any culture regime, while that of *D. tertiolecta* undergoes a general decrease after the exposure of the cells to the perturbation, which is more pronounced at high light.

Many articles correlate the reduction in Fv: Fm ratio to the presence of damage of photosynthetic system PSII (eg Wykoff et al. 1998, Schroda et al. 1999, Gomez et al. 2004 and Aguilera et al. 2008). Photoinhibition may be due to the prolonged joint action of high irradiation and high temperature (Yamane 1998; Butler and Kitajima, 1975), but it is also could due to the absence of hydrogenase which may serve as a sink for electrons that are produced in excess during photosynthesis at high light (Kessler 1973). It is also interesting to notice that differences have been reported in the sensitivity to photoinhibition among algal species subjected to anaerobiosis. Kessler (1973), for instance, showed that the photoinhibition was higher in algae that do not have hydrogenase, such as *D. tertiolecta* (Timmins et al. 2009), than in algal that possess hydrogenase, such as *C. reinhardtii* (Figure 1.2). This occurs thanks to the photoproduction of H_2 in the hydrogenase-containing algae, which dissipates reducing power and thus makes the oxidation of photosystem II possible.

6. CONCLUSION

i) The energy provided by the mitochondria seems essential for the long-term acclimation of *C. reinhardtii* to the S-starvation, which provides a reorganization of the main cell organic pools.

ii) The variation of certain cell components appears crucial for the acclimation of algae to the temperature change, since it occurs regardless of the external [O_2] and of the irradiance in the culture regime. The identity of such components and the direction of such changes, however, seem strictly specie-specific (i.e. an increase of protein in *C. reinhardtii*; a decrease of lipid for *D. tertiolecta*).
For what concerns the other cell organic pools, the external [O_2] and the irradiance determined either the direction of the change, and/or the acclimation timing, and/or the possibility to maintain the modifications at long-term, depending on the considered organic compound and on species-specific strategies.

7. REFERENCES

Aguilera, J., Figueroa, F. L., Häder, D. P., & Jiménez, C. (2008). Photoinhibition and photosynthetic pigment reorganisation dynamics in light/darkness cycles as photoprotective mechanisms of *Porphyra umbilicalis* against damaging effects of UV radiation. *Scientia Marina*, *72*(1), 87-97.

Aksoy, M., Pootakham, W., Pollock, S. V., Moseley, J. L., González-Ballester, D., & Grossman, A. R. (2013). Tiered regulation of sulfur deprivation responses in *Chlamydomonas reinhardtii* and identification of an associated regulatory factor. *Plant physiology*, *162*(1), 195-211.

Allen, J. F. (2002). Photosynthesis of ATP—electrons, proton pumps, rotors, and poise. *Cell*, *110*(3), 273-276.

Andersson, B., & Aro, E. M. (2001). Photodamage and D1 protein turnover in photosystem II. In *Regulation of photosynthesis* (pp. 377-393). Springer Netherlands.

Asada, K. (1999). The water-water cycle in chloroplasts: scavenging of active oxygens and dissipation of excess photons. *Annual review of plant biology*, *50*(1), 601-639.

Assunção, P., Jaén-Molina, R., Caujapé-Castells, J., de la Jara, A., Carmona, L., Freijanes, K., & Mendoza, H. (2012). Phylogenetic position of Dunaliella acidophila (Chlorophyceae) based on ITS and rbcL sequences. *Journal of applied phycology*, *24*(4), 635-639.

Atteia, A., Van Lis, R., Gelius-Dietrich, G., Adrait, A., Garin, J., Joyard, J., ... & Martin, W. (2006). Pyruvate formate-lyase and a novel route of eukaryotic ATP synthesis in *Chlamydomonas* mitochondria. *Journal of Biological Chemistry*, *281*(15), 9909-9918.

Atteia, A., Van Lis, R., Tielens, A. G., & Martin, W. F. (2013). Anaerobic energy metabolism in unicellular photosynthetic eukaryotes. *Biochimica et Biophysica Acta (BBA)-Bioenergetics*, *1827*(2), 210-223.

Bailleul, B., Berne, N., Murik, O., Petroutsos, D., Prihoda, J., Tanaka, A., ... & Krieger-Liszkay, A. (2015). Energetic coupling between plastids and mitochondria drives CO_2 assimilation in diatoms. *Nature*, *524*(7565), 366-369.

Baker, N. R., Harbinson, J., & Kramer, D. M. (2007). Determining the limitations and regulation of photosynthetic energy transduction in leaves. *Plant, Cell & Environment*, *30*(9), 1107-1125.

Behrenfeld, M. J., Prasil, O., Babin, M., & Bruyant, F. (2004). In search of a physiological basis for covariations in light-limited and light-saturated photosynthesis. *Journal of Phycology*, *40*(1), 4-25.

Behrenfeld, M. J., Halsey, K. H., & Milligan, A. J. (2008). Evolved physiological responses of phytoplankton to their integrated growth environment. *Philosophical Transactions of the Royal Society of London B: Biological Sciences*, *363*(1504), 2687-2703.

Ben-Amotz, A., & Avron, M. (1980). Glycerol, beta-carotene and dry algal meal production by commercial cultivation of Dunaliella. *Algae biomass: production and use [sponsored by the National Council for Research and Development, Israel and the Gesellschaft fur Strahlen-und Umweltforschung (GSF), Munich, Germany]; editors, Gedaliah Shelef, Carl J. Soeder*.

Ben-Amotz, A., & Avron, M. (1990). The biotechnology of cultivating the halotolerant algaDunaliella. *Trends in Biotechnology*, *8*, 121-126.

Ben-Amotz, A., Gressel, J., & Avron, M. (1987). Massive accumulation of phytoene induced by norflurazon in Dunaliella bardawil (Chlorophyceae) prevents recovery from photoinhibition. *Journal of phycology*, *23*(1), 176-181.

Boyer, T. H. (1975). Random electrodynamics: The theory of classical electrodynamics with classical electromagnetic zero-point radiation. *Physical Review D*, *11*(4), 790.

Büchel, C., & Wilhelm, C. (1993). In vivo analysis of slow chlorophyll fluorescence induction kinetics in algae: progress, problems and perspectives. *Photochemistry and Photobiology*, *58*(1), 137-148.

Buchheim, M. A., Lemieux, C., Otis, C., Gutell, R. R., Chapman, R. L., & Turmel, M. (1996). Phylogeny of the *Chlamydomonadales* (Chlorophyceae): a comparison of ribosomal RNA gene sequences from the nucleus and the chloroplast. *Molecular Phylogenetics and Evolution*, *5*(2), 391-402.

Butler, W. L., & Kitajima, M. (1975). Fluorescence quenching in photosystem II of chloroplasts. *Biochimica et Biophysica Acta (BBA)-Bioenergetics*, *376*(1), 116-125.

Cardol, P., Alric, J., Girard-Bascou, J., Franck, F., Wollman, F. A., & Finazzi, G. (2009). Impaired respiration discloses the physiological significance of state transitions in *Chlamydomonas*. *Proceedings of the National Academy of Sciences*, *106*(37), 15979-15984.

Catalanotti, C., Dubini, A., Subramanian, V., Yang, W., Magneschi, L., Mus, F., ... & Grossman, A. R. (2012). Altered fermentative metabolism in *Chlamydomonas reinhardtii* mutants lacking pyruvate formate lyase and both pyruvate formate lyase and alcohol dehydrogenase. *The Plant Cell*, *24*(2), 692-707.

Catalanotti, C., Yang, W., Posewitz, M. C., & Grossman, A. R. (2013). Fermentation metabolism and its evolution in algae. *Frontiers in plant science*, *4*.

Davies, J. M., Poole, R. J., & Sanders, D. (1993). The computed free energy change of hydrolysis of inorganic pyrophosphate and ATP: apparent significance. for inorganic-pyrophosphate-driven reactions of intermediary metabolism. *Biochimica et Biophysica Acta (BBA)-Bioenergetics*, *1141*(1), 29-36.

de Hostos, E. L., Schilling, J., & Grossman, A. R. (1989). Structure and expression of the gene encoding the periplasmic arylsulfatase of *Chlamydomonas reinhardtii*. *Molecular and General Genetics MGG*, *218*(2), 229-239.

De La Rocha, C. L., & Passow, U. (2004). Recovery of Thalassiosira weissflogii from nitrogen and silicon starvation. *Limnology and oceanography*, *49*(1), 245-255.

Domenighini, A., & Giordano, M. (2009). Fourier transform infrared spectroscopy of microalgae as a novel tool for biodiversity studies, species identification, and the assessment of water quality. *Journal of phycology*, *45*(2), 522-531.

Dubini, A., Mus, F., Seibert, M., Grossman, A. R., & Posewitz, M. C. (2008). Flexibility in anaerobic metabolism as revealed in a mutant of *Chlamydomonas reinhardtii* lacking hydrogenase activity. *Journal of Biological Chemistry*.

Falkowski, P., & Kiefer, D. A. (1985). Chlorophyll *a* fluorescence in phytoplankton: relationship to photosynthesis and biomass. *Journal of Plankton Research*, *7*(5), 715-731.

Fanesi, A., Raven, J. A., & Giordano, M. (2014). Growth rate affects the responses of the green alga Tetraselmis suecica to external perturbations. *Plant, cell & environment*, *37*(2), 512-519.

Fernie, A. R., Aharoni, A., Willmitzer, L., Stitt, M., Tohge, T., Kopka, J., ... & DeLuca, V. (2011). Recommendations for reporting metabolite data. *The Plant Cell*, *23*(7), 2477-2482.

Gaffron, H., & Rubin, J. (1942). Fermentative and photochemical production of hydrogen in algae. *The Journal of General Physiology*, *26*(2), 219-240.

Gfeller, R. P., & Gibbs, M. (1984). Fermentative metabolism of *Chlamydomonas reinhardtii*. *Plant Physiology*, *75*(1), 212-218.

Ghirardi, M. L., Maness, P. C., & Seibert, M. (2008). Photobiological methods of renewable hydrogen production. In *Solar hydrogen generation* (pp. 229-271). Springer New York.

Ghirardi, M. L., Zhang, L., Lee, J. W., Flynn, T., Seibert, M., Greenbaum, E., & Melis, A. (2000). Microalgae: a green source of renewable H_2. *Trends in biotechnology*, *18*(12), 506-511.

Giordano, M. (2001). Interactions between C and N metabolism in Dunaliella salina cells cultured at elevated CO_2 and high N concentrations. *Journal of Plant Physiology*, *158*(5), 577-581.

Giordano, M. (2013). Homeostasis: an underestimated focal point of ecology and evolution. *Plant science*, *211*, 92-101.

Giordano, M., Kansiz, M., Heraud, P., Beardall, J., Wood, B., & McNaughton, D. (2001). Fourier transform infrared spectroscopy as a novel tool to investigate changes in intracellular macromolecular pools in the marine microalga Chaetoceros muellerii (Bacillariophyceae). *Journal of Phycology*, *37*(2), 271-279.

Giordano, M., & Raven, J. A. (2014). Nitrogen and sulfur assimilation in plants and algae. *Aquatic botany*, *118*, 45-61.

Gómez, I., López-Figueroa, F., Ulloa, N., Morales, V., Lovengreen, C., Huovinen, P., & Hess, S. (2004). Patterns of photosynthesis in 18 species of intertidal macroalgae from southern Chile. *Marine Ecology Progress Series*, *270*, 103-116.

González-Ballester, D., Casero, D., Cokus, S., Pellegrini, M., Merchant, S. S., & Grossman, A. R. (2010). RNA-seq analysis of sulfur-deprived *Chlamydomonas* cells reveals aspects of acclimation critical for cell survival. *The Plant Cell Online*, *22*(6), 2058-2084.

Grossman, A. R., Croft, M., Gladyshev, V. N., Merchant, S. S., Posewitz, M. C., Prochnik, S., & Spalding, M. H. (2007). Novel metabolism in *Chlamydomonas* through the lens of genomics. *Current opinion in plant biology*, *10*(2), 190-198.

Guiry, M.D. & Guiry, G.M. 2017. AlgaeBase. World-wide electronic publication, National University of Ireland, Galway. http://www.algaebase.org.

Gupta, R., He, Z., & Luan, S. (2002). Functional relationship of cytochrome c 6 and plastocyanin in *Arabidopsis*. *Nature*, *417*(6888), 567.

Guschina, I. A., & Harwood, J. L. (2006). Lipids and lipid metabolism in eukaryotic algae. *Progress in lipid research*, *45*(2), 160-186.

Happe, T., & Naber, J. D. (1993). Isolation, characterization and N-terminal amino acid sequence of hydrogenase from the green alga *Chlamydomonas reinhardtii*. *The FEBS Journal*, *214*(2), 475-481.

Harris, E. H. (1989). Culture and storage methods. *The Chlamydomonas Sourcebook: A Comprehensive Guide to Biology and Laboratory Use. Academic Press, San Diego*, 25-63.

Heber, U. (1974). Metabolite exchange between chloroplasts and cytoplasm. *Annual Review of Plant Physiology*, *25*(1), 393-421.

Heineke, D., Riens, B., Grosse, H., Hoferichter, P., Peter, U., Flügge, U. I., & Heldt, H. W. (1991). Redox transfer across the inner chloroplast envelope membrane. *Plant Physiology*, *95*(4), 1131-1137.Heldt, H. W. (1969). Adenine nucleotide translocation in spinach chloroplasts. *FEBS letters*, *5*(1), 11-14.

Heldt, H. W. (1969). Adenine nucleotide translocation in spinach chloroplasts. *FEBS letters*, *5*(1), 11-14.

Hemschemeier, A., Fouchard, S., Cournac, L., Peltier, G., & Happe, T. (2008a). Hydrogen production by *Chlamydomonas reinhardtii*: an elaborate interplay of electron sources and sinks. *Planta*, *227*(2), 397-407.

Hemschemeier, A., & Happe, T. (2005). The exceptional photofermentative hydrogen metabolism of the green alga *Chlamydomonas reinhardtii*. *International Hydrogenases Conference 2004*.

Hemschemeier, A., Jacobs, J., & Happe, T. (2008b). Biochemical and physiological characterization of the pyruvate formate-lyase Pfl1 of *Chlamydomonas reinhardtii*, a typically bacterial enzyme in a eukaryotic alga. *Eukaryotic cell*, *7*(3), 518-526.

Hoefnagel, M. H., Atkin, O. K., & Wiskich, J. T. (1998). Interdependence between chloroplasts and mitochondria in the light and the dark. *Biochimica et Biophysica Acta (BBA)-Bioenergetics*, *1366*(3), 235-255.

Holmer, M., & Bondgaard, E. J. (2001). Photosynthetic and growth response of eelgrass to low oxygen and high sulfide concentrations during hypoxic events. *Aquatic Botany*, *70*(1), 29-38.

Kennedy, R. A., Rumpho, M. E., & Fox, T. C. (1992). Anaerobic metabolism in plants. *Plant Physiology*, *100*(1), 1-6.

Kessler, E. (1973). Effect of anaerobiosis on photosynthetic reactions and nitrogen metabolism of algae with and without hydrogenase. *Archiv für Mikrobiologie*, *93*(2), 91-100.

Kim, J., Fabris, M., Baart, G., Kim, M. K., Goossens, A., Vyverman, W., ... & Lun, D. S. (2016). Flux balance analysis of primary metabolism in the diatom *Phaeodactylum tricornutum*. *The Plant Journal*, *85*(1), 161-176.

Kramer, D. M., & Evans, J. R. (2011). The importance of energy balance in improving photosynthetic productivity. *Plant Physiology*, *155*(1), 70-78.

Krebs, H. A., & Johnson, W. A. (1937). Metabolism of ketonic acids in animal tissues. *Biochemical Journal*, *31*(4), 645.

Kromer, S. (1995). Respiration during photosynthesis. *Annual review of plant biology*, *46*(1), 45-70.

Lapaille, M., Escobar-Ramírez, A., Degand, H., Baurain, D., Rodríguez-Salinas, E., Coosemans, N., ... & Cardol, P. (2010). Atypical subunit composition of the chlorophycean mitochondrial F1FO-ATP synthase and role of Asa7 protein in stability and oligomycin resistance of the enzyme. *Molecular biology and evolution*, *27*(7), 1630-1644.

Lea, P. J., & Miflin, B. J. (1975). The occurrence of glutamate synthase in algae. *Biochemical and biophysical research communications*, *64*(3), 856-862.

Lehninger, A. L. (1962). Water uptake and extrusion by mitochondria in relation to oxidative phosphorylation. *Physiological reviews*, *42*(3), 467-517.

Leliaert, F., & Lopez-Bautista, J. M. (2015). The chloroplast genomes of Bryopsis plumosa and Tydemania expeditiones (Bryopsidales, Chlorophyta): compact genomes and genes of bacterial origin. *Bmc Genomics*, *16*(1), 204.

Liaud, M. F., Lichtl, C., Apt, K., Martin, W., & Cerff, R. (2000). Compartment-specific isoforms of TPI and GAPDH are imported into diatom mitochondria as a fusion protein: evidence in favor of a mitochondrial origin of the eukaryotic glycolytic pathway. *Molecular biology and evolution*, *17*(2), 213-223.

Melis, A., & Happe, T. (2001). Hydrogen production. Green algae as a source of energy. *Plant physiology*, *127*(3), 740-748.

Merchant, S. S., Prochnik, S. E., Vallon, O., Harris, E. H., Karpowicz, S. J., Witman, G. B., ... & Marshall, W. F. (2007). The *Chlamydomona*s genome reveals the evolution of key animal and plant functions. *Science*, *318*(5848), 245-250.

Mitchell, P. (1966). Chemiosmotic coupling in oxidative and photosynthetic phosphorylation. *Biological Reviews*, *41*(3), 445-501.

Montechiaro, F., Hirschmugl, C. J., Raven, J. A., & Giordano, M. (2006). Homeostasis of cell composition during prolonged darkness. *Plant, cell & environment*, *29*(12), 2198-2204.

Mus, F., Dubini, A., Seibert, M., Posewitz, M. C., & Grossman, A. R. (2007). Anaerobic acclimation in *Chlamydomonas reinhardtii* anoxic gene expression, hydrogenase induction, and metabolic pathways. *Journal of Biological Chemistry*, *282*(35), 25475-25486.

Noctor, G., & Foyer, C. H. (1998). Ascorbate and glutathione: keeping active oxygen under control. *Annual review of plant biology*, *49*(1), 249-279.

Ohad, I., Sonoike, K., & Andersson, B. (2000). Photoinactivation of the two photosystems in oxygenic photosynthesis: mechanisms and regulations. *Probing Photosynthesis: Mechanisms, Regulation and Adaptation. Taylor and Francis Publishers–London*, 293-309.

Padmasree, K., Padmavathi, L., & Raghavendra, A. S. (2002). Essentiality of mitochondrial oxidative metabolism for photosynthesis: optimization of carbon assimilation and protection against photoinhibition. *Critical Reviews in Biochemistry and Molecular Biology*, *37*(2), 71-119.

Palmucci, M., Ratti, S., & Giordano, M. (2011). Ecological and evolutionary implications of carbon allocation in marine phytoplankton as a function of nitrogen availability: a Fourier transform infrared spectroscopy approach. *Journal of phycology*, *47*(2), 313-323.

Palmucci, M., Britun, N., Konstantinidis, S., & Snyders, R. (2013). Rarefaction windows in a high-power impulse magnetron sputtering plasma. *Journal of applied physics*, *114*(11), 113302.

Pape, M., Lambertz, C., Happe, T., & Hemschemeier, A. (2012). Differential expression of the *Chlamydomonas* [FeFe]-hydrogenase-encoding HYDA1 gene is regulated by the copper response regulator1. *Plant physiology*, *159*(4), 1700-1712.

Peterson, G. L. (1977). A simplification of the protein assay method of Lowry et al. which is more generally applicable. *Analytical biochemistry*, *83*(2), 346-356.

Pfaffl, M. W. (2001). A new mathematical model for relative quantification in real-time RT–PCR. *Nucleic acids research*, *29*(9), e45-e45.

Philipps, G., Krawietz, D., Hemschemeier, A., & Happe, T. (2011). A pyruvate formate lyase-deficient *Chlamydomonas reinhardtii* strain provides evidence for a link between fermentation and hydrogen production in green algae. *The Plant Journal*, *66*(2), 330-340.

Pootakham, W., Gonzalez-Ballester, D., & Grossman, A. R. (2010). Identification and regulation of plasma membrane sulfate transporters in *Chlamydomonas*. *Plant physiology*, *153*(4), 1653-1668.

Raghavendra, A. S., & Padmasree, K. (2003). Beneficial interactions of mitochondrial metabolism with photosynthetic carbon assimilation. *Trends in plant science*, *8*(11), 546-553.

Raghavendra, A. S., Padmasree, K., & Saradadevi, K. (1994). Interdependence of photosynthesis and respiration in plant cells: interactions between chloroplasts and mitochondria. *Plant Science*, *97*(1), 1-14.

Ratti, S., Knoll, A. H., & Giordano, M. (2011). Did sulfate availability facilitate the evolutionary expansion of chlorophyll *a + c* phytoplankton in the oceans?. *Geobiology*, *9*(4), 301-312.

Raven, J. A. (1982). The energetics of freshwater algae; energy requirements for biosynthesis and volume regulation. *New Phytologist*, *92*(1), 1-20.

Raven, J. A. (2005). Cellular location of starch synthesis and evolutionary origin of starch genes. *Journal of phycology*, *41*(6), 1070-1072.

Raven, J. A. (2011). The cost of photoinhibition. *Physiologia Plantarum*, *142*(1), 87-104.

Raven, J. A., & Beardall, J. (2017). Consequences of the genotypic loss of mitochondrial Complex I in dinoflagellates and of phenotypic regulation of Complex I content in other photosynthetic organisms. *Journal of Experimental Botany*, *68*(11), 2683-2692.

Raven, J. A., & Geider, R. J. (2003). Adaptation, acclimation and regulation in algal photosynthesis. In *Photosynthesis in algae* (pp. 385-412). Springer Netherlands.

Renaud, S. M., Thinh, L. V., Lambrinidis, G., & Parry, D. L. (2002). Effect of temperature on growth, chemical composition and fatty acid composition of tropical Australian microalgae grown in batch cultures. *Aquaculture*, *211*(1), 195-214.

Rismani-Yazdi, H., Haznedaroglu, B. Z., Bibby, K., & Peccia, J. (2011). Transcriptome sequencing and annotation of the microalgae *Dunaliella tertiolecta*: pathway description and gene discovery for production of next-generation biofuels. *BMC genomics*, *12*(1), 148.

Roberts, K., Gurney-Smith, M., & Hills, G. J. (1972). Structure, composition and morphogenesis of the cell wall of Chlamydomonas reinhardi: I. Ultrastructure and preliminary chemical analysis. *Journal of ultrastructure research*, *40*(5-6), 599-613.

Saradadevi, K., & Raghavendra, A. S. (1992). Dark respiration protects photosynthesis against photoinhibition in mesophyll protoplasts of pea (Pisum sativum). *Plant Physiology*, *99*(3), 1232-1237.

Scheibe, R. (2004). Malate valves to balance cellular energy supply. *Physiologia plantarum*, *120*(1), 21-26.

Schreiber, U., Schliwa, U., & Bilger, W. (1986). Continuous recording of photochemical and non-photochemical chlorophyll fluorescence quenching with a new type of modulation fluorometer. *Photosynthesis research*, *10*(1-2), 51-62.

Schroda, M., Vallon, O., Wollman, F. A., & Beck, C. F. (1999). A chloroplast-targeted heat shock protein 70 (HSP70) contributes to the photoprotection and repair of photosystem II during and after photoinhibition. *The Plant Cell*, *11*(6), 1165-1178.

Smith, B. C. (1998). Infrared spectral interpretation: a systematic approach. *CRC Press LLC* ISBN 0-8493-1463-7.

Spilling, K., Ylöstalo, P., Simis, S., & Seppälä, J. (2015). Interaction effects of light, temperature and nutrient limitations (N, P and Si) on growth, stoichiometry and photosynthetic parameters of the cold-water diatom Chaetoceros wighamii. *PloS one*, *10*(5), e0126308.

Takahashi, H., Braby, C. E., & Grossman, A. R. (2001). Sulfur economy and cell wall biosynthesis during sulfur limitation of *Chlamydomonas reinhardtii*. *Plant physiology*, *127*(2), 665-673.

Timmins, J. M., Ozcan, L., Seimon, T. A., Li, G., Malagelada, C., Backs, J., ... & Tabas, I. (2009). Calcium/calmodulin-dependent protein kinase II links ER stress with Fas and mitochondrial apoptosis pathways. *The Journal of clinical investigation*, *119*(10), 2925.

Tran, Q. H., & Unden, G. (1998). Changes in the proton potential and the cellular energetics of Escherichia coli during growth by aerobic and anaerobic respiration or by fermentation. *The FEBS Journal*, *251*(1-2), 538-543.

Woods, H. A., & Wilson, J. K. (2013). An information hypothesis for the evolution of homeostasis. *Trends in ecology & evolution*, *28*(5), 283-289.

Wykoff, D. D., Davies, J. P., Melis, A., & Grossman, A. R. (1998). The regulation of photosynthetic electron transport during nutrient deprivation in *Chlamydomonas reinhardtii*. *Plant physiology*, *117*(1), 129-139.

Wykoff, D. D., Davies, J. P., Melis, A., & Grossman, A. R. (1998). The regulation of photosynthetic electron transport during nutrient deprivation in *Chlamydomonas reinhardtii*. *Plant physiology*, *117*(1), 129-139.

Yamane, Y., Kashino, Y., Koike, H., & Satoh, K. (1998). Effects of high temperatures on the photosynthetic systems in spinach: oxygen-evolving activities, fluorescence characteristics and the denaturation process. *Photosynthesis Research*, *57*(1), 51-59.

Yildiz, F. H., Davies, J. P., & Grossman, A. R. (1994). Characterization of sulfate transport in *Chlamydomonas reinhardtii* during sulfur-limited and sulfur-sufficient growth. *Plant Physiology*, *104*(3), 981-987.

8. INDEX OF FIGURES

9. INDEX OF TABLE